ROLE OF MAIZE OXYLIPINS IN REGULATING INDUCED SYSTEMIC RESISTANCE TRIGGERED BY BENEFICIAL FUNGUS TRICHODERMA VIRENS

A Dissertation

by

KEN-DER WANG

Submitted to the Office of Graduate and Professional Studies of
Texas A&M University
in partial fulfillment of the requirements for the degree of

DOCTOR OF PHILOSOPHY

Chair of Committee,	Michael Kolomiets
Co-Chair of Committee	Charles Kenerley
Committee Members,	Libo Shan
	Gregory Sword
Head of Department,	Leland Pierson III

December 2018

Major Subject: Plant Pathology

ABSTRACT

Plants benefit from interactions with symbiotic microorganisms, with enhancements ranging from improved growth to activation of induced systemic resistance (ISR) against a broad range of pathogens. While pathogen-triggered systemic acquired resistance (SAR) is well understood with multiple signal molecules identified, ISR mobile signals remain unknown. Jasmonic acid (JA), a 13-lipoxygenase (LOX)-derived oxylipin, and ethylene (ET) have long been established as the main phytohormone regulators of ISR, although conclusive evidence for these two molecules as ISR mobile signals is lacking. However, there is increasing evidence that other oxylipin signals, especially those derived from 9-LOX activity, have roles in ISR. For instance, the maize 9-LOX, LOX3, has been identified as a negative regulator of ISR, with *lox3* mutants displaying constitutive ISR against a broad range of pathogens. The objective of this study is to identify oxylipin biosynthesis genes and specific molecules that govern ISR. Maize wild-type and near-isogenic mutants disrupted for several LOX, JA biosynthesis, and ET biosynthesis and ISR-positive and -negative mutants of the beneficial fungus *Trichoderma virens* were used to identify key oxylipin regulators of ISR by metabolite and transcriptome profiling. Both the JA-producing 13-LOX, *LOX10*, and the 9-LOX, *LOX12*, were overexpressed in *lox3* roots and found to be required for *T. virens*-induced ISR. *T. virens*-colonized *lox10* and *lox12* mutants became more susceptible to infection by *Colletotrichum graminicola*, causal agent of anthracnose leaf blight, leading to an induced systemic susceptibility (ISS) phenotype. Oxylipin profiling of xylem sap from maize exhibiting different defense responses after treatment with mutant or WT *T. virens* identified JA precursor, 12-oxo-phytodienoic acid (12-OPDA), and a 9-LOX-derived α-ketol, 9-hydroxy-10-oxo-12(Z),15(Z)-octadecadienoic acid (KODA) as

molecular signals involved in induction of ISR. Treatment with 12-OPDA or KODA enhanced resistance against infection in a dose-dependent effect, confirming signaling roles. Surprisingly, *T. virens*-induced ISR in either JA- or ET-deficient mutants, suggesting neither were required for ISR. Transcriptome analysis of *T. virens*-treated maize revealed upregulation of 12-OPDA biosynthesis and response genes, but downregulation of subsequent JA biosynthesis genes and JA response genes. These results show that OPDA and KODA, but not JA, are required for activation of *T. virens*-induced ISR in maize.

DEDICATION

To my mother Liao Shu Chi Wang, my father Yue Swei Wang, and my sister Sandy Wang.

ACKNOWLEDGEMENTS

I would like to thank my committee chair, Dr. Kolomiets, my co-chair, Dr. Kenerley, and my committee members, Dr. Shan and Dr. Sword, for their guidance and encouragement throughout the course of my research. I would also like to thank my colleagues, friends, and the department faculty and staff for making my time at Texas A&M University a great experience. Special thanks to the undergraduate assistants Joseph Vasselli, Briana Hankinson, and Kacey Wilson for their hard work for my project. Finally, thanks to my mother, father, and sister for their patience and support.

CONTRIBUTORS AND FUNDING SOURCES

This work was supervised by a committee consisting of Professors Michael Kolomiets and Charles Kenerley, who acted as co-advisors, and Professor Libo Shan of the Department of Plant Pathology and Microbiology, and Professor Gregory Sword of the Department of Entomology.

Transcript sequencing was conducted by the Texas A&M Agrilife Research Genomics and Bioinformatics Services. LC/MS-MS analysis for phytohormones, oxylipins, and metabolites in the xylem sap was conducted by Dr. Eli Borrego. Work on transgenic *Arabidopsis* expressing *pLOX12::GUS* was done by Shihang Liu in Dr. Hisashi Koiwa's lab of the Department of Horticulture at Texas A&M University. All other work for the dissertation was completed independently by the student.

This work was made possible in part by USDA-NIFA Agriculture and Food Research Initiative under grant number 2016-67013-24730. Graduate study was also supported by a fellowship from Texas A&M University.

TABLE OF CONTENTS

Page

LIST OF FIGURES

LIST OF TABLES

CHAPTER I

INTRODUCTION

The advances in large-scale transcriptomics, proteomics, and genomics have driven microbiome studies with the goal of improving crop productivity by utilizing beneficial microbes to enhance plant growth and resistance to biotic and abiotic stresses. Manipulating and engineering the plant microbiome could revolutionize the field of medicine and agriculture (Mueller and Sachs, 2015). The rhizosphere of plants offers a diverse microbiome that ranges from pathogens to beneficial microbes. This area of diverse and heightened activity has been termed the rhizobiome. Plants interact with microbes within the rhizobiome through the secretion of plant exudates and signaling compounds to promote mutualistic relationships (Mendes et al., 2013). Many of these beneficial microbes can be characterized as plant growth promoting rhizobacteria/fungi (PGPR/PGPF), as they can enhance growth and development of the plant hosts they interact with. In addition to growth, these PGPR/PGPF can also heighten host systemic resistance against a broad range of pathogens and pests by a mechanism called induced systemic resistance (ISR) (Pieterse et al., 2014a). Upon induction of ISR, plants undergo transcriptomic and metabolomic reprogramming to prime defense responses to respond rapidly and robustly against pathogen infection (Wang et al., 2005; Conrath et al., 2006; Pieterse et al., 2014b).

The ISR pathway is poorly understood compared to the well-characterized systemic acquired resistance (SAR) pathway (Pieterse et al., 2014a). SAR is activated by prior infection by pathogens and is regulated by salicylic acid (SA) signaling, while ISR occurs upon root colonization by beneficial microbes and is long believed to be regulated by jasmonic acid (JA)

and ethylene (ET) signaling (Pieterse et al., 2014b). SAR signaling requires activation of Nonexpressor of pathogenesis-related genes 1 (NPR1), which monomerizes and moves to the nucleus to activate the TGACG (TGA) motif-binding family of transcriptional factors to promote expression of SA-responsive defense genes (Vlot et al., 2009; Pieterse et al., 2012). Interestingly, several long-distance signals for SAR have been identified and include azelaic acid (AzA), pipecolic acid (Pip), methyl salicylate (MeSA), glycerol-3-phosphate (G3P), and dehydroabietinal (DA), but not SA itself (Klessig et al., 2018; Shan and He, 2018). Much less is known about the ISR signaling pathway; however, NPR1 activity in the cytoplasm is required (Pieterse et al., 1998; Pieterse et al., 2012).

Among the fungal members of the rhizobiome, *Trichoderma* spp., which include the agriculturally relevant *T. virens* and *T. harzianum*, have been identified as prominent PGPF from many soil environments (Lorito et al., 2010; Harman, 2011; Hermosa et al., 2012; Mukherjee et al., 2013). Their benefits to host plants include growth promotion, biocontrol activity through antibiosis and mycoparasitism, and triggering ISR (Yedidia et al., 1999; Howell et al., 2000; Druzhinina et al., 2011). Several species of *Trichoderma* interact with a diverse species of plants, such as *Arabidopsis*, cotton, tomato, and maize, resulting in ISR against a wide array of pathogens (Djonovic et al., 2006; Djonovic et al., 2007; Shoresh et al., 2010; Contreras-Cornejo et al., 2011).

The process of communication between *Trichoderma* and its plant host is pivotal for providing eventual plant benefits. However, even before root colonization or contact, various secreted fungal elicitors contribute to form compatible interactions. One elicitor in particular is Sm1, a small secreted cysteine-rich protein (SSCP) from *T. virens* that is required for induction of ISR in host plants (Djonovic et al., 2006; Djonovic et al., 2007). Expression of *SM1* was

greatly induced when *T. virens* grew in the presence of plants compared to when grown alone (Djonovic et al., 2007; Moran-Diez et al., 2015). Presence of Sm1 induced maize defense genes locally in roots and systemically, while the knockout mutant *Δsm1* lost the ability to induce ISR completely. *T. atroviride* Epl1, a homolog of *T. virens* Sm1, is required for ISR in tomato and improves plant resistance against necrotrophic pathogens such as *Alternaria solani* and *Botrytis cinerea* or the biotroph *Pseudomonas syringae* pv. *tomato* (*Pst* DC3000) (Salas-Marina et al., 2015). In addition to Sm1, *T. virens* also secretes many other SSCPs, some of which act as negative regulators of ISR and reduce plant defense response (Lamdan et al., 2015). Knockout mutant of protein ID 77560, now named Suppressor of Induced Resistance 1 (Sir1), induced enhanced ISR in maize against a necrotroph *Cochliobolus heterostrophus* compared to wild-type *T. virens*. Importantly, during *T. virens* colonization of maize, expression of a 9-lipoxygenase (LOX) gene, *LOX3,* was suppressed in a Sm1-dependent manner, and *lox3* knockout mutant displayed constitutively active ISR (Constantino et al., 2013), prompting the need to better understand the role of plant oxylipins and their role in regulating ISR.

Plant oxylipins are involved in cross-kingdom signal communication and play major roles in regulating many aspects of plant physiology, such as growth and development and defense responses to pathogens, herbivores, and abiotic stresses (Feussner and Wasternack, 2002; Christensen and Kolomiets, 2011; Borrego and Kolomiets, 2016). Oxylipins are produced through enzymatic or nonenzymatic oxygenation of polyunsaturated fatty acids such as linoleic acid (C18:2, LA) and linolenic acid (C18:3, α-LeA) in plants and arachidonic acid (C20:4) in mammals. Human oxylipins, such as prostaglandins, leukotrienes, and thromboxanes, have been well characterized as hormone regulators of various developmental, physiological, and pathological processes (Funk, 2001). Compared to mammalian oxylipins, plant oxylipins are

poorly characterized, with only JA and its derivatives as the exceptions. The LOX pathway is the enzymatic pathway for oxylipin biosynthesis, which begins with 9- or 13-LOX enzymes oxygenating polyunsaturated fatty acids (PUFAs) at carbon position 9 or 13, respectively (Feussner and Wasternack, 2002; Andreou et al., 2009; Kachroo and Kachroo, 2009). The products of LOXs are immediately fed into seven different branches of the LOX pathway. One such branch is the 13-allene oxide synthase (13-AOS) pathway, which produces JA-precursor, 12-oxo-phytodienoic acid (12-OPDA), and the hormone JA-Ile, and other JA derivatives from 13-hydroperoxy octadecatrienoic acid (13-HPOTE), and the hydroperoxide lyase (HPL) pathway, which converts 13-HPOTE to several short chain C6-compounds called green leaf volatiles (GLVs) in maize (Matsui, 2006; Christensen et al., 2013). GLVs attract parasitoid wasps in response to herbivory (Whitman and Eller, 1990; Christensen et al., 2013), regulate plant-plant communications (Engelberth et al., 2004), and enhance JA response against herbivory (Farag and Pare, 2002).

Aside from JA, over 650 other oxylipins have been identified in plants with largely unknown functions, especially the 9-oxylipins derived from 9-LOX activity (Borrego and Kolomiets, 2016). While JA and its derivatives are derived from linolenic acid and produced by 13-LOX activity through the 13-AOS branch, products of the 9-AOS pathway include death acids (Christensen et al., 2015), which can trigger potent programmed cell death, and 9-oxylipin ketols including 9-hydroxy-10-oxo-12(Z), 15(Z)-octadecadienoic acid (KODA), the function of which is not clearly established (Vick and Zimmerman, 1984). The 9-oxylipins have been mostly characterized for their roles in regulating germination, root growth, and defense against infection and herbivory (Vellosillo et al., 2007; Nalam et al., 2012). Maize 9-LOXs, LOX4 and LOX5, share ~95% amino acid sequence identity, but are expressed in different tissue and in response to

different stimuli (Park et al., 2010). *LOX4* expression is detected in below-ground tissue and in response to JA, while *LOX5* expression is detected in above-ground tissue and in response to JA, SA, wounding, and insect herbivory. Furthermore, *lox4* mutants were significantly more susceptible to *Colletotrichum graminicola*, causal agent of anthracnose stalk rot and leaf blight, while *lox5* mutants were more resistant (Park, 2012; Damarwinasis, 2018). Another maize 9-LOX, *LOX12*, is expressed in below-ground tissue and greatly induced upon infection by *Fusarium verticillioides* (Christensen et al., 2014). Furthermore, *lox12* mutants are more susceptible to *F. verticillioides* infection due to reduced accumulation of 12-OPDA and JA (Christensen et al., 2014; Battilani et al., 2018). The specific 9-oxylipin product of LOX12 has not been yet identified.

While 13-LOXs in plants are better characterized because of their involvement in JA biosynthesis, the 9-LOXs and their products are poorly understood. Most work with 9-oxylipins focus on growth and development, and defense against infection and herbivory (Vellosillo et al., 2007; Gao et al., 2008; Nalam et al., 2012; Christensen et al., 2014). However, there is increasing evidence that 9-oxylipins also have major roles in regulating ISR. For example, disruption of maize *LOX3*, a root-specific 9-LOX, resulted in dramatic increase in systemic resistance against a variety of seed, stalk, root, and foliar pathogens, such as *C. heterostrophus*, *Exserohilum pedicellatum*, *Fusarium verticillioides,* and *C. graminicola* (Gao et al., 2007; Isakeit et al., 2007). The *lox3* mutant roots constitutively overexpressed genes involved in biosynthesis of GLVs and JA (*HPL1* and *LOX10*) and defense phytohormones SA, and ET, and over-accumulated those hormones even in the absence of pathogen infection (Gao et al., 2008). Because LOX3 gene is not expressed in leaf tissue even when infected with pathogens and transfusion of xylem sap collected from *lox3* mutants conferred increased systemic resistance

to receiver wild-type (WT) plants to levels comparable to ISR phenotype of *T. virens*-treated WT plants, it was concluded that *lox3* mutant produces potent xylem-sap resident ISR signal and thus, displays constitutively active ISR (Constantino et al., 2013). As previously mentioned, expression of *LOX3* in WT plant roots was suppressed by *T. virens* colonization in a Sm1-dependent manner, suggesting that LOX3 is a negative regulator of ISR. Additionally, recent studies demonstrated that as-yet-unidentified 9-LOX derivatives are involved in plant-arbuscular mycorrhizal (AM) fungus interactions that result in mycorrhizae-induced resistance (MIR) akin to ISR (León-Morcillo et al., 2012; Morcillo et al., 2016).

The focus of this project is to elucidate the major oxylipin biosynthesis genes and their metabolites as signals for ISR induction upon maize root colonization by *T. virens*. The main objectives of this project are: 1) Identify specific oxylipin biosynthesis genes responsible for activation of ISR; and 2) identity specific oxylipin signals required for ISR induction in response to *T. virens* colonization of roots.

CHAPTER II

MATERIALS AND METHODS

Plant and Fungal Material

The maize inbred lines B73, W438, and Tx714 and mutator transposon knockout mutants *lox3-4* (Gao et al., 2007), *lox10-2, lox10-3* (Christensen, 2011), and double mutants *opr7opr8* (Yan et al., 2012) and *acs2acs6* were used in this study. The double mutant of *lox3lox10* was generated in this study by conventional breeding. The mutant maize lines are all near-isogenic (NILs) at the backcross seven (BC7) genetic stage in the B73 background. Strains Gv29-8 (TvWT) (Baek and Kenerley, 1998), *Δsm1* (Djonovic et al., 2006), and *Δsir1* (formerly *Δ77560*) (Lamdan et al., 2015) of *T. virens* were grown on Potato Dextrose Agar (PDA, Difco Laboratories, Detroit) at 27°C from stock glycerol cultures maintained at -80 C. Chlamydospores of *T. virens* were obtained from cultures grown in molasses-yeast extract medium (Mukherjee and Kenerley, 2010). After 2 weeks, the incubated cultures were vacuum filtered, air dried, and the mycelial mat containing chlamydospores was ground to fine powder. *Colletotrichum graminicola* (1.001 strain) on PDA and *Cochliobolus heterostrophus* on complete medium with xylose (substituted for glucose to improve conidiation) were grown at room temperature (21-23°C) under fluorescent lights. (Tzeng et al., 1992).

Soil Growth Conditions

Maize seeds were surface sterilized with 70% EtOH wash for 5 min, followed with a 0.6% sodium hypochlorite wash for 5 min, and then rinsed 3-5 times with sterile water. The seeds were planted in sterilized MetroMix 366 soil (steam sterilized for 1 hour, cooled overnight, and sterilized again for 1 hour) in long conical tubes (20.5 x 4 cm conetainers, Stewe and Sons).

ISR Assay

Infection with C. *graminicola* and *C. heterostrophus* was performed in this study as described by (Gao et al., 2007). Seven days after maize seeds were planted, and similarly developed seedlings that germinated were either left untreated (control) or treated with 0.1 g of *T. virens* chlamydospore (added to the soil at a depth of 4-5 cm). When the plants reached vegetative stage four (V4), the third true leaves were infected with *C. graminicola* or *C. heterostrophus*. Briefly, the plants were placed in trays (78.5 cm x 63 cm x 7 cm) lined with paper towels with the third leaves taped down flat facing up. Sterile distilled water (SDW) was added to *C. graminicola* or *C. heterostrophus* plates, which were then scraped with an inoculating loop to free the conidia. The suspension was then filtered through sterile cheesecloth into a 50 mL Falcon tube to remove mycelia. The conidial suspension was centrifuged twice at 3000 rpm for 3 minutes, with the water being replaced each time with fresh SDW. The initial conidia concentration was determined using a hemocytometer. The suspension was finally diluted to a concentration of 1×10^6 spores per mL. The spores were used immediately after preparation, as they lose viability after 2 hr in room temperature. Ten μL of the spore

suspensions (10,000 spores) were inoculated to 6 individual areas of the center of the leaf without contacting the midvein. Paper towels were moistened with sterile water, which were then covered with GLAD Press'n'Seal (The Glad Products Company, Oakland, CA, U.S.A) to create a humid chamber. The humidity chambers were placed in darkness for 24 hours at 25°C. The plants were then positioned upright and allowed to continue to grow under 14:10 light:dark photoperiod at room temperature (21-23°C). Leaves were scanned 4 days after inoculation, and lesion area was determined using the ImageJ software (https://imagej.nih.gov/ij/). Data were analyzed by ANOVA and Tukey's HSD test ($p < 0.05$).

Xylem-Enriched Sap Collection

Xylem-enriched sap was collected from B73, *lox3-4*, and *lox10-3* plants at V4-stage treated with WT or *Δsm1* strains of *T. virens* or left untreated. One day before sap collection, the plants were placed on light shelves (150 μmol m^{-2} s^{-1} (Quantum Meter; Apogee Instruments, Logan, UT, USA) and kept well-watered (Constantino et al., 2013). The following day the plants were watered until the soil was saturated, and then decapitated by a diagonal cut with a scalpel above the first leaf. The first droplet of sap was discarded to avoid collecting any wounding signals. The droplets after that were collected for 8 hours and stored on ice. The plants were also periodically recut when sap flow declined, with the first new droplet being discarded. The final sap collections were stored in -80°C until needed for experiments.

Xylem Sap Transfusion Assay

Xylem-enriched root sap was collected from a donor plant and introduced into a small cut along the pseudo-stem below the first true leaf of the receiver plants (B73 or Tx714) at the V4 stage (Constantino et al., 2013). Receiver plants were allowed to reach V4 stage and placed on their sides in trays lined with paper towels with the third true leaves taped down flat. One incision was made with a scalpel between the first and second leaves, and 10 μL H_2O or 1:1 diluted plant sap was added into each incision. For assays that transfuse 12-OPDA, KODA, or JA-Ile, the protocol for xylem sap transfusion assay was slightly modified. Xylem sap from untreated B73 was diluted 1:1 with either water for control or a concentration of the phytohormone to achieve the desired final concentrations. After 3 hours, plant leaves were inoculated with *C. graminicola*. Lesions were measured as an indication of plant resistance as described in the ISR assay section.

Quantification of Plant Sap Hormones and Metabolites

Xylem-enriched sap and fresh maize tissue hormones and metabolites were quantified using LC-MS/MS. For xylem-enriched sap, 90 μL of a 1:1 diluted sap solution was mixed with 10 μL of 5 μM internal standards (d-ABA ([2 H6](+)-cis,trans-ABA; [Olchem]), d-IAA ([2 H5] indole-3- acetic acid, Olchem) and d-JA (2,4,4-d3; acetyl-2,2-d2 JA; CDN Isotopes), and d-SA (d6-SA, Sigma)). For fresh tissue, hormones and metabolites were extracted via extraction, methylation, vapor-phase extraction, and liquid chromatography mass spectrometry-based quantification. Briefly, 0.1 g tissue was ground and mixed with 10 μL of 5 μM internal standards

(d-ABA ([2 H6](+)-cis,trans-ABA; [Olchem]), d-IAA ([2 H5] indole-3- acetic acid, Olchem) and d-JA (2,4,4-d3; acetyl-2,2-d2 JA; CDN Isotopes), and d-SA (d6-SA, Sigma)) and 500 µL phytohormone extraction buffer (1-propanol/water/HCl [2:1:0.002 vol/vol/vol]). The samples were agitated for 30 minutes at 4°C under darkness, and 500 µL dichloromethane was added to each sample. The samples were agitated again for 30 minutes at 4°C under darkness and then centrifuged at 13,000 × g for 5 minutes. The lower layer of each sample was transferred to a glass vial for evaporation under a nitrogen gas stream. They were resuspended in 150 µL methanol, transferred to a 1.5 mL microcentrifuge tube, and centrifuged at 14,000 × g for 2 minutes to pellet any debris. Supernatant (100uL) of each sample was transferred into autosampler vials to feed into the LC-MS/MS. The samples were transferred into autosampler vials with glass inserts, and a 15 µL aliquot was injected directly into an API 3200 LC-MS/MS on negative electrospray ionization mode with multiple reactions mentoring (MRM). The simultaneous detection of several hormones utilized methods by Muller and associates (2013) with modifications. The chromatography was performed with an Ascentis Express C-18 Column (3 cm × 2.1 mm, 2.7 µm). The mobile phase was set at 400 mL/minute consisting of Solution A (0.05% acetic acid in water) and Solution B (0.05% acetic acid in acetonitrile) with a gradient consisting of (time in minutes – %B): 0.3 – 1%, 2 – 45%, 5 – 100%, 8 – 100%, 9 – 1%, 11 – stop.

Hydroponic Growth Conditions for RNA-Seq

To study the effects of colonization by *T. virens* on maize roots, a hydroponic system as described by Djonovic et al., 2007 was used to prevent contamination and minimize mechanical

damage. Maize B73 seeds were surface sterilized with a 70% ethanol wash for 5 minutes, rinsed with sterile water, washed with 10% hydrogen peroxide for 2 hours, and finally rinsed with sterile water. The seeds were plated on Luria-Bertani (LB) (Difco Laboratories, Detroit) agar plates and incubated at 28°C in humidity chambers (boxes with wet paper towels lining the bottom with plates separated by glass petri plates). The seeds were checked every day for signs of bacterial or fungal contamination, and clean seeds were carefully moved to fresh LB plates. After 7 days, clean and uniformly germinated seeds were selected and placed in hydroponic units, which consist of wide mouth 16 oz mason jars (Ball wide mouth canning jar 16 oz) with a 125mL shaker clamp (Thermo Scientific™ MaxQ™ Shaker Universal Clamps, model 30153) supporting a plastic mesh stage, and filled with 200-225 mL of half strength Murashige and Skoog media with Gamborg vitamins (pH = 5.6, Sigma-Aldrich, St. Louis, MO, U.S.A). Each jar contained five seedlings positioned so that the tap roots of each seedling were threaded through the mesh and partly submerged in the MS media. The jars were then capped with the bottom of sterile plastic petri plates (100 x 15mm) and placed on shakers (50 rpm) at 25-27°C with a 16:8 light:dark photoperiod. Twenty-four hours before treatment, TvWT was cultured in 1L potato dextrose broth (PDB) in a Fernbach flask at a concentration of 1×10^5 spores/mL. After 24 hours, mycelia were collected by filtration with sterile nylon and washed with sterile water. One gram of fresh weight of the mycelial inoculum was added to the jars, after which a second mason jar (24oz Ball wide mouth canning jar) was placed atop the first jar and held in place with parafilm. This design allowed continued unimpeded shoot growth.

Tissue Harvesting

Plant root tissue was harvested 6, 30, and 54 hours after adding inoculation of the hydroponic jars with *T. virens*. The shoot tissue included all parts above the maize mesocotyl, while the root tissue included the radicle root and the lateral seminal roots. The roots were not rinsed with water when collected, especially at 30 and 54 hours when the *T. virens* tissue was inextricable from maize root tissue. At 6, 30, and 54 hours, the *T. virens* biomass not associated with maize roots was collected by filtering the MS medium through nylon filters and gently rinsing with sterile water. All the tissue samples collected were immediately flash frozen in liquid nitrogen and preserved at -80°C until RNA extraction.

RNA Extraction

Plant shoot and root tissue and fungal biomass were harvested and stored in -80°C. RNA was extracted from root and biomass of *T. virens* using a modified method for the Qiagen RNeasy Plant Mini Kit. The tissue samples were first ground in liquid nitrogen, and 1 μg of the tissue was aliquoted for RNA extraction. While the samples were still chilled in liquid nitrogen, 1 mL TRI reagent (Molecular Research Center Inc, Cat. TR118) was added to each sample and mixed well. The samples were then left at room temperature for 5 minutes before 200 μL chloroform was added and mixed well. The samples were stored at room temperature for 10 minutes before being centrifuged at 13,000 × g at 4°C for 15 minutes. The supernatant was transferred to a new tube containing 500 μL isopropanol. The samples were gently mixed and

stored at room temperature for 10 minutes prior to transfer into the Qiagen RNeasy spin columns. The samples were then processed following the manufacturer's instructions.

RNA-Sequencing

RNA was submitted to the Texas A&M AgriLife Genomics and Bioinformatics Service as total genomic RNA. For the 30 hr TvWT-treated maize, the submitted RNA comprised both maize and *T. virens* RNA. Preliminary sequencing determined that the ratio between maize:fungal RNA was roughly 2:8 maize to fungus in origin. The 6 hr samples were subsequently recombined in a 2:8 fungus:maize ratio to allow for sufficient coverage of maize genome. The cDNA libraries were created with the NEXTflex® Rapid Illumina Directional RNA-Seq Library Prep Kit. Sequencing parameters were 50 bp paired end reads, to a depth of 250 million reads, on a NovaSeq 6000.

RNA-Seq Data Analysis

Base-calling, quality checking, and removal of adaptor sequences was performed by the Texas A&M AgriLife Genomic and Bioinformatics Service as per their standard operating procedure. Raw, paired end, 50bp reads were then aligned back to the B73 reference genome sequence (AGPv4 release 38) via the TopHat2 v2.1.0 pipeline (Kim et al., 2013). Alignment rates varied depending on whether the samples were comprised of only maize RNA or a mixture of maize:fungal RNA. Uniquely aligned reads were counted with the HT-Seq 0.6.1 pipeline (Anders et al., 2015) using the Ensembl GCA_000005005.6 Zm-B73-REFERENCE-

GRAMENE-4.0 for annotation. The FPKM (Fragments Per Kilobase of exon model per Million mapped reads) values were determined using the Ballgown (v2.10.0) pipeline.

qRT-PCR Analysis

RNA-seq results were validated with real time quantitative PCR (qRT-PCR) using RNA extracted from samples not submitted for RNA-seq. The qRT-PCR reactions were set up using the Verso 1-step RT-qPCR Kit, SYBR Green, ROX (ThermoFisher Scientific) following manufacturer's procedure with 10 µL volume reactions and were run in the StepOne™ Real-Time PCR System (Applied Biosystems) using the following conditions: 48°C for 30 minutes, 95°C for 10 minutes, followed by 40 cycles of 95°C for 15 seconds, 54°C for 30 seconds, 72°C for 30 seconds. Melt curve conditions were 95°C for 15 seconds, 60°C for 1 minute, 95°C for 15 seconds. Relative expression was determined between control plants (untreated B73) and TvWT treatment using the $2^{-\Delta\Delta CT}$ method using maize *α-TUBULIN* as the reference gene (Czechowski et al., 2005; Xia et al., 2014). Expression of *LOX10* in B73 roots in response to treatment with TvWT, *Δsm1*, or *Δsir1* was performed in a similar manner, with all three treatments being compared to control plants.

GUS Staining

Transgenic *Arabidopsis* plants expressing β-glucuronidase (*GUS*) controlled by maize *LOX12* promoter (*pLOX12::GUS*) were developed and utilized to determine induction and localization of *LOX12* by *T. virens.* Two-week-old transgenic *Arabidopsis* plants were

germinated on solid MS medium, then transferred to new solid MS medium and inoculated 10 μL 10×10^3 WT *T.virens* spores on roots for 4 days. For high-resolution GUS staining, plant were incubated at 37℃ for 4 h in a solution containing 2 mM 5-bromo-4-chloro-4-3-indolyl glucuronide, 5 mM $K_3Fe(CN)_6$, 5 mM $K_4Fe(CN)_6$, 100 mM sodium phosphate buffer (pH 7.0), and 0.1% Triton X-100. After GUS staining, plants were observed and photographed under a dissecting microscope.

CHAPTER III

JA PRECURSOR, 12-OPDA, AND α-KETOL KODA, NOT JASMONIC ACID, ARE REQUIRED FOR INDUCED SYSTEMIC RESISTANCE (ISR) TRIGGERED BY *TRICHODERMA VIRENS* COLONIZATION OF MAIZE ROOTS

INTRODUCTION

Plants are sessile organisms and must constantly contend with various microorganisms that range from beneficial to harmful. Within the rhizosphere, plant roots interact with the ever-present microbes. Through these interactions, plants must discern beneficial microbes such as plant growth promoting rhizobacteria/fungi (PGPR/PGPF) from pathogens and respond accordingly by either dampening host defenses when colonized by beneficial microbes or heightening defenses against pathogens. For these reasons, plants have evolved sophisticated mechanisms to recognize friends from foes, and specifically tailor their responses (Heil and Bostock, 2002; Katagiri and Tsuda, 2010). One such response to beneficial microorganisms is heightened resistance to a wide range of pathogens termed induced systemic resistance (ISR). ISR is triggered following root colonization by PGPR and/or PGPF, and results in priming rapid and robust defense responses against future pathogen infections (Pieterse et al., 2014a). While the primed plants display strong systemic resistance upon infection, they display little to no discernable changes in their defense status in the absence of pathogens (Wang et al., 2005; Conrath et al., 2006; Pieterse et al., 2014b). The mechanisms by which these PGPR/PGPF enhance both plant growth and defenses remain a mystery, since allocation of resources to growth means loss of limited resources for defense (Havko et al., 2016).

The specific signaling mechanisms of ISR are much less understood compared to the pathogen-triggered systemic acquired resistance (SAR). While SAR relies mostly on salicylic acid (SA) signaling, SA itself is not the long-distance signal (Pieterse et al., 2014a). Several of the signals, which include azelaic acid (AzA), pipecolic acid (Pip), methyl salicylate (MeSA), glycerol-3-phosphate (G3P), and dehydroabietinal (DA), have been identified as the signals involved with SAR (Klessig et al., 2018; Shan and He, 2018). SAR signaling occurs with activation of Nonexpressor of *PR* genes 1 (NPR1), which is monomerized and moves from the cytoplasm to the nucleus, where it interacts with TGA family of transcriptional factors to promote expression of SA-responsive defense genes (Vlot et al., 2009; Pieterse et al., 2012). ISR induction is postulated to require jasmonic acid (JA) and ethylene (ET) in a SA-independent manner (Pieterse et al., 2014b). In *Arabidopsis*, several JA-signaling mutants, such as *jar1* and *jin1*, and ET-signaling mutants, such as *etr1* and *ein2*, lacked the capacity for ISR (Knoester et al., 1999; Korolev et al., 2008; Pozo et al., 2008). Furthermore, treating cucumber roots with the JA-biosynthesis inhibitor diethyldithiocarbamic acid (DIECA) blocked *T. asperellum*-triggered ISR (Shoresh et al., 2005). Tomato mutant *spr2* (*Suppressor of prosystemin-mediated responses 2*), impaired in wound-induced JA biosynthesis and defense signaling, could not establish *Funneliformis mosseae* (an arbuscular mycorrhiza)-primed disease resistance against *Alternaria solani* (Song et al., 2015). Interestingly, establishment of ISR also requires NPR1 activity, which occurs without induction of *PR* genes (Pieterse et al., 1998). Unlike during SAR, NPR1 activity relevant to ISR does not occur in the nucleus, but rather in the cytoplasm (Pieterse et al., 2012).

Trichoderma spp. are soil-borne filamentous fungi found ubiquitously around the world, including agriculturally relevant *T. virens* and *T. harzianum*. They have been studied extensively for their beneficial effects on plants, such as enhancing growth and development of shoots and

roots, directing attacks against harmful soil-borne pathogens through antibiosis and mycoparasitism, and triggering ISR (Yedidia et al., 1999; Howell et al., 2000; Lorito et al., 2010; Druzhinina et al., 2011; Hermosa et al., 2012). *T. virens*-induced ISR against diverse pathogens was demonstrated in several plant species including *Arabidopsis*, cotton, tomato, and maize (Djonovic et al., 2006; Djonovic et al., 2007; Contreras-Cornejo et al., 2011).

The signal communications between *Trichoderma* and host plants that result in ISR is poorly understood; however, a plethora of fungal molecules has been identified that trigger ISR in plants. Sm1, a small secreted cysteine-rich protein (SSCP) from *T. virens*, plays an integral role in ISR signaling. The deletion mutant *Δsm1* can no longer trigger ISR in either maize or cotton, while the mutants over-expressing *SM1* enhanced plant resistance against pathogens to levels greater than wild-type *T. virens* (Djonovic et al., 2006; Djonovic et al., 2007). Similarly, Epl1, a homolog of Sm1 in *T. atroviride,* induces ISR in tomato and improves resistance against necrotrophic pathogens such as *Alternaria solani*, *Pseudomonas syringae* pv. *tomato* (*Pst* DC3000), and *B. cinerea* (Salas-Marina et al., 2015). *T. virens* also produces several other SSCPs, some of which can be characterized as negative regulators of ISR. For example, deletion of several SSCPs (protein IDs 111486, 92810, 71692, or 77560) greatly enhanced ISR of maize against *Cochliobolus heterostrophus,* a necrotrophic pathogen and causal agent of Southern corn leaf blight (Lamdan et al., 2015). The specific mechanisms of SSCPs in regulating ISR remain unknown. Recent evidence suggests that one function of Sm1 is to regulate synthesis of oxylipins with signaling properties (Constantino et al., 2013).

Oxylipins are a large group of oxidized lipid signals that include, among others, jasmonates, which regulate many aspects of plant physiology, such as growth and development, defense responses to pathogens and herbivores and abiotic stresses (Borrego and Kolomiets,

2016). They are mainly produced through enzymatic oxygenation of polyunsaturated fatty acids, linoleic acid (C18:2), and linolenic acid (C18:3) at carbon position 9 or 13, by 9- or 13-lipoxygenases (LOX), respectively (Feussner and Wasternack, 2002; Andreou et al., 2009). These products are fed into the seven sub-branches, which include the allene oxide synthase (AOS) pathway that produces JA and the hydroperoxide lyase (HPL) pathway, which converts 13-hydroperoxy octadecatrienoic acid (13-HPOTE) to several C6 compounds called green leaf volatiles (GLVs) in maize (Matsui, 2006; Christensen et al., 2013). GLVs attract parasitoid wasps in response to herbivory (Whitman and Eller, 1990; Christensen et al., 2013), regulate plant-plant communications (Engelberth et al., 2004), and enhance JA response against herbivory (Farag and Pare, 2002).

JA is produced by 13-LOX action through the 13-AOS branch, while the products of 9-AOS include death acids (Christensen et al., 2015) and 9-oxylipin ketols including 9-hydroxy-10-oxo-12(Z), 15(Z)-octadecadienoic acid (KODA), the function of which is not clearly established (Vick and Zimmerman, 1984). JA biosynthesis begins in plastids, where 13-LOX activity converts linolenic acid (18:3) to 13-hydroperoxy octadecatrienoic acid (13-HPOT) (Borrego and Kolomiets, 2016). Allene oxide synthase (AOS) activity converts 13-HPOT to 12, 13-epoxy octadecatrienoic acid (12, 13-EOT), which is then converted by allene oxide cyclase (AOC) to 12-oxo-phytodienoic acid (12-OPDA). 12-OPDA moves to the peroxisome, where it is catalyzed to 3-oxo-2-(2′(Z)-pentenyl)-cyclopentane-1 octanoic acid (OPC-8:0) by OPDA reductase (OPR). The OPC-8:0 undergoes three rounds of β-oxidation by acyl-coenzyme A oxidase (ACX), multi-functional protein (MFP), and ketoacyl-coenzyme A thiolase (KAT), resulting in JA. Finally, JAR1 (jasmonate resistant 1) activity in the cytoplasm conjugates isoleucine to JA to produce JA-Ile, the biologically active jasmonate required for JA signaling.

JA signaling occurs when JA-Ile binds to coronatine insensitive 1 (COI1), an F-box protein and part of the E3 ubiquitin-ligase Skip-Cullin-F-box complex (SCF^{COI1}) (Song et al., 2013). This activates the SCF complex, which targets Jasmonate-ZIM domain (JAZ) repressor proteins, transcriptional repressors of JA signaling, for degradation via proteasome and allows transcription of various JA-responsive genes such as MYC and WRKY transcription factors. Undoubtedly, the best characterized oxylipin in terms of relevance to ISR is JA.

In addition to jasmonates, plants produce an estimated 650 oxylipins, the functions of which are largely unknown (Borrego and Kolomiets, 2016). Silencing bean *PvLOX2*, a 9-LOX not involved with JA biosynthesis, resulted in the abolishment of mycorrhizae-induced resistance against the foliar pathogen *Sclerotinia sclerotiorum* (Mora-Romero et al., 2015a; Mora-Romero et al., 2015b). Additionally, the negative role of 9-LOX activity in regulating ISR has recently been demonstrated with maize LOX3, a non-JA-producing LOX. The LOX3-deficient mutants demonstrated increased resistance against various seed, stalk, root, and foliar pathogens (Gao et al., 2007; Isakeit et al., 2007) due to constitutive production of unknown systemic signals derived from the roots (Constantino et al., 2013). Expression of *LOX3* has been observed exclusively in maize roots, with expression being suppressed by *T. virens* in a Sm1-dependent manner (Constantino et al., 2013). Roots of *lox3* mutants over-accumulated defense hormones JA, ET, and SA, and over-expressed many defense genes involved with biosynthesis and signaling of JA, ET, SA, and green leaf volatiles (GLV) (Gao et al., 2008). Furthermore, stem transfusion of xylem sap derived from *lox3-4* roots to wild-type maize confers systemic resistance against *Colletotrichum graminicola* infection, proving that systemic resistance signal(s) originate from the roots and travel systemically along the xylem (Constantino et al., 2013). Because LOX3-deficient mutants over-express several JA biosynthesis genes including

LOX10, in this study we have tested our central hypothesis that constitutively active ISR in the *lox3* mutant is due to overexpression of *LOX10* and overproduction of JA or other jasmonates. Maize knock-out *lox10* mutants are GLV-deficient and accumulated significantly lower wound-induced levels of 12-OPDA and JA in leaves (Christensen et al., 2013).

In support of this hypothesis, we showed that LOX10 function is indeed required to establish proper ISR, as instead of increased resistance to leaf pathogens, colonization of *lox10* mutant roots by *T. virens* resulted in increased susceptibility. Oxylipin and hormone profiling of xylem sap from B73 wild-type and *lox3* and *lox10* mutants treated with either wild-type or ISR-perturbed *T. virens* mutants along with pharmacological treatments indicated that 12-OPDA produced by LOX10 and KODA produced by an unknown 9-LOX are major ISR long-distance signals. Unexpectedly, the JA-deficient *opr7opr8* double mutant displayed normal ISR response induced by *T. virens*, suggesting that JA is not required for ISR signaling in maize. Moreover, analyses of the transcriptome response of maize roots to colonization by *T. virens* indicated that while the genes for OPDA synthesis are induced by this symbiont, the genes for conversion of 12-OPDA to JA-Ile were not altered. Taken together, our results present evidence that the JA precursor, 12-OPDA, and KODA, but not JA, are required for ISR induction in maize.

RESULTS

T. virens induces *LOX10* expression at the early stages of the interaction

To assess the involvement of LOX10 in maize-*T. virens* interactions, B73 maize seedlings were grown in hydroponic conditions and subsequently treated with WT, *Δsm1*, or *Δsir1* mutant strain, formerly designated as *Δ77560* (Lamdan et al., 2015). These three strains are contrasted in their ability to induce ISR in maize. Compared to wild-type *T. virens* (TvWT), *Δsm1* is unable to induce ISR (Djonovic et al., 2007), whereas *Δsir1* induces exceptionally strong ISR to leaf fungal pathogens including *Cochliobolus heterostrophus*, a necrotrophic pathogen and causal agent of Southern corn leaf blight (Lamdan et al., 2015). Treatment with TvWT strain resulted in upregulation of *LOX10* expression as early as 2, 3, and 6 hours ranging between 3- and 4- fold induction compared to untreated controls (Fig. 1A). This effect was diminished by 9 hours, suggesting that *LOX10* induction is transient. Interestingly, *Δsir1* induced *LOX10* 1 hour earlier than TvWT, with a peak at 3 hours. In contrast, *Δsm1* strain was unable to induce LOX10 transcript accumulation of *LOX10* at all time points, suggesting that *LOX10* expression in the host is dependent on the functional Sm1 protein in the fungus. Together, these results suggested that *LOX10* expression was induced at both transcript and protein level and that induction is positively regulated by ISR-promoting secreted protein Sm1, but negatively by another secreted protein Sir1. To determine whether the more robust induction of LOX10 expression by *Δsir1* was due to altered expression of *SM1*, transcript accumulation of *SM1* and *SIR1* was measured in TvWT and both mutants. Expression of *SM1* was 3-fold greater in *Δsir1* mutant compared to TvWT, whereas *SIR1* expression in *Δsm1* was not altered (Fig. 1C). These results indicate that

the most likely reason for *Δsir1* being more effective in induction of *LOX10* is due to increased expression of *SM1* in this mutant and confirming that *LOX10* is indeed one host target positively regulated by Sm1 peptide to promote ISR.

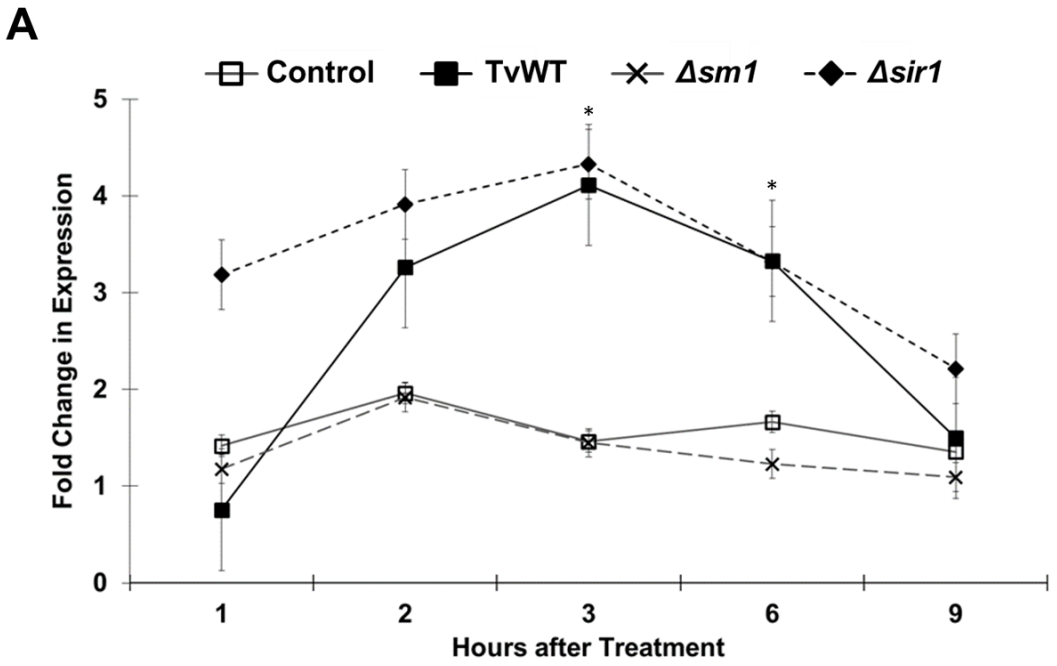

FIGURE 1. *LOX10* expression is induced by *T. virens* in a Sm1-dependent manner.

(A) Expression of *LOX10* via qPCR was determined in B73 seedling roots after treatment with *T. virens* (WT, ISR-deficient strain *Δsm1*, or ISR-enhancing strain *Δsir1*) at 1, 2, 3, 6, and 9 hours after treatment compared to untreated control plants. Relative expression was calculated from cycle threshold values using the $2^{-\Delta\Delta Ct}$ method. Values represent means ± standard deviation SD (n=3) relative to control plants and were normalized to transcript levels of *α-Tubulin* (*α-TUB*). Statistical significance (* represents $p < 0.05$) was determined with Tukey's HSD test compared to control.

(B) Expression of *SM1* and *SIR1* via qPCR was determined in *T. virens* hyphal tissue grown in MS media for 6 hours. Expression of *SM1* in *Δsm1* mutant and expression of *SIR1* in *Δsir1* mutant were not tested, as the mutants were previously shown to not express the respective genes. Relative expression was calculated from cycle threshold values using the $2^{-\Delta\Delta Ct}$ method. Values represent means ± standard deviation SD (n=3) relative to control plants and were normalized to transcript levels of *β-Tubulin* (*β-TUB*). Statistical significance (* represents $p < 0.05$) was determined with Tukey's HSD test.

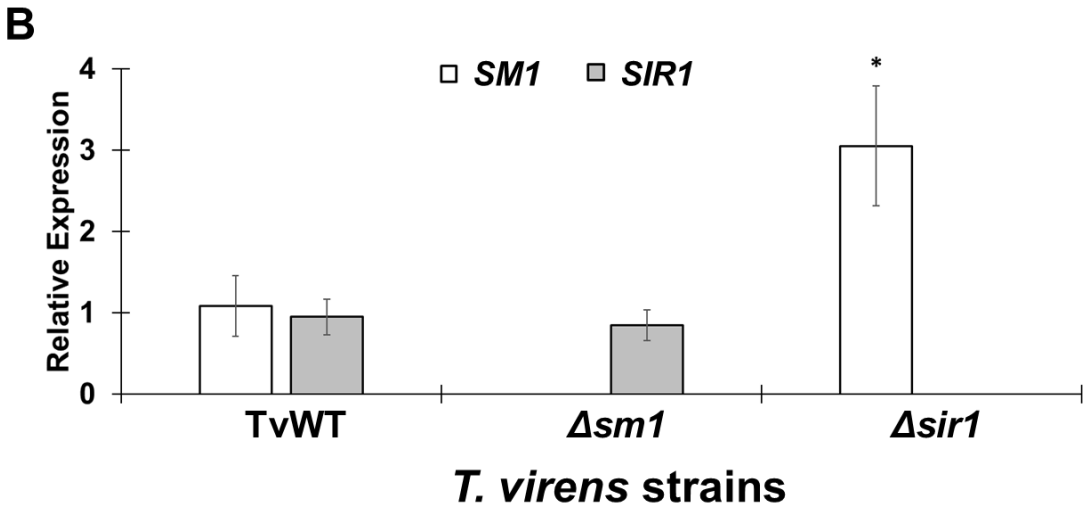

FIGURE 1. Continued

LOX10 is required for *T. virens*-mediated ISR

To further define the role of LOX10 in regulating maize-*T. virens* interactions, the B73 inbred line and near-isogenic *lox10* mutant alleles were treated with TvWT. As expected, TvWT-treated B73 displayed a characteristic ISR response, as evidenced by significantly reduced lesion areas and chlorosis caused by *C. graminicola* (Fig. 2A and 2B). As previously reported, both untreated *lox10-3* and *lox10-2* mutant alleles were significantly more resistant to *C. graminicola* (Christensen, 2011). Surprisingly, instead of ISR observed in B73, *T. virens* treatment of both mutant alleles resulted in significantly increased susceptibility, which we termed induced systemic susceptibility (ISS) (Fig. 2C and 2D). To test if the ISS phenotype can be observed in a different maize inbred line, W438 inbred line and *lox10-3* mutant in the W438 genetic background were treated with TvWT and challenged with *C. graminicola*. The results reflected those observed in B73; specifically, untreated *lox10-3* was more resistant than untreated W438, but TvWT-treated *lox10-3* became more susceptible (Fig. 2E and 2F). TvWT-treated *lox10-3* plants still had increased shoot and root dry weight compared to untreated plants, inferring that *T. virens* plant growth and development promotion occurred independently from ISR promotion (Fig. 3). To test whether the overexpression of *LOX10* was responsible for constitutive ISR in *lox3* mutant, we created *lox3lox10* double mutant at the BC7 stage. ISR response between B73 and single/double mutants was compared. The untreated double mutant was more susceptible compared to either single mutant, but still more resistant compared to B73, suggesting that deleting *LOX10* in *lox3* mutant only partially reduced the constitutive ISR phenotype of *lox3* mutant (Fig. 4). The striking phenotype of TvWT-treated *lox3lox10* was a total loss of ISS

phenotype observed in TvWT-treated *lox10-3*, suggesting that ISS in *lox10* mutants was completely dependent on LOX3 function.

ISR is effective against a broad range of pathogens. Because *C. graminicola* is a hemibiotroph, we tested whether LOX10 is required for ISR against a pathogen with a reported necrotrophic lifestyle. For this, B73 and both *lox10* mutant alleles were treated with TvWT and infected with *C. heterostrophus*, a necrotrophic causal agent of Southern corn leaf blight. Similar to *C. graminicola*, disease severity caused by *C. heterostrophus* was reduced in *T. virens*-colonized B73 and untreated *lox10-3* and *lox10-2* (Fig. 5A, 5B, 5C, and 5D). Furthermore, TvWT-treated *lox10-3* and *lox10-2* mutants became more susceptible to *C. heterostrophus* infection, as evidenced by significantly larger lesions compared to untreated controls. Increased susceptibility phenotype was also observed in the W438 background, as TvWT-treated *lox10-3* mutant in the W438 genetic background displayed larger lesions and greater chlorosis compared to untreated mutant (Fig. 5E and 5F). These results suggest that LOX10 plays an essential positive regulatory role in *T. virens*-triggered ISR against pathogens regardless of their lifestyle.

To test the role of the fungal peptide regulators of ISR, Sm1 and Sir1, in the ISS phenotype of *lox10-3* mutants, B73 and *lox10-3* mutants were treated with TvWT, *Δsm1*, or *Δsir1* and subsequently challenged with *C. graminicola*. While B73 exhibited ISR in response to TvWT, there was no increased resistance observed with *Δsm1* treatment (Fig. 6), consistent with previous reports (Djonovic et al., 2007). Root colonization by *Δsir1* conferred enhanced resistance against *C. graminicola* in WT maize to greater levels than TvWT, supporting a previous report of enhanced ISR by *Δsir1* against *C. heterostrophus* (Lamdan et al., 2015). While both TvWT and *Δsm1* treatments resulted in increased susceptibility in *lox10-3*, *Δsir1* had no such effect. Because lesions on Sm1-treated *lox10-3* were moderately but significantly smaller

than those on TvWT-treated *lox10-3*, we concluded that a functional Sm1 is partially responsible for the ISS phenotype observed. The loss of ISS triggered by *Δsir1*, on the other hand, suggests that functional Sir1 in *T. virens* is the primary elicitor of ISS in *lox10-3* mutant.

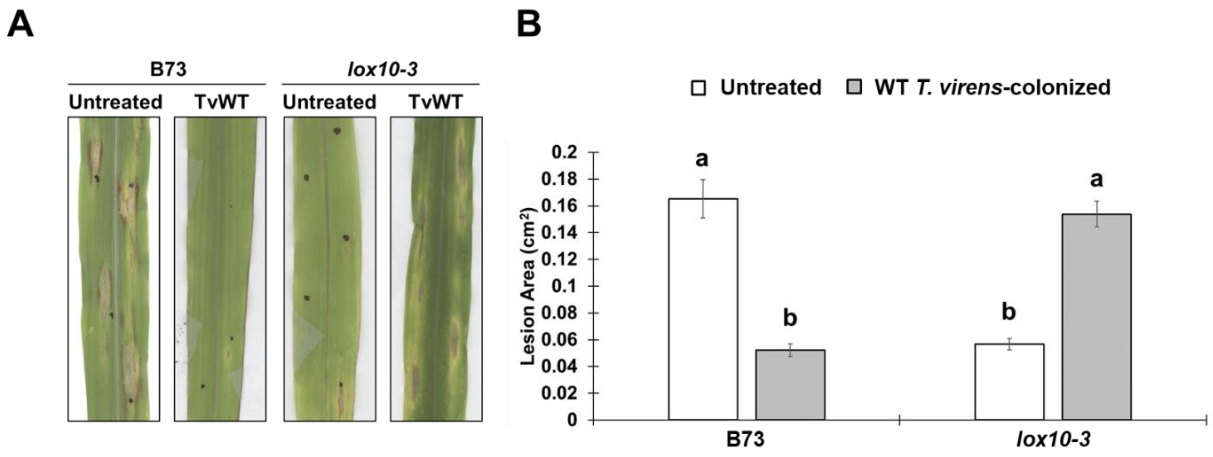

FIGURE 2. *LOX10* acts as a positive regulator of *T. virens*-triggered ISR against hemibiotrophic pathogen *C. graminicola*.

(A) Lesions developed on 3rd leaves of untreated or TvWT-treated B73 inbred line and *lox10-3* mutant plants infected with *C. graminicola*.

(B) Measurements of lesion area caused by *C. graminicola* infection on leaves of untreated and TvWT-treated B73 and *lox10-3* mutant plants. Values represent means ± standard deviation SD (n=5), with letters indicating significant differences between treatments (Tukey's HSD test, $p < 0.05$).

(C) Lesions developed on 3rd leaves of untreated or TvWT-treated B73 inbred line and *lox10-2* mutant plants infected with *C. graminicola*.

(D) Measurements of lesion area caused by *C. graminicola* infection on leaves of untreated and TvWT-treated B73 and *lox10-2* mutant plants. Values represent means ± standard deviation SD (n=5), with letters indicating significant differences between treatments (Tukey's HSD test, $p < 0.05$).

(E) Lesions developed on 3rd leaves of untreated or TvWT-treated W438 inbred line and *lox10-3* mutant plants infected with *C. graminicola*.

(F) Measurements of lesion area caused by *C. graminicola* infection on leaves of untreated and TvWT-treated W438 and *lox10-3* mutant plants. Values represent means ± standard deviation SD (n=5), with letters indicating significant differences between treatments (Tukey's HSD test, $p < 0.05$).

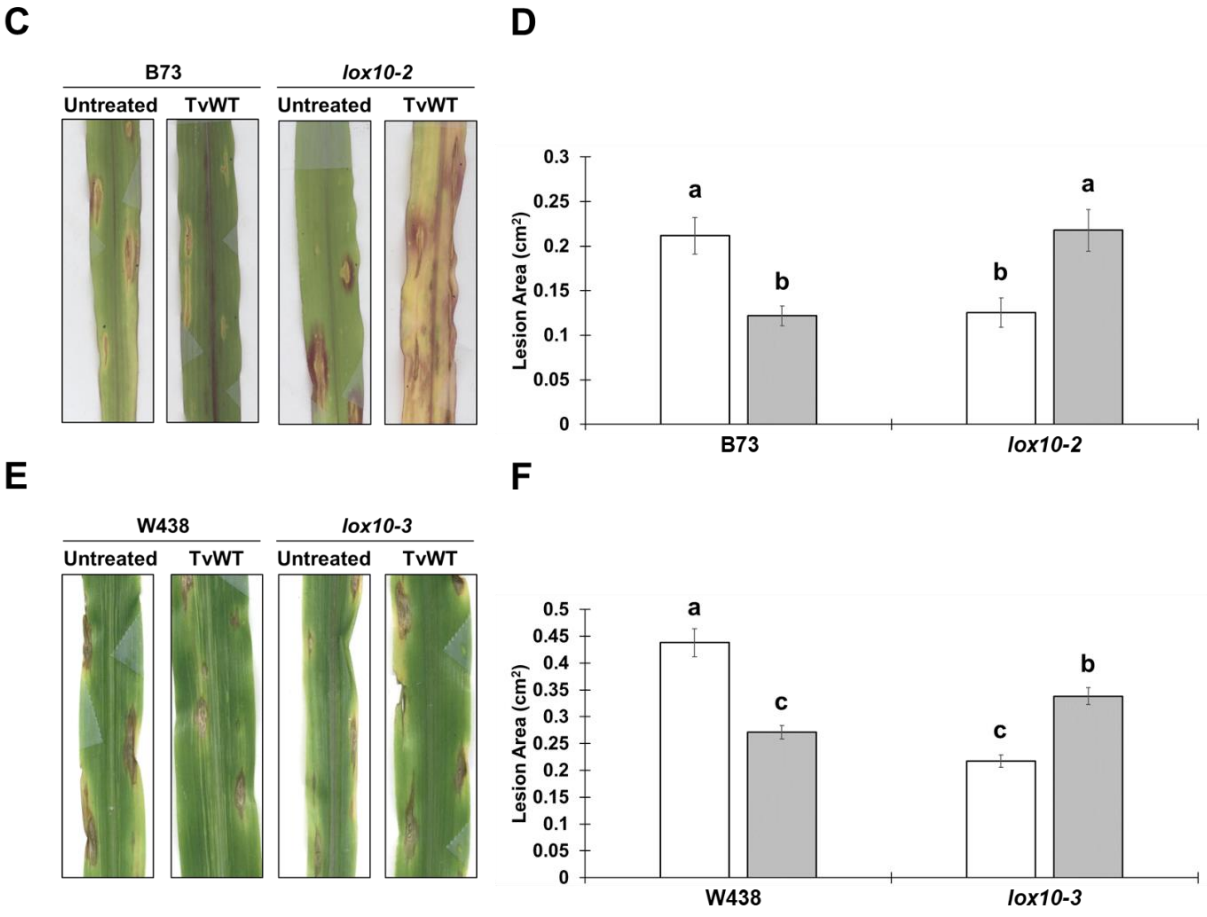

FIGURE 2. Continued

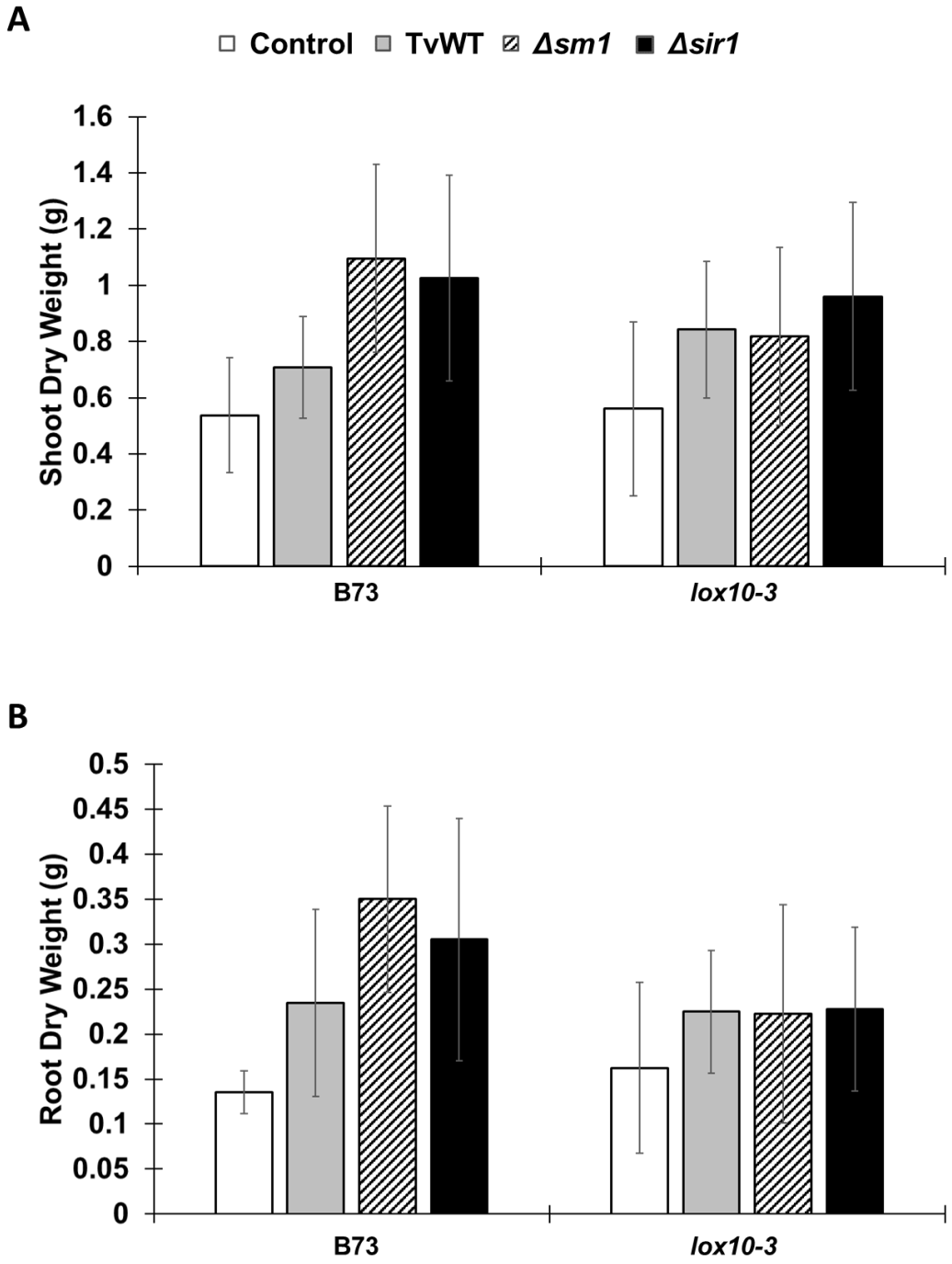

FIGURE 3. TvWT promotes plant growth and development independently from ISR. Measurements of average shoot and root tissue dry weight of untreated and TvWT-treated B73 and *lox10-3* plants. Values represent means ± standard deviation SD (n=5), with letters indicating significant differences between treatments (Tukey's HSD test, $p < 0.05$).

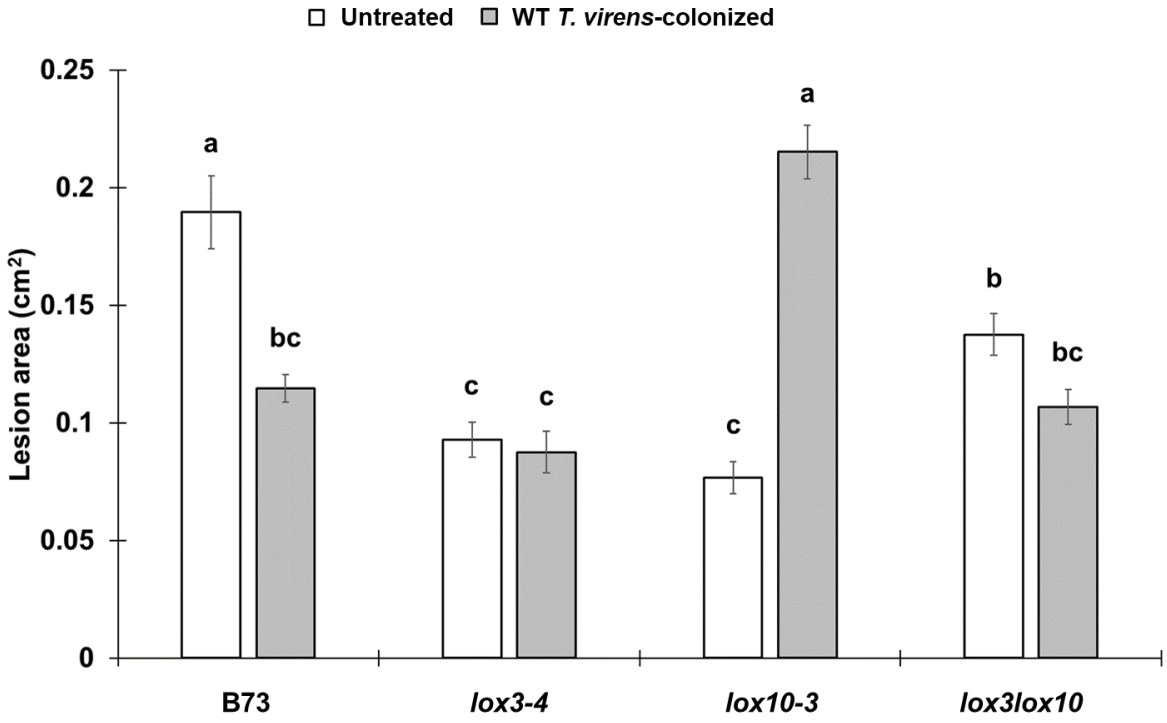

FIGURE 4. Loss of LOX3 function in *lox10-3* results in loss of ISS phenotype.
Measurements of lesion area caused by *C. graminicola* infection on leaves of untreated and TvWT-treated B73, *lox3-4*, *lox10-3*, and *lox3lox10* double mutant plants. Values represent means ± standard deviation SD (n=5), with letters indicating significant differences between treatments (Tukey's HSD test, $p < 0.05$).

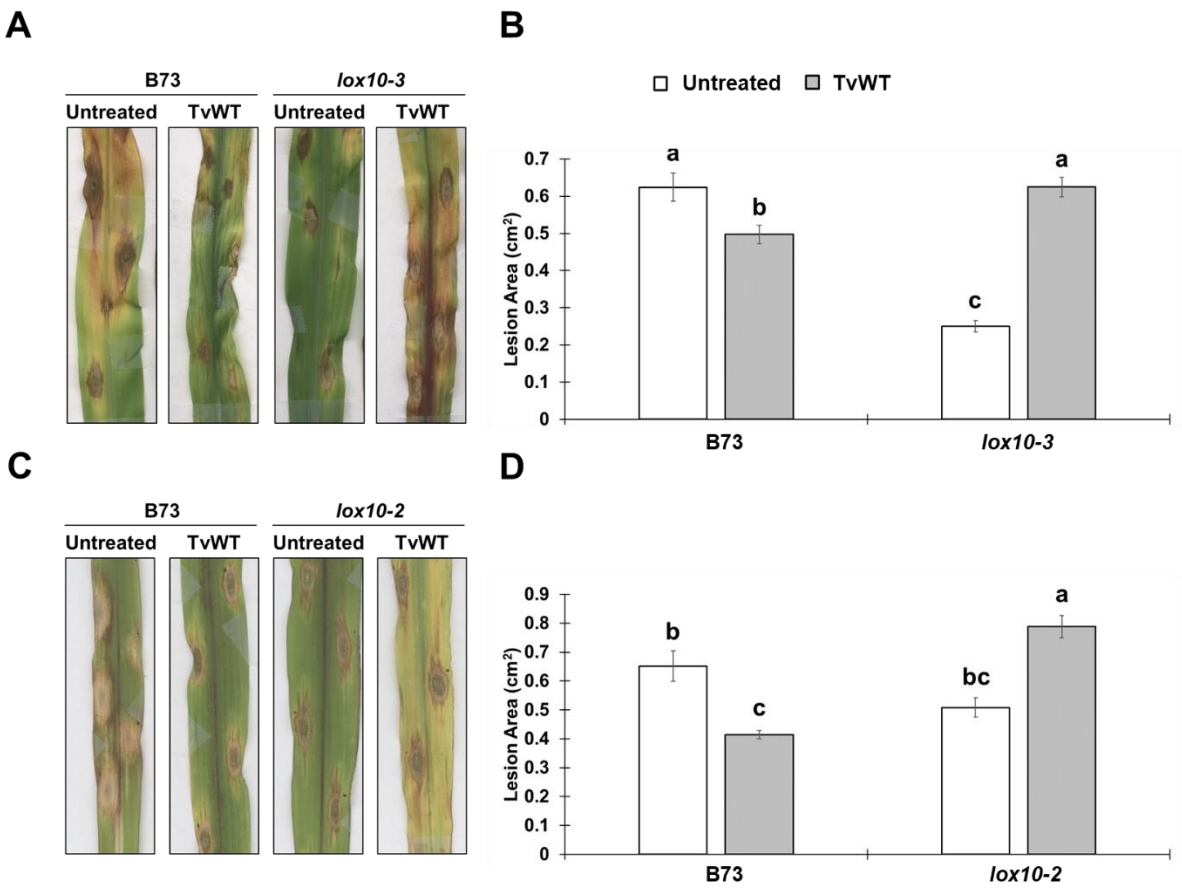

FIGURE 5. *LOX10* acts as a positive regulator of *T. virens*-triggered ISR against necrotrophic pathogen *Cochliobolus heterostrophus*.

(A) Lesions developed on 3rd leaves of untreated or TvWT-treated B73 inbred line and *lox10-3* mutant plants infected with *C. heterostrophus*.

(B) Measurements of lesion area caused by *C. heterostrophus* infection on leaves of untreated and TvWT-treated B73 and *lox10-3* mutant plants. Values represent means ± standard deviation SD (n=5), with letters indicating significant differences between treatments (Tukey's HSD test, $p < 0.05$).

(C) Lesions developed on 3rd leaves of untreated or TvWT-treated B73 inbred line and *lox10-2* mutant plants infected with *C. heterostrophus*.

(D) Measurements of lesion area caused by *C. heterostrophus* infection on leaves of untreated and TvWT-treated B73 and *lox10-2* mutant plants. Values represent means ± standard deviation SD (n=5), with letters indicating significant differences between treatments (Tukey's HSD test, $p < 0.05$).

(E) Lesions developed on 3rd leaves of untreated or TvWT-treated W438 inbred line and *lox10-3* mutant plants infected with *C. heterostrophus*.

(F) Measurements of lesion area caused by *C. heterostrophus* infection on leaves of untreated and TvWT-treated W438 and *lox10-3* mutant plants. Values represent means ± standard deviation SD (n=5), with letters indicating significant differences between treatments (Tukey's HSD test, $p < 0.05$).

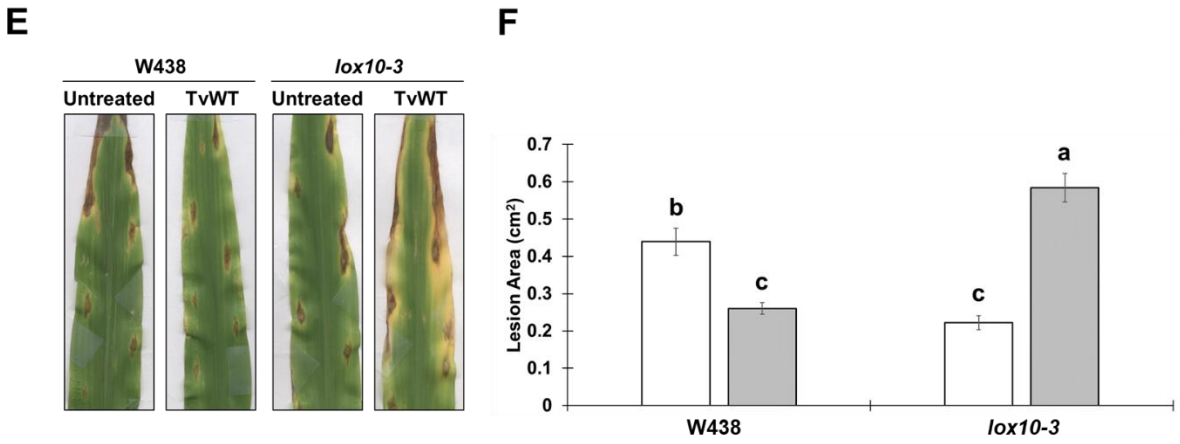

FIGURE 5. Continued

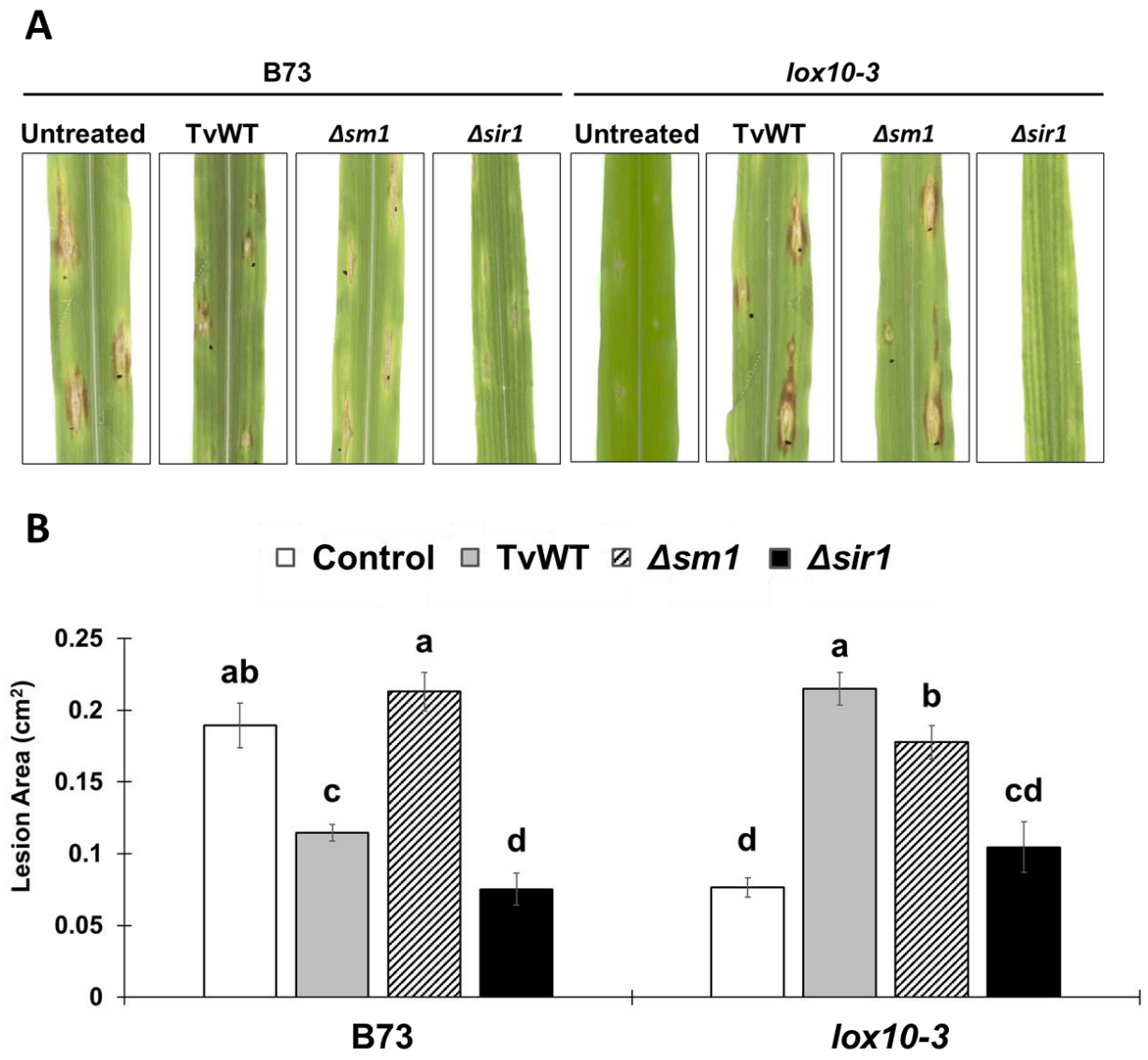

FIGURE 6. *T. virens* role of SSCPs Sm1 and Sir1 in regulating *T. virens*-triggered ISR.

(A) Lesions developed on 3rd leaves of untreated or TvWT-, *Δsm1*-, and *Δsir1*-treated B73 and *lox10-3* mutants plants infected with *C. graminicola*.

(B) Measurements of lesion area caused by *C. graminicola* infection on untreated or TvWT-, *Δsm1*-, and *Δsir1*-treated B73 and *lox10-3* leaves. Infected leaves were scanned and measured using ImageJ software to determine mean lesion area. Values represent means ± standard deviation SD (n=5), with letters indicating significant differences between treatments (Tukey's HSD test, $p < 0.05$).

Metabolite profiling of xylem sap identifies 12-OPDA and KODA as potential ISR signals

A previous study of *lox3* mutant revealed that the mutant constitutive systemic resistance could be conferred using xylem sap collected from the mutant (Constantino et al., 2013). To determine whether *lox10* mutant sap is altered in its ability to enhance resistance, we have taken advantage of the sap transfusion methodology developed by Constantino et al., 2013 to circumvent the inability to graft monocots. Xylem sap was collected from untreated or TvWT-treated B73, *lox3-4*, and *lox10-3*. 10µL aliquots of the diluted sap were transfused into untreated B73 receiver plants prior to infection with *C. graminicola*. Corroborating efficacy of the transfusion method, plants treated with sap collected from TvWT-treated B73 showed enhanced systemic resistance, as lesions were significantly smaller compared to those that developed on control plants treated with sap from untreated B73 (Fig. 7A). Importantly, increase in resistance due to TvWT-treated B73 sap treatment resembles TvWT-triggered ISR in B73. Transfusion with xylem sap from untreated or TvWT-treated *lox3-4* plants also resulted in significantly enhanced resistance, consistent with previous study (Constantino et al., 2013). While transfusion with sap from untreated *lox10-3* led to enhanced resistance, sap from TvWT-treated *lox10-3* resulted in lack of ISR compared to untreated B73 sap, but increased susceptibility compared to untreated *lox10-3* sap, mirroring the ISS phenotype of TvWT-treated *lox10-3* mutants (Fig. 2 and 5). In order to better understand how sap of untreated *lox10-3* could confer resistance to receiver plants, the sap samples were analyzed by liquid chromatography tandem mass spectrometry (LC-MS/MS), which revealed significantly higher levels of 10-oxo-11-phytoenoic acid (10-OPEA) in sap of untreated *lox3-4* and *lox10-3* mutants (Fig. 8). The 9-LOX-derived oxylipin was found to have antimicrobial and anti-herbivory properties and accumulated locally in response to fungal

and insect attack (Christensen et al., 2016), and exogenous application of 10-OPEA led to programmed cell death (Christensen et al., 2015). The sap transfusion results were not restricted to B73, as Tx714 inbred line also displayed phenotypes that resemble those seen in B73 (Fig. 7B). These results confirm that the ISR signal(s) are root-derived, transported along the xylem to above-ground organs to confer systemic resistance, and require functional LOX10. Interestingly, xylem sap from TvWT-treated *lox10-3* conferred ISS to *lox10-3* receiver plants, suggesting that sap from TvWT-treated *lox10-3* contains as-yet unknown signal(s) responsible for ISS (Fig. 7C). Unfortunately, among the metabolites measured in the xylem sap (Supplemental Table 1), none unambiguously correlated with increased susceptibility.

To determine whether xylem sap carries ISR signals from plants colonized by *Δsm1* or *Δsir1*, saps were collected from *Δsm1*- and *Δsir1*-treated B73, *lox3-4*, and *lox10-3* plants and transfused into B73 receiver plants. The results showed that sap from *Δsir1*-treated B73 and *Δsir1*-treated *lox10-3* conferred resistance to *C. graminicola*; however, sap from *Δsir1*-treated *lox3-4* and all *Δsm1*-treated plants did not (Fig. 9). These results, together with results described in Fig. 7, pointed out that TvWT- and *Δsir1*-treated B73 and untreated and TvWT-treated *lox3-4* sap samples were enriched with ISR positive signal and therefore, were ideal for metabolite profiling in our search for ISR long-distance signal. This analysis also identified saps lacking ISR activity, which include untreated and *Δsm1*-treated B73 and *Δsm1*- and *Δsir1*-treated *lox3-4*.

The collected xylem saps were analyzed by LC-MS/MS using quantification standards for approximately 60 diverse oxylipins and several phytohormones (Table 1). To reduce the number of ISR-relevant candidate metabolites, the following criteria were used for selection of an ISR signal candidate. This molecule(s) had to accumulate at: **1)** increased levels in sap from TvWT- and *Δsir1*-treated B73 and untreated and TvWT-treated *lox3-4*, **2)** reduced levels in

untreated and *Δsm1*-treated B73 and *Δsm1*- and *Δsir1*-treated *lox3-4*, and **3)** statistically lower levels in *lox10-3* plants regardless of treatment compared to TvWT-treated B73. Out of the oxylipins and phytohormones screened, only 12-OPDA and KODA, a 9-LOX- and 9-AOS-derived α-ketol (Vick and Zimmerman, 1984), met all three criteria. Though the function of KODA remains obscure, these data suggest that it plays a role in ISR. Specifically, both were enriched in saps with potent ISR activity, which include TvWT- and *Δsir1*-treated B73 and untreated and TvWT-treated *lox3-4* (Fig. 10A and 10B). Xylem sap from plants not displaying ISR, which consist of untreated B73, *Δsm1*-treated B73, and *Δsm1*- and *Δsir1*-treated *lox3-4*, accumulated 12-OPDA and KODA at much lower levels. Surprisingly, neither JA nor JA-Ile met the three criteria, as their levels did not correlate with sap ISR activity. Specifically, JA levels were significantly elevated in B73 when treated with all three strains of *T. virens*, including *Δsm1*, which is unable to induce ISR (Fig. 10C). Interestingly, JA-Ile levels were not elevated in TvWT-treated B73 and untreated *lox3-4* (Fig. 10D). Not surprisingly, low levels of 12-OPDA, KODA, JA, and JA-Ile were detected in all *lox10-3* plants regardless of treatment (Fig. 10), consistent with previous reports that *lox10* mutants were unable to accumulate both compounds (Christensen et al., 2013). Because traumatic acid synthesis requires functional LOX10 in leaves (Christensen et al., 2013), this molecule was considered a potential ISR signal; however, traumatic acid content was reduced in B73 treated with all *T. virens* strains (Fig. 10E). Lastly, SA levels had no patterns that correlated with resistance, and levels were not greatly altered between the different treatments (Fig. 10F). This data suggests that out of all the LOX10 products, only 12-OPDA appears to be relevant for ISR. Levels of KODA, a 9-LOX product, appears to be influenced by, but not directly produced by LOX10.

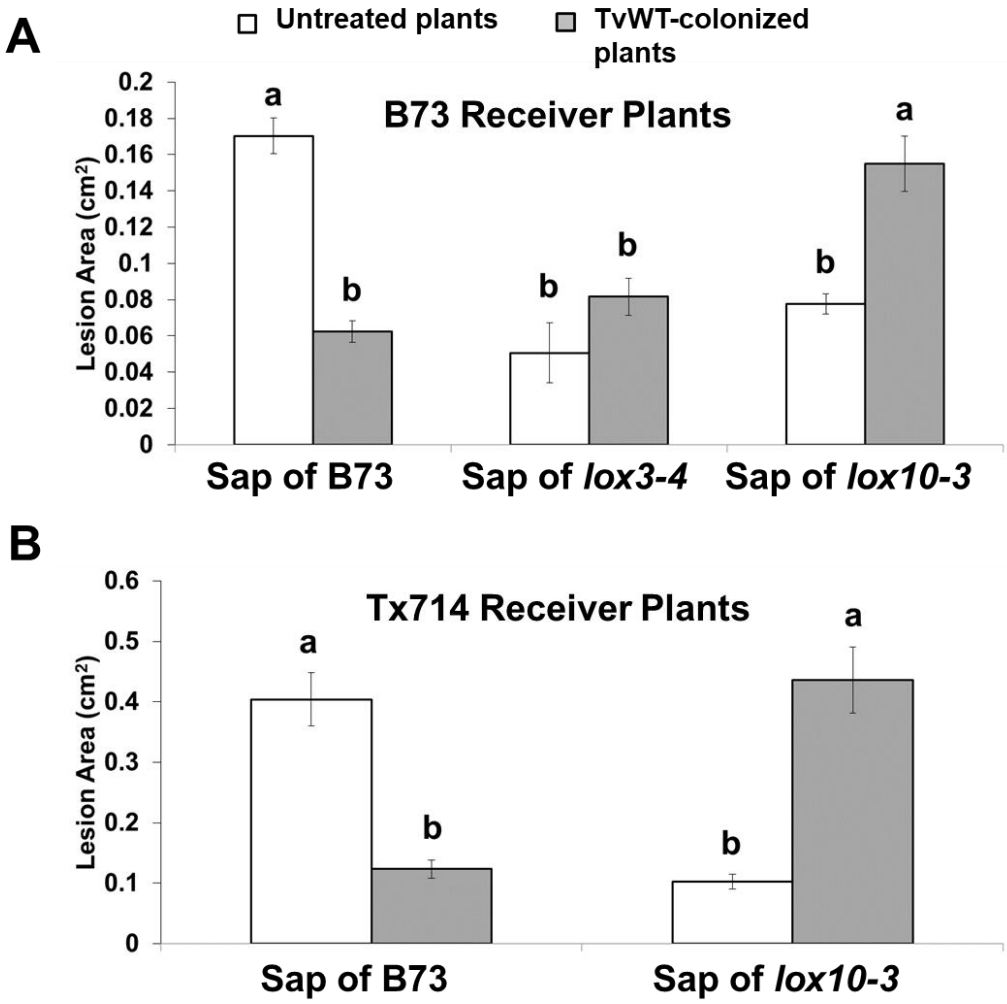

FIGURE 7. Xylem-derived sap from *T. virens*-treated plants contains ISR signals.

(A) Measurements of lesion area caused by *C. graminicola* infection on B73 inbred line receiver plants transfused with xylem sap from untreated or TvWT-treated B73, *lox3-4*, and *lox10-3* plants. Values represent means ± standard deviation SD (n=5), with letters indicating significant differences between treatments (Tukey's HSD test, $p < 0.05$).

(B) Measurements of lesion area caused by *C. graminicola* infection on Tx714 inbred line receiver plants transfused with xylem sap from untreated or TvWT-treated B73 and *lox10-3* plants. Values represent means ± standard deviation SD (n=5), with letters indicating significant differences between treatments (Tukey's HSD test, $p < 0.05$).

(C) Measurements of lesion area caused by *C. graminicola* infection on *lox10-3* receiver plants transfused with xylem sap from untreated or TvWT-treated B73, *lox3-4*, and *lox10-3* plants. Values represent means ± standard deviation SD (n=5), with letters indicating significant differences between treatments (Tukey's HSD test, $p < 0.05$).

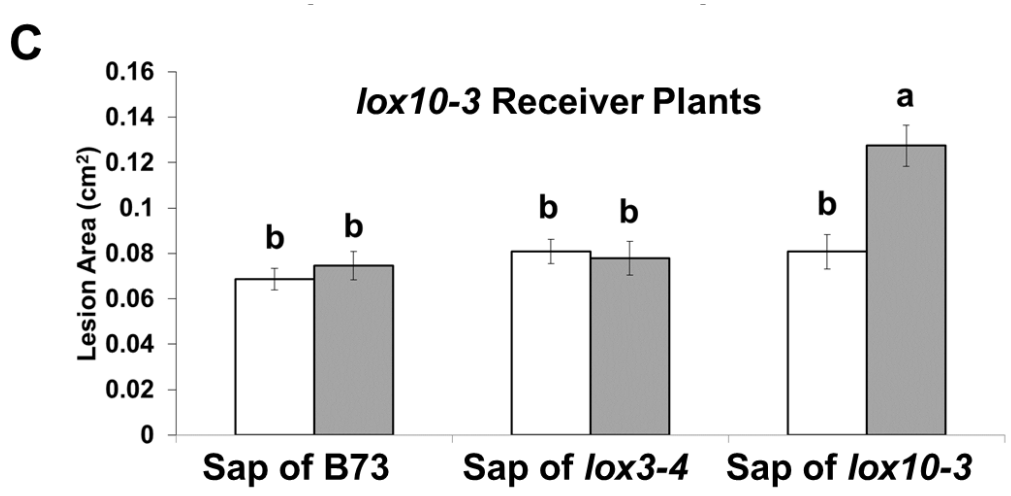

Figure 7. Continued

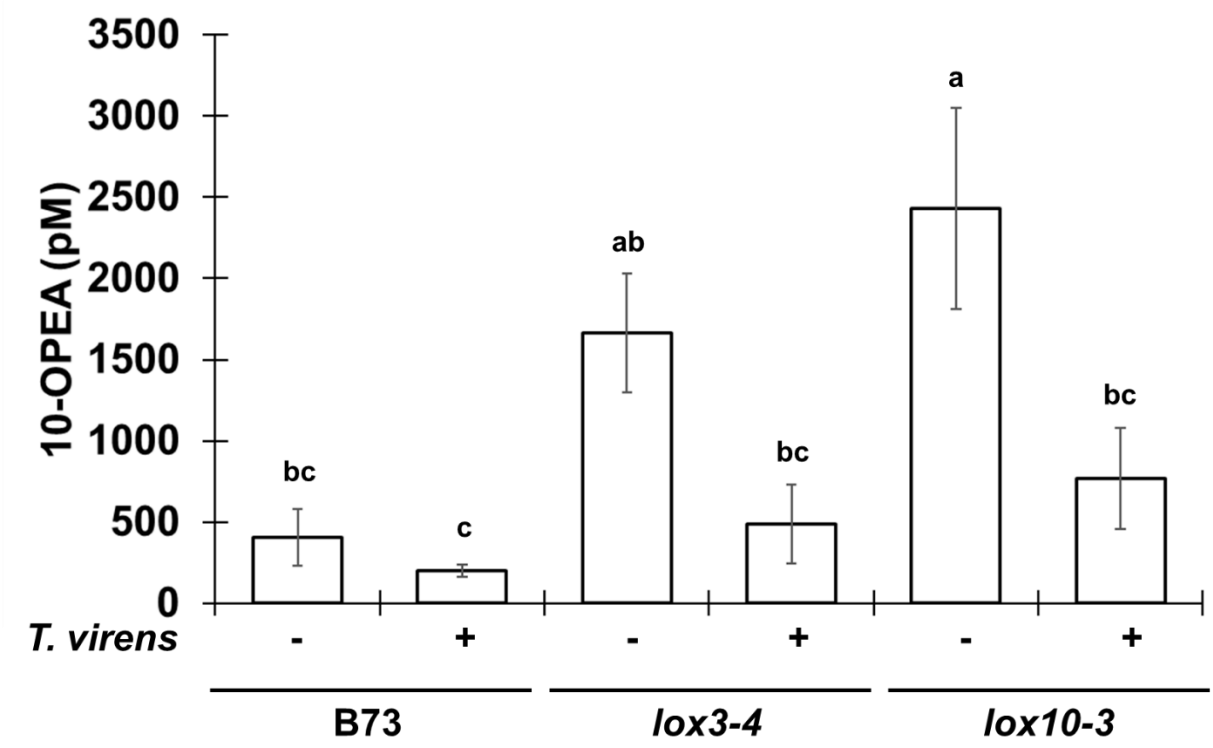

FIGURE 8. 10-OPEA levels decrease significantly with *T. virens* root colonization. LC-MS/MS measurement of 10-OPEA levels in xylem sap collected from B73, *lox3-4*, and *lox10-3* treated with TvWT. Values represent means ± standard deviation SD (n=5), with letters indicating significant differences between treatments (Tukey's HSD test, $p < 0.05$).

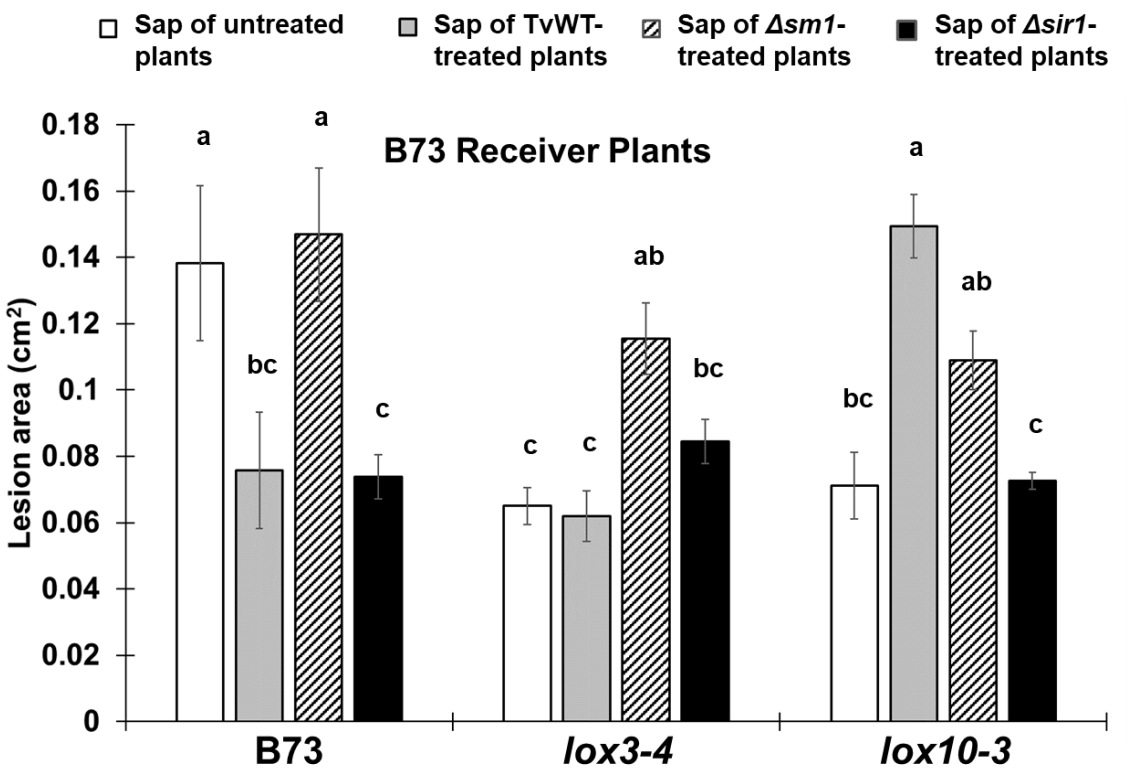

FIGURE 9. Xylem-derived sap from *T. virens*-treated plants contain ISR signals. Measurements of lesion area caused by *C. graminicola* infection on B73 inbred line receiver plants transfused with xylem sap from untreated or TvWT-, *Δsm1*-, or *Δsir1*-treated B73, *lox3-4*, and *lox10-3* plants. Values represent means ± standard deviation SD (n=5), with letters indicating significant differences between treatments (Tukey's HSD test, $p < 0.05$).

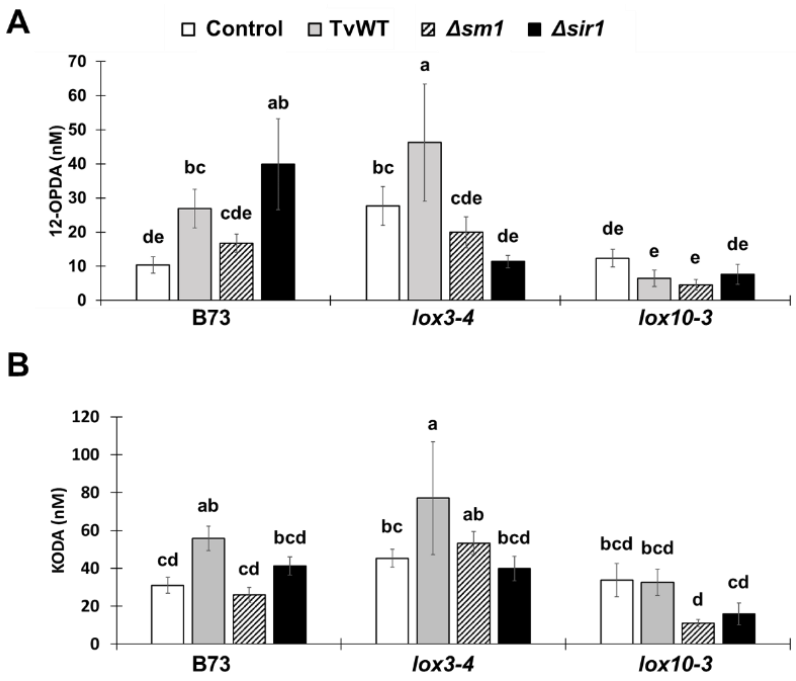

FIGURE 10. Metabolite analysis identified 12-OPDA and KODA as potential ISR signals.

(A) LC-MS/MS measurement of 12-OPDA levels in xylem sap collected from untreated, TvWT-, *Δsm1*-, or *Δsir1*-treated B73, *lox3-4*, and *lox10-3* plants. Values represent means ± standard deviation SD (n=5), with letters indicating significant differences between treatments (Tukey's HSD test, $p < 0.05$).

(B) LC-MS/MS measurement of KODA levels in xylem sap collected from untreated, TvWT-, *Δsm1*-, or *Δsir1*-treated B73, *lox3-4*, and *lox10-3* plants. Values represent means ± standard deviation SD (n=5), with letters indicating significant differences between treatments (Tukey's HSD test, $p < 0.05$).

(C) LC-MS/MS measurement of JA levels in xylem sap collected from untreated, TvWT-, *Δsm1*-, or *Δsir1*-treated B73, *lox3-4*, and *lox10-3* plants. Values represent means ± standard deviation SD (n=5), with letters indicating significant differences between treatments (Tukey's HSD test, $p < 0.05$).

(D) LC-MS/MS measurement of JA-Ile levels in xylem sap collected from untreated, TvWT-, *Δsm1*-, or *Δsir1*-treated B73, *lox3-4*, and *lox10-3* plants. Values represent means ± standard deviation SD (n=5), with letters indicating significant differences between treatments (Tukey's HSD test, $p < 0.05$).

(E) LC-MS/MS measurement of traumatin levels in xylem sap collected from untreated, TvWT-, *Δsm1*-, or *Δsir1*-treated B73, *lox3-4*, and *lox10-3* plants. Values represent means ± standard deviation SD (n=5), with letters indicating significant differences between treatments (Tukey's HSD test, $p < 0.05$).

(F) LC-MS/MS measurement of SA in xylem sap collected from untreated, TvWT-, *Δsm1*-, or *Δsir1*-treated B73, *lox3-4*, and *lox10-3* plants. Values represent means ± standard deviation SD (n=5), with letters indicating significant differences between treatments (Tukey's HSD test, $p < 0.05$).

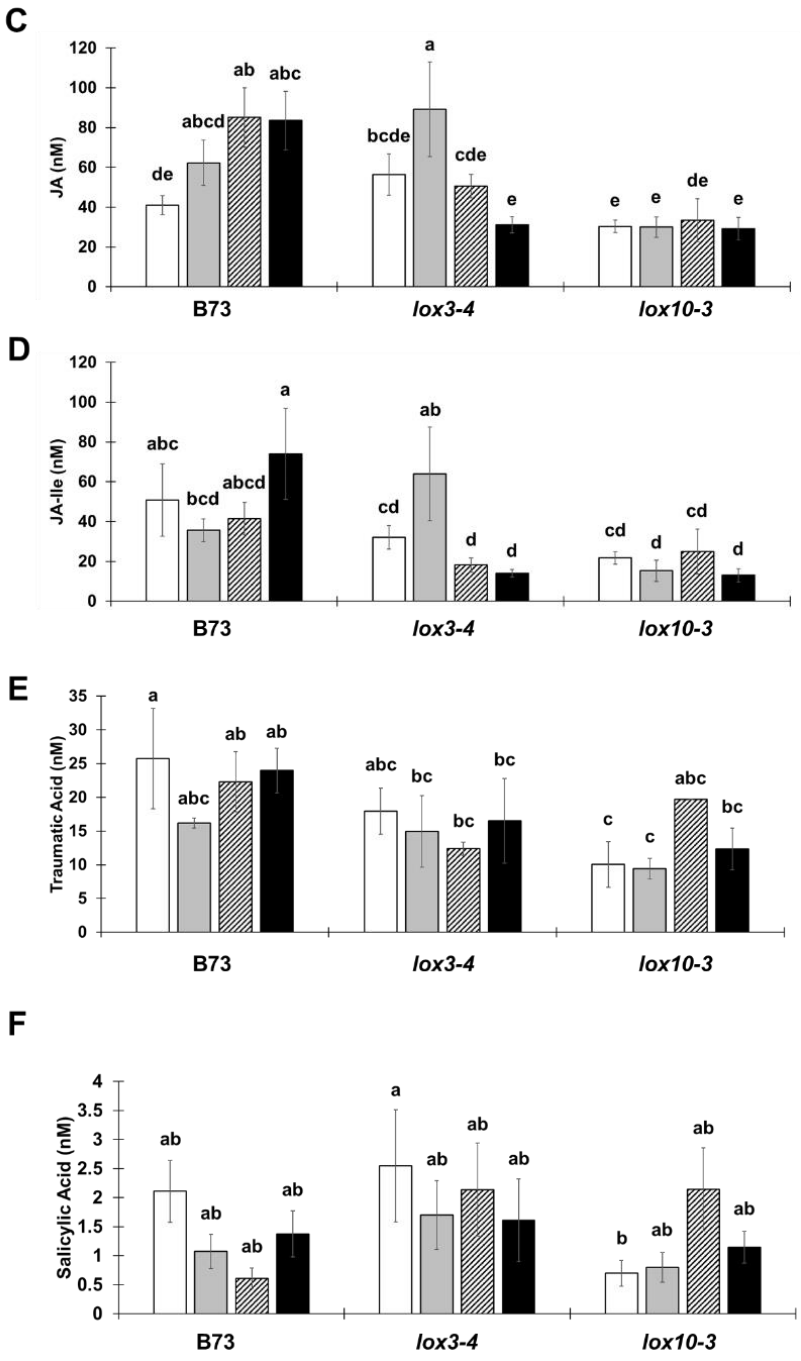

Figure 10. Continued

	B73				*lox3-4*				*lox10-3*			
Metabolite	Untreated	TvWT	*Δsm1*	*Δsir1*	Untreated	TvWT	*Δsm1*	*Δsir1*	Untreated	TvWT	*Δsm1*	*Δsir1*
nM p10HOD	0.8±0.2	1.2±0.6	0.7±0.2	1.3±0.3	1.0±0.3	0.8±0.2	0.6±0.2	0.9±0.2	1.1±0.4	1.2±0.1	0.8±0.2	1.3±0.6
nM 12,13-diHOM	45.1±3.3	32.2±4.6	28.9±1.4	29.4±2.3	36.0±1.5	34.7±2.5	41.3±5.5	31.7±1.5	27.3±3.1	35.8±6.6	23.9±3.4	127.4±92.7
nM 12,13-EpOM	3.7±0.7	2.3±0.7	1.7±0.2	1.3±0.2	4.2±0.8	3.4±0.9	3.1±0.5	1.7±0.5	3.2±0.5	4.1±0.6	2.3±0.7	2.8±0.7
nM 12OH-JA	17.6±1.1	19.1±1.4	21.6±2.2	19.1±0.2	18.5±1.0	82.6±27.4	25.9±5.2	12.1±0.8	11.4±0.4	16.5±5.9	17.6±5.3	258.4±245.2
nM 12OH-JA-Ile	27.4±7.8	30.8±7.6	58.6±17.7	99.8±34.2	47.2±17.9	110.2±50.1	12.4±2.3	10.1±2.1	21.2±3.2	24.5±12.8	27.6±18.8	13.2±3.3
nM 13HOD	31.0±10.9	17.1±5.6	11.8±5.0	15.5±4.2	34.4±4.5	24.3±3.1	16.8±4.5	8.3±0.6	44.8±18.2	20.0±3.0	12.1±2.8	12.1±4.7
nM 13HOT	6.7±2.4	7.6±1.2	3.9±1.1	7.8±1.6	7.2±2.1	6.7±1.5	7.1±2.1	4.3±0.7	7.0±2.1	6.3±0.9	2.4±0.8	4.7±2.2
nM 13OH-12KOM	10.8±3.2	11.3±5.8	8.4±4.6	21.9±4.8	69.8±11.1	48.9±22.4	18.0±3.7	6.3±1.4	32.6±14.5	18.4±7.9	3.8±1.5	2.1±0.7
nM 9,10,13-THOM	1472.6±278.0	912.1±187.4	1186.1±250.9	2408.9±112.8	1108.9±140.8	680.2±171.6	932.5±194.5	676.5±74.2	1156.4±360.5	670.7±64.0	671.9±162.9	1006.6±257.4
nM 9,10-EpOM	54.9±13.8	37.5±13.3	22.8±6.0	24.7±4.1	74.6±14.6	55.9±10.2	62.9±12.2	27.9±9.9	55.1±16.7	57.0±10.1	18.7±7.2	36.3±13.4
nM 9,12,13-THOM	723.1±101.9	598.8±73.0	789.5±84.3	1075.2±121.7	628.0±80.7	542.5±141.0	881.2±73.9	687.1±45.0	384.1±102.5	527.6±76.6	302.5±78.9	438.2±235.5
nM 9HOD	39.0±10.4	20.6±4.5	17.6±1.9	24.5±3.8	18.1±1.1	12.3±1.3	8.0±1.6	6.4±0.8	43.1±16.1	19.7±1.8	14.8±6.0	20.1±3.6
nM 9HOT	6.3±1.7	6.3±1.1	6.3±1.4	7.5±1.1	4.4±0.5	4.9±1.4	4.7±0.5	3.9±0.9	4.1±1.0	5.1±0.5	3.2±2.1	4.5±0.7
nM 9OH-10KOM	1880.4±127.2	1769.1±85.7	1588.4±54.9	1406.2±57.3	1342.4±24.4	818.9±147.1	610.2±136.8	889.4±24.1	958.9±81.4	1084.5±298.4	531.3±61.8	4192.1±3416.9
nM 9OH-12KOM	115.4±29.5	65.3±15.7	46.4±9.9	53.7±21.9	77.4±10.2	84.6±20.5	71.6±10.6	40.9±13.8	137.0±30.8	56.1±15.4	24.5±13.5	34.0±16.8
nM ABA	3.8±0.4	3.4±0.7	7.0±1.0	5.7±2.2	2.6±0.6	13.5±5.0	4.7±1.1	2.5±0.6	3.4±0.9	3.7±1.2	3.9±0.4	8.3±2.1
nM Azelaic acid	20.0±4.9	12.3±3.6	10.8±1.6	19.9±7.8	14.3±1.2	6.8±1.5	5.3±0.3	6.8±1.4	27.8±18.4	10.5±2.6	22.6±11.5	54.5±45.3
nM Benzoate	33.5±5.2	32.6±1.4	39.3±2.2	92.2±46.1	41.4±5.0	40.5±2.9	36.9±2.3	55.3±21.7	38.3±5.7	45.8±7.8	88.9±11.1	119.5±35.8
nM CA	4.1±3.6	0.9±0.4	1.5±0.1	3.9±3.0	19.3±17.1	0.7±0.1	3.0±2.5	22.5±20.9	2.5±0.8	1.0±0.3	260.6±156.1	18.4±7.5
nM IAA	1.7±0.2	2.8±0.8	3.4±2.1	3.4±0.2	2.2±0.7	2.2±0.9	2.9±0.4	41.1±38.1	1.6±0.3	1.8±0.4	92.9±31.2	9.3±4.6

Table 1. Detected metabolites and phytohormones in collected xylem sap samples.

LC-MS/MS measurement of metabolite and phytohormone levels in xylem sap collected from untreated or TvWT-, *Δsm1*-, and *Δsir1*-treated B73, *lox3-4*, and *lox10-3*. Values represent means ± standard deviation SD.

12-OPDA and KODA, but not JA, increases plant resistance in a dose-dependent manner

To directly test the effect of 12-OPDA and KODA, B73 plants were transfused with different concentrations of 12-OPDA or KODA to identify its effects on maize systemic resistance in a dose-dependent manner. To mimic the sap transfusion methods used previously, 12-OPDA or KODA was added to sap from untreated B73 plants and transfused to B73 receiver plants. Positive control for ISR activity was transfusion with sap from TvWT-treated B73 plants, while negative control was transfusion with sap from untreated B73. After transfusion with 12-OPDA, the leaves of treated B73 plants were subsequently challenged with *C. graminicola* infection. Sap transfusion with 12-OPDA enhanced B73 resistance against *C. graminicola* in a dose-dependent manner, with 25 nM 12-OPDA moderately increasing resistance, peaking at 100 nM (Fig. 11A and 11B). Further increases in 12-OPDA concentration, including 1000 nM and beyond, had no additional enhancement in resistance (data not shown). Similarly, transfusion with KODA also showed a dose-dependent effect on enhancing plant resistance against *C. graminicola*, with the strongest effect occurring with 1000 nM (Fig. 11C and 11D). Further increases in KODA concentration had no additional effect on plant resistance (data not shown). Furthermore, B73 transfused with low concentrations of 12-OPDA and KODA simultaneously displayed better resistance than single treatments, suggesting an additive or synergistic effect (Fig. 12).

Because JA-Ile has been implicated in ISR regulation in other species, sap transfusion experiments were also carried out with JA-Ile within the same range of concentrations. JA-Ile concentrations from 1 to 100 nM had no impact on lesion area. Unexpectedly, addition of JA-Ile at 1000 nM led to enhanced susceptibility (Fig. 11E and 11F). Furthermore, transfusion with JA-

Ile precursor, JA, at 1000 nM concentration also led to the same increased susceptibility (data not shown). Taken together, these results suggest that 12-OPDA, not JA or JA-Ile, is an oxylipin signal that positively regulates ISR effect at physiologically relevant nM concentrations.

To test whether ISR-deficiency of *Δsm1*-treated B73 is due to low 12-OPDA content, we supplemented the sap samples from untreated B73 (no ISR signal) and *Δsm1*-treated B73 (no ISR signal) with 12-OPDA. Both untreated B73 and *Δsm1*-treated B73 displayed significantly increased resistance to *C. graminicola* when supplemented with 12-OPDA (Fig. 13A and 13B). These results suggest that 12-OPDA can complement the lack of ISR activity in both ISR-negative saps. To test if 12-OPDA can reverse the ISS phenotype of TvWT-colonized *lox10-3*, sap samples from untreated and TvWT-treated *lox10-3* were supplemented with 12-OPDA and transfused into untreated *lox10-3* and TvWT-treated *lox10-3*. The results showed that 12-OPDA supplementation complemented *lox10-3* inability to induce ISR, as evidenced by significantly decreased lesion area (Fig. 13C and 13D), suggesting that LOX10-dependent ISR requires 12-OPDA signaling.

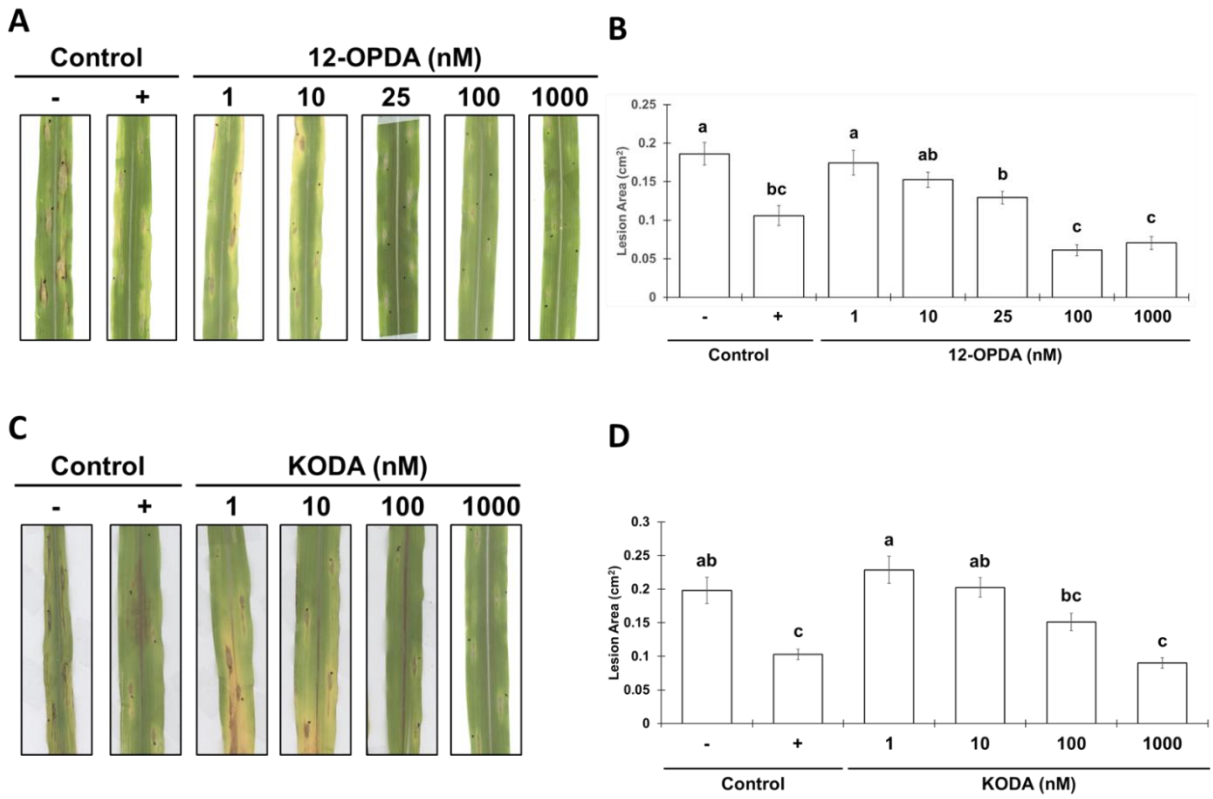

FIGURE 11. Transfusion of 12-OPDA or KODA increased resistance in a dose-dependent manner, while transfusion with of JA-Ile increases susceptibility.

(A) Lesions developed on 3rd leaves of 12-OPDA-transfused B73 receiver plants and infected with *C. graminicola*. Positive control treatment was transfusion with TvWT-treated B73 sap, while negative control treatment was transfusion with untreated B73 sap.

(B) Measurements of lesion area caused by *C. graminicola* infection on 12-OPDA-transfused B73. Infected leaves were scanned and measured using ImageJ software to determine mean lesion area. Values represent means ± standard deviation SD (n=5), with letters indicating significant differences between treatments (Tukey's HSD test, $p < 0.05$).

(C) Lesions developed on 3rd leaves of KODA-transfused B73 receiver plants and infected with *C. graminicola*. Positive control treatment was transfusion with TvWT-treated B73 sap, while negative control treatment was transfusion with untreated B73 sap.

(D) Measurements of lesion area caused by *C. graminicola* infection on KODA-transfused B73. Infected leaves were scanned and measured using ImageJ software to determine mean lesion area. Values represent means ± standard deviation SD (n=5), with letters indicating significant differences between treatments (Tukey's HSD test, $p < 0.05$).

(E) Lesions developed on 3rd leaves of JA-Ile-transfused B73 receiver plants and infected with *C. graminicola*. Positive control treatment was transfusion with TvWT-treated B73 sap, while negative control treatment was transfusion with untreated B73 sap.

(F) Measurements of lesion area caused by *C. graminicola* infection on JA-Ile-transfused B73. Infected leaves were scanned and measured using ImageJ software to determine mean lesion area. Values represent means ± standard deviation SD (n=5), with letters indicating significant differences between treatments (Tukey's HSD test, $p < 0.05$).

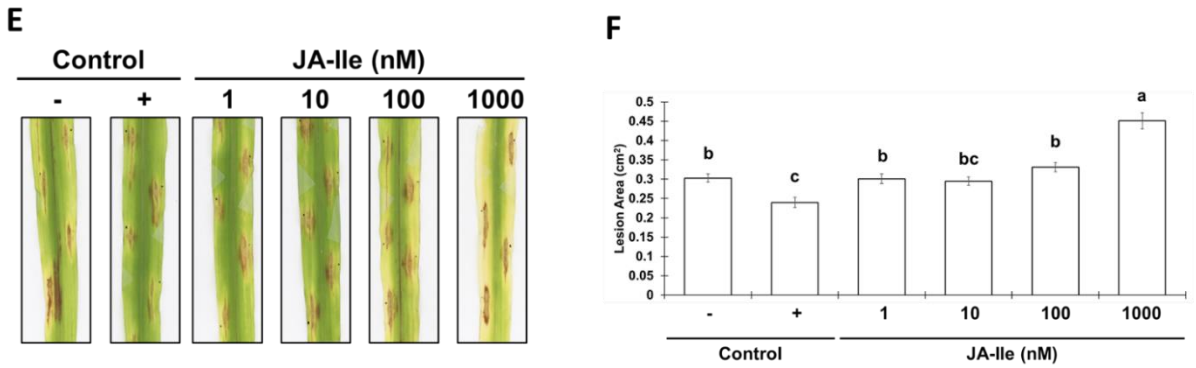

Figure 11. Continued

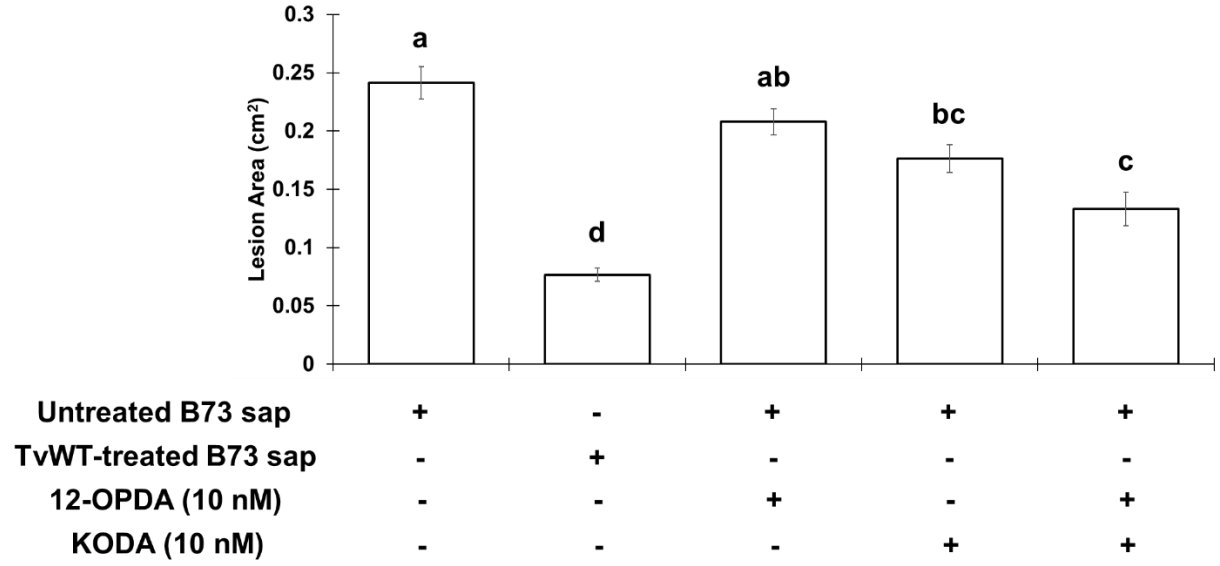

FIGURE 12. Transfusion of 12-OPDA and KODA displayed additive effect on plant resistance.

Measurements of lesion area caused by *C. graminicola* infection on B73 transfused with 12-OPDA (10 nM), KODA (10 nM), or both. Controls were transfusion with untreated B73 sap and TvWT-treated B73 sap without 12-OPDA or KODA added. Infected leaves were scanned and measured using ImageJ software to determine mean lesion area. Values represent means ± standard deviation SD (n=5), with letters indicating significant differences between treatments (Tukey's HSD test, $p < 0.05$).

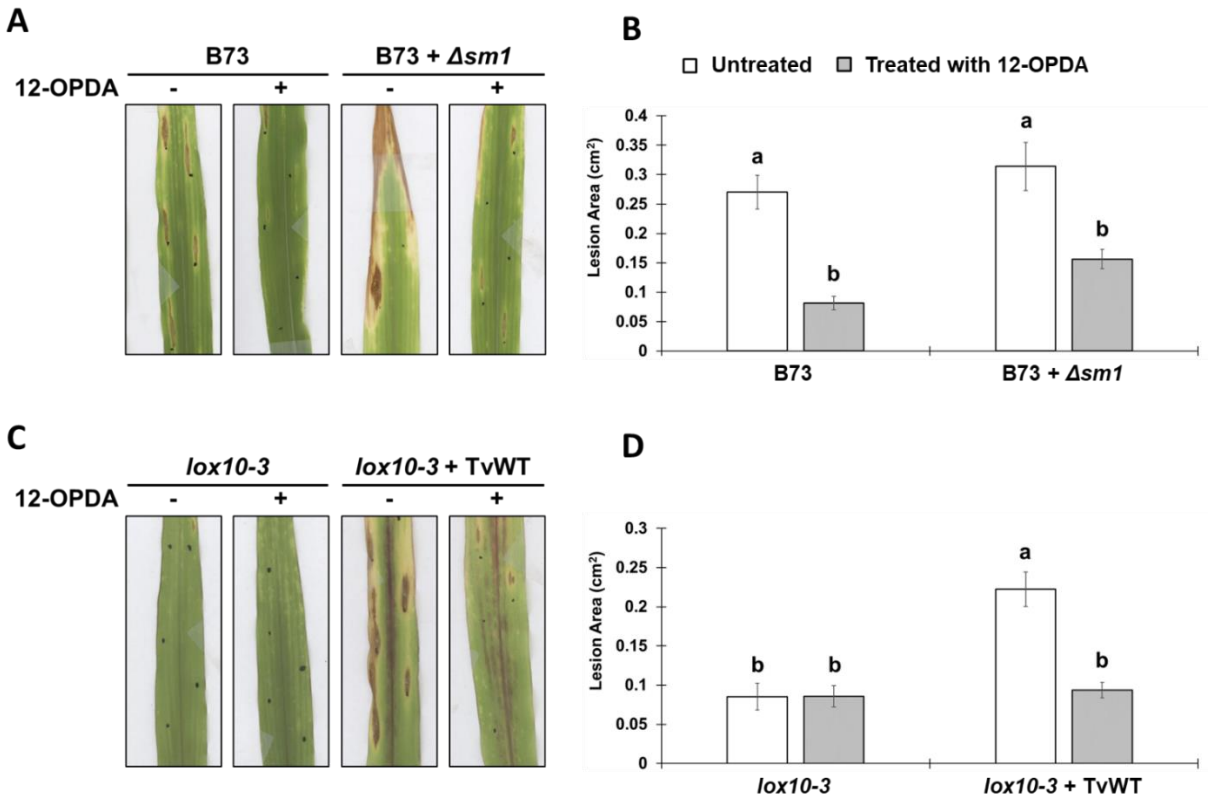

FIGURE 13. Transfusion of 12-OPDA enhanced resistance in B73 and rescued susceptibility of *Δsm1*-treated B73 and TvWT-treated *lox10-3*.

(A) Lesions developed on 3rd leaves of 12-OPDA-transfused untreated and *Δsm1*-treated B73 receiver plants and infected with *C. graminicola*. Control plants were transfused with untreated B73 sap or *Δsm1*-treated B73 sap without 12-OPDA added.

(B) Measurements of lesion area caused by *C. graminicola* infection on 12-OPDA-transfused untreated and *Δsm1*-treated B73. Infected leaves were scanned and measured using ImageJ software to determine mean lesion area. Values represent means ± standard deviation SD (n=5), with letters indicating significant differences between treatments (Tukey's HSD test, $p < 0.05$).

(C) Lesions developed on 3rd leaves of 12-OPDA-transfused untreated and TvWT-treated *lox10-3* receiver plants and infected with *C. graminicola*. Control plants were transfusion with untreated *lox10-3* sap or TvWT-treated *lox10-3* sap without 12-OPDA added.

(D) Measurements of lesion area caused by *C. graminicola* infection on 12-OPDA-transfused untreated or TvWT-treated *lox10-3*. Infected leaves were scanned and measured using ImageJ software to determine mean lesion area. Values represent means ± standard deviation SD (n=5), with letters indicating significant differences between treatments (Tukey's HSD test, $p < 0.05$).

Phytohormones JA and ET are not required for *T. virens*-mediated ISR in maize

The unexpected results from JA-Ile-enriched sap transfusion poised the question of JA-Ile relevance to ISR. To directly address this question and test whether JA is important for ISR in maize, we utilized the JA-deficient *opr7opr8* double mutant, which is devoid of JA-biosynthesis in every organ tested, but produces normal levels of 12-OPDA (Yan et al., 2012). This mutant was treated with TvWT and subsequently infected with *C. graminicola*. As previously reported, the untreated *opr7opr8* mutants were significantly more resistant to anthracnose leaf blight than untreated B73 plants (Gorman et al., 2017). Surprisingly, in response to TvWT-colonization, lesion area significantly decreased not only on B73 leaves, but also on *opr7opr8* leaves, indicating that the JA-deficient mutant was still capable of ISR (Fig. 14A and 14B). This was in stark contrast to *lox3-4* plants, whose resistance did not benefit further with TvWT treatment (Constantino et al., 2013). These results provide strong genetic evidence that JA is not required for ISR induction in maize.

This striking finding prompted the hypothesis that ET may have greater significance for ISR in maize compared to JA. ET has been widely implicated for ISR signaling (Pieterse et al., 2014a; Pieterse et al., 2014b) alongside JA. To test the role of ET in regulating *T. virens*-triggered ISR in maize, we have tested the ET-deficient *acs2acs6* double mutant for *T. virens*-triggered ISR response. The TvWT-treated *acs2acs6* double mutants displayed ISR phenotype similar to TvWT-treated B73 (Fig. 14C and 14D). Furthermore, the metabolite analysis of xylem sap samples detected that levels of 1-aminocyclopropane-1-carboxylic acid (ACC), the precursor for ET biosynthesis, were reduced significantly in saps from TvWT-treated plants regardless of maize genotype (Fig. 15). ACC functions not only as a precursor for ET biosynthesis, but can

also function as a mobile signal independent of ET, as evidenced by its release into the rhizosphere to attract PGPRs (Penrose et al., 2001). Furthermore, knocking out multiple *Arabidopsis ACS* genes, which produce ACC, resulted in lethality, which did not occur with ET signaling mutants (Tsuchisaka et al., 2009). These results suggest that ET may not play an integral role in regulating *T. virens*-triggered ISR.

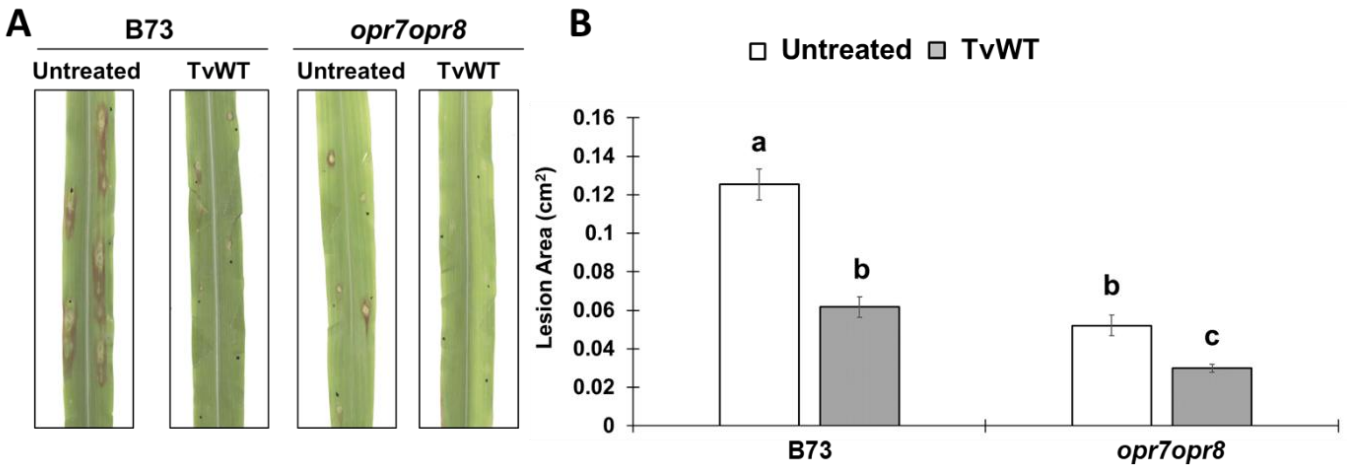

FIGURE 14. *T. virens* conferred ISR to JA-deficient mutant *opr7opr8* and ET-deficient mutant *acs2acs6*.

(A) Lesions developed on 3rd leaves of untreated or TvWT-treated B73 inbred line and *opr7opr8* double mutant plants infected with *C. graminicola*.

(B) Measurements of lesion area caused by *C. graminicola* infection on leaves of untreated or TvWT-treated B73 and *opr7opr8* double mutant plants. Values represent means ± standard deviation SD (n=5), with letters indicating significant differences between treatments (Tukey's HSD test, $p < 0.05$).

(C) Lesions developed on 3rd leaves of untreated or TvWT-treated B73 inbred line and *acs2acs6* double mutant plants infected with *C. graminicola*.

(D) Measurements of lesion area caused by *C. graminicola* infection on leaves of untreated or TvWT-treated B73 and *acs2acs6* double mutant plants. Values represent means ± standard deviation SD (n=5), with letters indicating significant differences between treatments (Tukey's HSD test, $p < 0.05$).

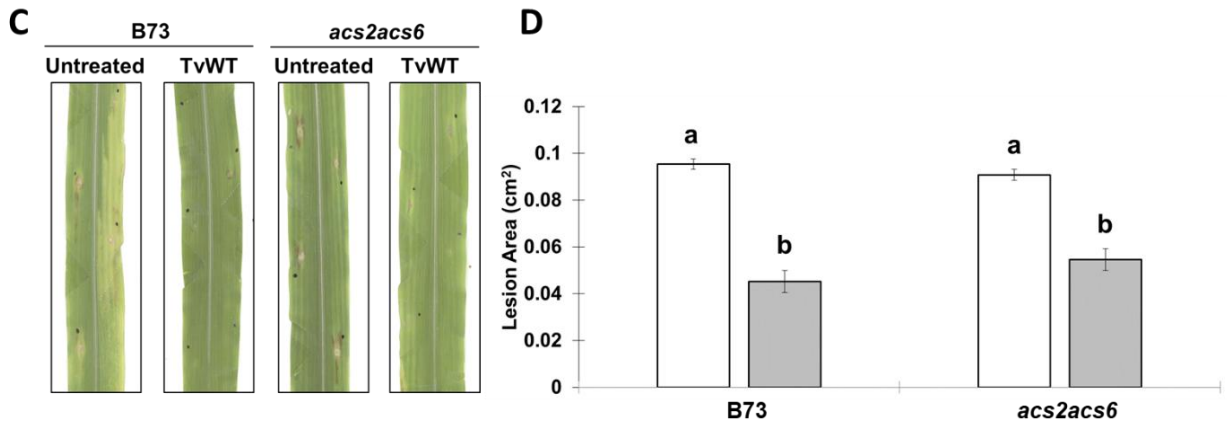

Figure 14. Continued

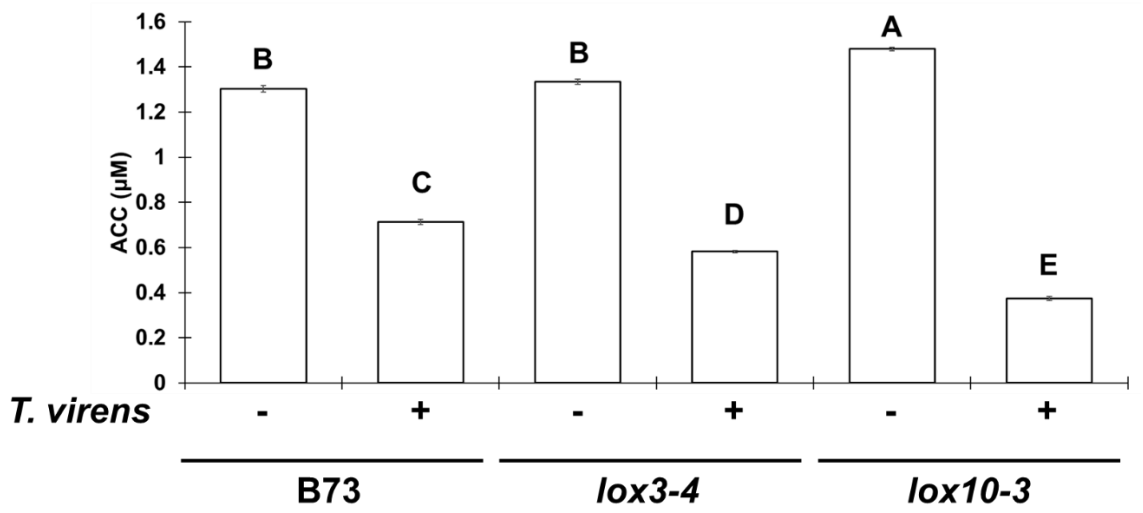

FIGURE 15. ACC levels decrease significantly with *T. virens* root colonization.
LC-MS/MS measurement of ACC levels in xylem sap collected from B73, *lox3-4*, and *lox10-3* treated with TvWT. Values represent means ± standard deviation SD (n=5), with letters indicating significant differences between treatments (Tukey's HSD test, $p < 0.05$).

Transcriptomic analysis reveals induction of genes involved in 12-OPDA, but not JA, biosynthesis

The data above showing that 12-OPDA, but not JA, is required for *T. virens*-mediated ISR in maize prompted the hypothesis that JA biosynthesis and 12-OPDA biosynthesis genes may be regulated differently by *T. virens* colonization. We tested this hypothesis by performing RNA-seq analysis on B73 seedlings grown in hydroponic conditions and treated with TvWT at 6 and 54 hr. The time points represented fungal recognition at 6 hr and advanced colonization at 54 hr (data not shown). Importantly, the 54 hr time point reflects 2 days after initial recognition stage at 6 hr to avoid any transcriptome changes associated with the circadian clock. The genes involved in JA-biosynthesis in the AOS branch of the LOX pathway, perception, and downstream JA response have been previously identified (Borrego and Kolomiets, 2016), with 12-OPDA biosynthesis occurring in plastids and involving 13-LOX, 13-AOS, and 13-AOC. The JA biosynthesis portion of the AOS branch occurs in peroxisome and cytoplasm, with OPRs, β-oxidation enzymes, and cytoplasmic JAR1.

12-OPDA biosynthesis begins in the plastid with 13-LOX (*LOX7*, *LOX8*, *LOX9*, *LOX10*, *LOX11*, and *LOX13*) activity, which converts linolenic acid to 13-HPOT (Fig. 16A). As measured by FPKM (Fragments Per Kilobase of transcript per Million mapped reads), only *LOX10* expression was induced in response to TvWT recognition, with ~6-fold increase in transcript abundance compared to untreated controls, consistent with earlier qPCR results (Fig. 1A). *LOX7* and *LOX13* transcripts were not detected in any samples. *LOX8* and *LOX9* were expressed only in untreated control plants, but were suppressed by TvWT at both time points. While expression of *LOX11* was unchanged between control and TvWT-treated B73 at 6 hr, its

expression was downregulated at 54 hr. These data point to LOX10 as the sole 13-LOX that was rapidly induced by TvWT even before root colonization took place, supporting the previous data that *LOX10* is induced by secreted peptide Sm1 (Fig. 1A). The next steps occur with AOS conversion of 13-HPOT to 12,13-EOT, which is further converted by AOC to 12-OPDA. Expression of *AOS1a*, *AOS1b*, *AOS1c*, and *AOC1* were upregulated after advanced TvWT-colonization at 54 hr. *AOC2* expression, on the other hand, was suppressed by TvWT. Several OPDA-specific response genes (ORGs) were differentially regulated in response to TvWT treatment (Fig. 16B). More specifically, a glycosyl hydrolase (*GH9B8*), known to be downregulated in response to 12-OPDA, was repressed in maize roots at both 6 and 54 hr after TvWT treatment. Expression of several other genes known to be upregulated by 12-OPDA, such as Calcium-binding EF-hand family protein (*CML41*), zinc finger transcription factor (*ZBF4*), ABC transporter (*PDR11*), and glutathione transferase (*GST5*), were all induced by TvWT at both 6 and 54 hr.

After 12-OPDA is transported to the peroxisome, the next step in JA biosynthesis is the conversion of 12-OPDA to OPC-8:0 by OPR7 and OPR8 (Yan et al., 2012). Expression of both *OPR7* and *OPR8* were downregulated steadily upon recognition and were completely undetectable during advanced colonization (Fig. 16A). OPC-8:0 undergoes three rounds of β-oxidation by ACX, MFP, and KAT activities to produce JA. Remarkably, expression of most of these genes were downregulated, with all *ACX* genes, *MFP*, and *KAT2* transcripts completely undetectable at 54 hr. Lastly, among the 5 *JAR1* maize homologs responsible for the conjugation of isoleucine to JA, *JAR1b*, closest maize homolog to *AtJAR1* (Borrego and Kolomiets, 2016) was expressed in the roots. Expression of *JAR1b* steadily decreased upon recognition and was undetectable at 54 hr. Taken together, these results suggested that genes responsible for 12-

OPDA biosynthesis were upregulated in response to TvWT colonization, but the expression of genes responsible for converting 12-OPDA to JA-Ile were downregulated. qPCR validation of *AOS1c*, *AOC1*, *OPR7,* and *JAR1b* was in agreement with RNA-seq data, though the degree of increase or decrease were not conserved (Fig. 17).

JA-Ile interaction with COI1-JAZ co-receptor complex results in activation of SCF complex, which results in degradation of JAZ proteins to allow transcriptional activation of MYC and WRKY that eventually lead to JA downstream signaling (Song et al., 2013). To determine if genes downstream of JA-Ile were differentially regulated with TvWT root colonization, we measured expression of JA signaling and response genes. Of the 5 detected *COI1* genes out of 6 that exist in maize, three were rapidly induced upon recognition of TvWT, but all five were substantially downregulated by 54 hr (Fig. 16B). Of the *JAZ* genes expressed in roots, *JAZ5*, *JAZ6*, and *JAZ8* transcripts steadily increased upon recognition and increased ~4-, 7-, and 11-fold, respectively, at 54 hr. This is in contrast to *JAZ1*, *JAZ2*, and *JAZ11*, which were induced at 6 hr but suppressed at 54 hr. Expression of transcription factors *MYC7*, *WRKY14*, and *WRKY46*, implicated in positive regulation of JA-responsive genes, steadily decreased at 6 hr and was completely repressed at 54 hr. In agreement with repression of transcription factors, expression of most JA-dependent genes, which include 9-LOX genes (*LOX1* and *LOX5*), OPR genes (*OPR2*, *OPR3*, and *OPR5*), and lipase *PLC* (Yan et al., 2012), were downregulated at 54 hr. The notable exceptions were *LOX4*, a 9-LOX, and *MPI*, a JA-responsive proteinase inhibitor which were both upregulated at 6 hr and 54 hr. qPCR validation of *MYC7* and *LOX1* expression was in agreement with the RNA-seq results, showing that both transcripts decreased over time (Fig. 17). Overall, upregulation of several *JAZ* genes and downregulation of JA-dependent genes suggest that *T. virens* colonization results in early suppression of JA responses.

In agreement with observed suppression of JA signaling, SA biosynthesis and signaling appear to be significantly upregulated at the time of colonization, likely due to well documented SA-JA antagonism. Specifically, expression of all phenylalanine ammonia lyase (*PAL*) genes were strongly upregulated at 54 hr, with the exception of *PAL4* (Fig. 17). Corroborating SA biosynthesis genes, expression of SA-responsive genes, *PR1*, *PR5*, and *PR10*, were significantly upregulated at 54 hr, displaying ~63-, 225-, and 68-fold increases in transcript levels, respectively. qPCR validation of *PR1* and *PR5* expression was in agreement with RNA-seq results, showing that both transcripts were increased incrementally from 6 to 54 hr (Fig. 18). Both *NPR1* and *TGA2*, components of SAR signaling, were upregulated at 6 hr, but only *TGA2* expression stayed upregulated at 54 hr. Overall, the results point to upregulation of SA biosynthesis and downstream signaling gene by TvWT treatment, which may be explained by the negative cross-talk between SA and JA signaling (Pieterse et al., 2012).

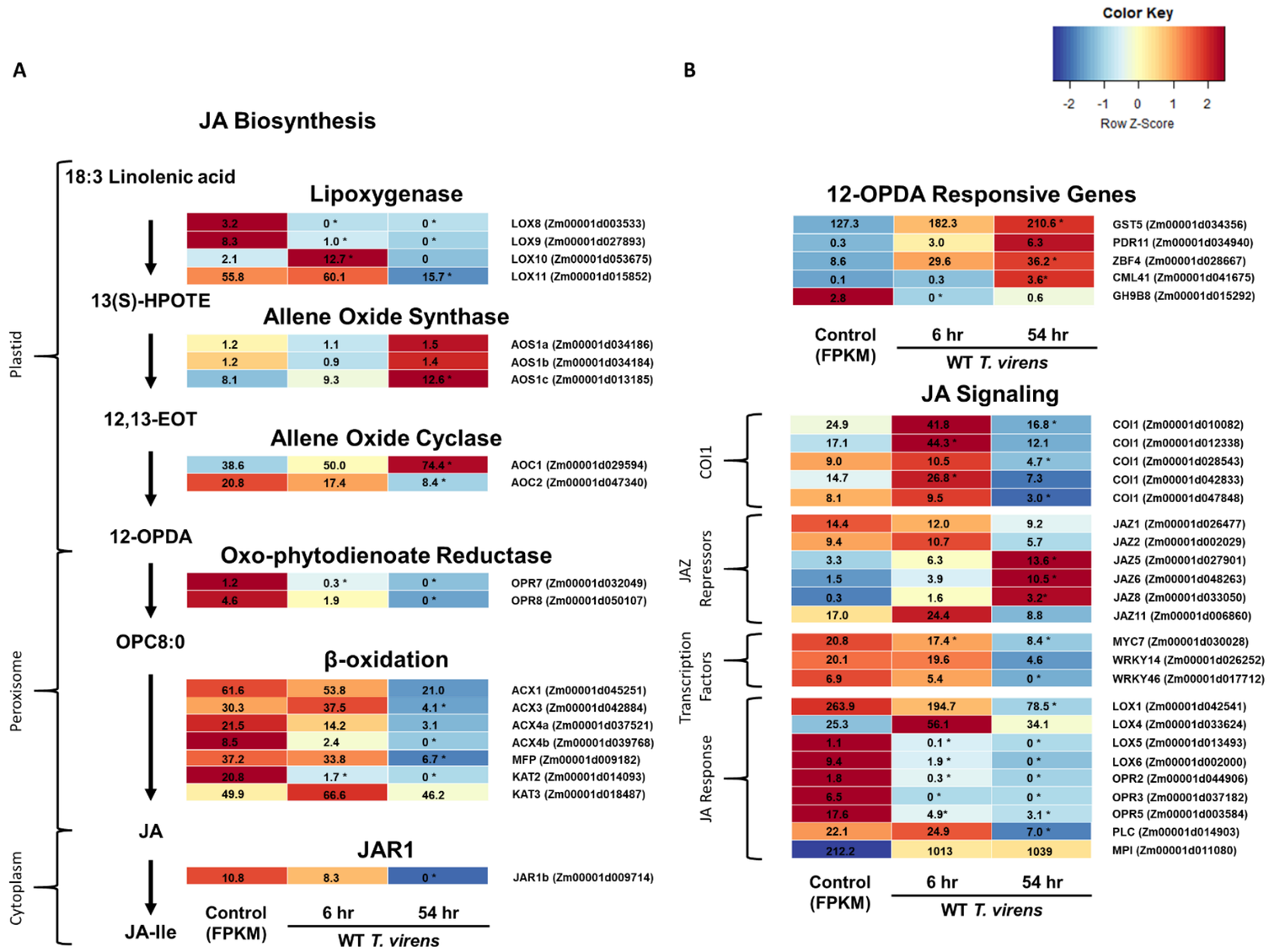

FIGURE 16. Maize-*T. virens* interactions induce biosynthesis of 12-OPDA, but not JA-Ile or JA downstream signaling.

(A) Schematic of the AOS branch genes, with heat maps representing Z-score transformed FPKM. Values in each block representing raw FPKM, with asterisks (*) denoting significant differences (Tukey's HSD test, $p < 0.05$). Treatments comprised of untreated B73 plants (n=4), and TvWT-treated plants (n=10) at 6 hr and 54 hr.

(B) Schematic of 12-OPDA-responsive genes and the JA downstream signaling genes, with heat maps representing Z-score transformed FPKM. Values in each block representing raw FPKM, with asterisks (*) denoting significant differences (Tukey's HSD test, $p < 0.05$). Treatments comprised of untreated B73 plants (n=4), and TvWT-treated plants (n=10) at 6 hr and 54 hr.

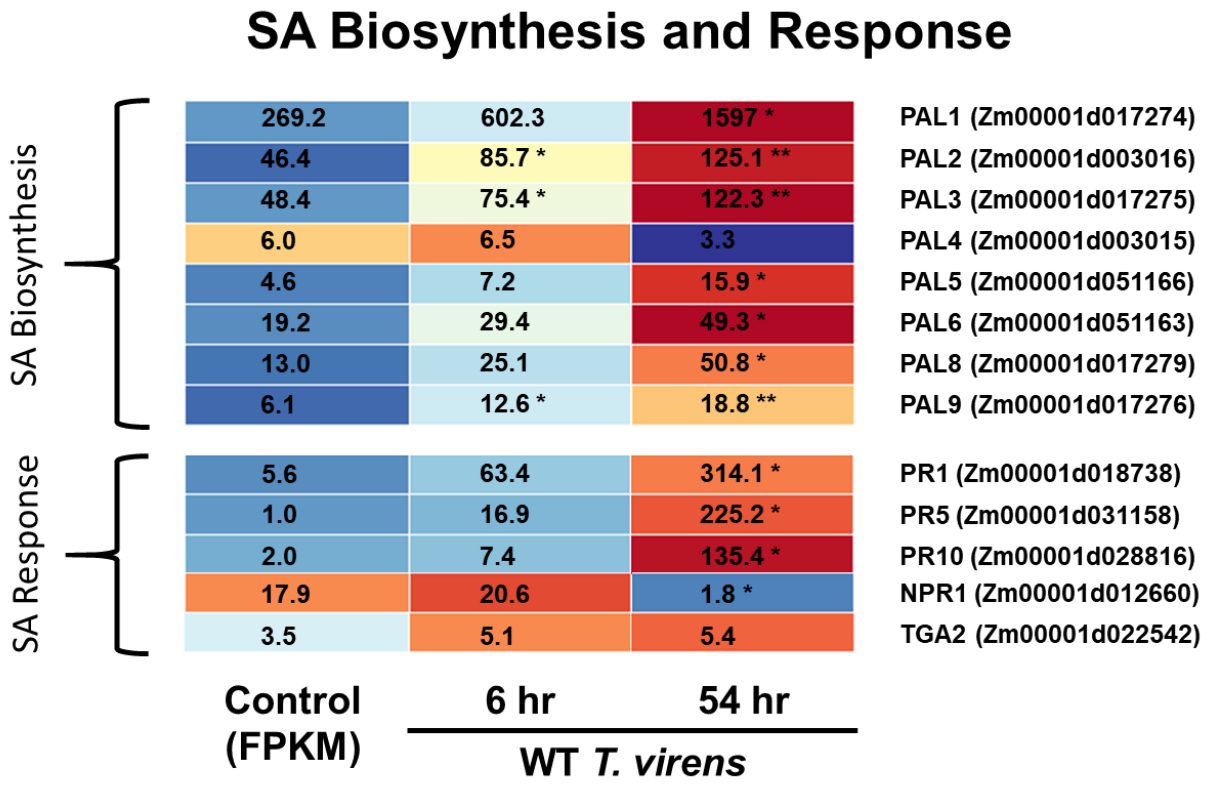

FIGURE 17. Maize-*T. virens* interactions induce SA biosynthesis and response genes. Schematic of the SA biosynthesis and response, with heat maps representing Z-score transformed FPKM. Values in each block representing raw FPKM, with asterisks (*) denoting significant differences (Tukey's HSD test, $p < 0.05$). Treatments comprised of untreated B73 plants (n=4), and TvWT-treated plants (n=10) at 6 hr and 54 hr.

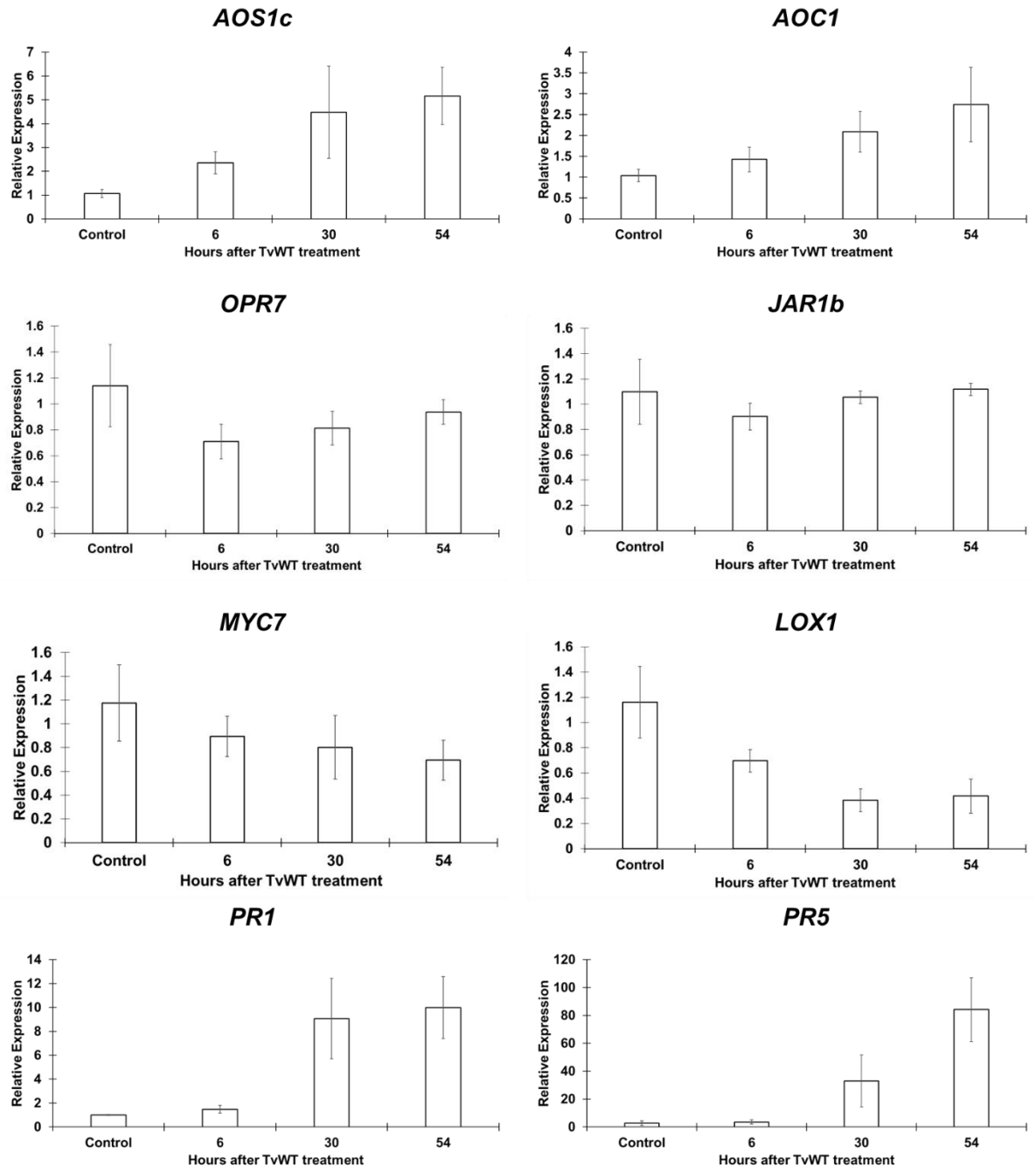

FIGURE 18. qPCR confirmation of RNA-seq transcriptomic analysis.

Expression of select JA and SA genes via qPCR was determined in TvWT-treated B73 seedling roots at 6, 30, and 54 hours after treatment compared to untreated control plants. Relative expression was calculated from cycle threshold values using the $2^{-\Delta\Delta Ct}$ method. Values represent means ± standard deviation SD (n=3) relative to control plants and were normalized to transcript levels of *α-Tubulin* (*α-TUB*). Statistical significance (* represents $p < 0.05$) was determined with Tukey's HSD test.

DISCUSSION

12-OPDA signaling is distinct from JA and is required for ISR

Multiple long-distance signaling molecules that regulate SAR have been identified (Klessig et al., 2018; Shan and He, 2018). In contrast, long-distance signals responsible for establishing ISR remain less characterized, with most bodies of work pointing to JA and ET as the two main signals (Pieterse et al., 2014a). In this study, we utilized genetic, biochemical, and pharmacological approaches with ISR-positive and -negative mutants of both *T. virens* (*Δsm1* and *Δsir1*) and maize (*lox3* and *lox10*) to identify the JA precursor, 12-OPDA, as the major signal responsible for regulating *T. virens*-triggered ISR in maize. The *lox10* mutants, reduced in 12-OPDA content (Christensen et al., 2013), lost the capacity for *T. virens*-induced ISR, as seen with ISS phenotype in response to infections by both hemibiotrophic and necrotrophic pathogens (Fig. 2 and 3). Moreover, the mutant became significantly more susceptible when colonized by this symbiont, a response coined ISS. In agreement with the major role of 12-OPDA in ISR signaling, *lox3* mutants, displaying constitutive ISR, or WT plants colonized by TvWT or *Δsir1* mutant accumulated significantly greater amounts of 12-OPDA in xylem sap (Fig. 10A). In contrast, xylem saps of ISR-negative B73 WT plants, whether untreated or treated with *Δsm1*, contained much lower levels of 12-OPDA. Transfusion with xylem sap supplemented with nM concentrations of 12-OPDA conferred robust ISR phenotype, with 100 nM showing strongest effect (Fig. 11A and 11B). This provides proof that OPDA has signaling properties in ISR, as we showed that OPDA transfusion with increasing nM range concentrations induced ISR in a dose-dependent manner, as has been shown for JA-like compounds (Blechert et al., 1999; Miersch et

al., 1999). Importantly, OPDA transfusion into TvWT-treated *lox10-3* rescued ISR phenotype to the levels observed with TvWT-treated WT plants (Fig. 13), indicating that OPDA-deficiency is the reason for lack of ISR in *lox10* mutants. Surprisingly, JA and JA-Ile levels in xylem sap did not correlate with ISR phenotype; furthermore, transfusion with supplemented JA-Ile at concentrations comparable to OPDA resulted in enhanced susceptibility (Fig. 11E and 11F). These results prompted the question of whether JA is actually required for inducing ISR. Analysis of ISR competency of JA-deficient mutant *opr7opr8* (Yan et al., 2012) showed that they were still capable of mounting ISR response with TvWT (Fig. 14A). Moreover, transcriptome analysis of TvWT-treated B73 plants showed upregulation of plastid-localized 12-OPDA biosynthesis genes (*LOX10*, *AOS1a, b, c*, and *AOC1*) and several ORGs (marker genes induced by 12-OPDA, but not JA), but gradual downregulation of JA biosynthesis genes downstream of 12-OPDA (*OPR7*, *8*, β-oxidation genes, and *JAR1*) during colonization (Fig. 16).Finally, several *JAZ* genes were significantly upregulated, signifying suppression of JA signaling upon TvWT colonization. Taken together, these results implicate 12-OPDA, not JA, as the major signal required for ISR induction in maize.

These results raise the question of why previous research has not identified 12-OPDA, rather than JA, as a major ISR signal. While 12-OPDA is a precursor of JA biosynthesis, there is growing evidence that it also functions as a signal with functions vastly different than that of JA (Maynard et al., 2018). Microarray analysis of *Arabidopsis* treated with 12-OPDA, JA, or methyl-JA (MeJA) revealed a set of genes, which included many genes involved with signaling, transcriptional factors, and stress responses, that responded only to 12-OPDA in a COI1-independent manner (Taki et al., 2005; Mueller et al., 2008). Recent studies revealed that there exists OPDA-Ile conjugate, lending credence to 12-OPDA being an independent signal in the

same manner as JA (Floková et al., 2016). Additionally, *Arabidopsis* resistance to root-knot nematodes was reliant on the accumulation of 12-OPDA, not JA, as mutants deficient in production of 12-OPDA and JA were hyper-susceptible, but mutants deficient in JA only were as resistant as wild-type plants (Gleason et al., 2016). *OPR3*-silenced tomato mutants showed dramatically lower levels of 12-OPDA and downstream JA products and biosynthesis genes; however, treatment with 12-OPDA, not JA, had significant effects in restoring plant basal resistance against *Botrytis cinerea* (Scalschi et al., 2015). In *AOC* over-expresser lines of rice, higher accumulation of 12-OPDA led to significant resistance against brown planthoppers (BPH), a piercing-sucking insect (Guo et al., 2014). Additionally, treatment with 12-OPDA, but not JA or JA-Ile, led to enhanced resistance to BPH in rice. Supporting our findings, tomato *def1* mutant lost the capacity for ISR against *Fusarium* infection when treated with *T. virens* (Jogaiah et al., 2018). While the authors assigned the lack of ISR to loss of JA in *def1*, the authors did not examine whether OPDA may have been responsible for the loss of ISR, as the mutant was determined to be disrupted in both 12-OPDA and JA biosynthesis (Howe et al., 1996). Increase in OPDA, but not JA, content also correlated with tendril coiling (Stelmach et al., 1998; Blechert et al., 1999). Interestingly, liverwort *Marchantia polymorpha*, a non-vascular plant considered to be one of the earliest land plants still existing, accumulated 12-OPDA in response to wounding, but not JA (Yamamoto et al., 2015). Similarly, moss *Physcomitrella patens* was found to lack the enzymes that convert 12-OPDA to JA, but still maintained the components for JA perception and signaling (Stumpe et al., 2010; Ponce De Leon et al., 2012). Furthermore, a recent study found that *M. polymorpha* COI1 was functionally conserved with AtCOI1, but recognized dinor-OPDA (dn-OPDA) as ligands rather than JA-Ile (Monte et al., 2018). A single amino acid substitution between MpCOI1 and AtCOI1 was responsible for the switch in ligand specificity, suggesting

that OPDA is the more ancient jasmonate signal and that JA-Ile arose later on. These revelations on COI1 also raise the possibility that, unlike the single COI1 in *Arabidopsis*, some of the 6 distinct COI1 proteins of maize may also recognize oxylipins other than JA-Ile.

An additional potential reason for discrepancy between our results and the reports implicating JA in ISR responses is that studies on the role of JA in regulating ISR have typically been performed on dicots such as *Arabidopsis* and tomato. One possible reason for the discrepancy is that JA was considered to be the primary functional outcome of the AOS branch pathway. For example, mutants used in some studies were JA-signaling mutants and not those disrupted in biosynthesis of JA (Pozo et al., 2008). *Pseudomonas fluorescens* WCS417r, a nonpathogenic and biocontrol bacterium, could no longer induce ISR in *jin1*, a JA-insensitive mutant disrupted in *MYC2*. Since JA downstream signaling also results in a positive feedback loop for JA biosynthesis (Wasternack, 2007), JA-insensitive mutants would lack that positive feedback and be unable to trigger upregulation of both JA and 12-OPDA biosynthesis. Tomato *spr2*, the mutant reported to be impaired in wound-induced JA biosynthesis and defense signaling and unable to establish mycorrhiza induced resistance (MIR) (Song et al., 2015), has also been shown to have over 90% decreased 18:3 content in leaves (Li et al., 2003). The decrease in 18:3 content results in a decrease of not only JA, but also 12-OPDA. The mechanisms behind *spr2*MIR-deficient phenotype cannot be unequivocally assigned to only JA, and may instead be due to increased 12-OPDA content.

KODA signaling is also required for ISR

Another key finding of this study is the identification of KODA as another potential ISR signal. The function of KODA has not been extensively studied, with several reports indicating that KODA has flowering-promotion effects in *Lemna paucicostata* (duckweed), apple trees, and Japanese pears (Yokoyama et al., 2000; Kittikorn et al., 2010; Sakamoto et al., 2010). KODA was also reported to accumulate at high levels in duckweed after exposure to abiotic stresses such as drought, heat, or osmotic stresses (Yokoyama et al., 2000). Wheat treated with KODA displayed enhanced abiotic stress tolerance by promoting root elongation at normal and high pH conditions, increasing germination rate and seedling growth, and improving drought tolerance (Haque et al., 2016). One study demonstrated that exogenous application of KODA enhanced grape resistance against *Glomerella cingulate* (Wang et al., 2016). Interestingly, KODA treatment induced high levels of *LOX* and *AOS* expression, which may indicate that KODA induces OPDA biosynthesis as well. While JA and OPDA have been reported to inhibit root growth, increased KODA production in response to *T. virens* may shed some light behind simultaneous growth promotion and ISR induction. While transfusion with concentrations of KODA and 12-OPDA alone were more effective at >100 nM, co-transfusion with 12-OPDA and KODA at 10 nM each resulted in enhanced resistance, suggesting an additive effect (Fig. 12).

In contrast to JA pathway, SA pathway is upregulated during colonization

In agreement with our data showing the downregulation of JA biosynthesis and signaling pathway, transcriptome analysis revealed the upregulation of SA biosynthesis and signaling

pathway, likely due to the SA-JA antagonism well documented in many different plants (Pena-Cortés et al., 1993; Pieterse et al., 2012; Thaler et al., 2012). Genes involved with SA biosynthesis (*PAL1*, *PAL2*, *PAL3*, *PAL5*, *PAL6*, *PAL8*, and *PAL9*) and SA responsive genes (*PR1*, *PR5*, and *PR10*) were mostly upregulated at both 6 and 54 hr (Fig. 17). Recent studies have shown that induction of SA defense is necessary to limit *Trichoderma* colonization of roots to apoplast and excluded from the vascular tissue (Alonso-Ramirez et al., 2014; Martinez-Medina et al., 2017). *T. atroviride* was also demonstrated to induce in *Arabidopsis* defense response genes of both SA and JA/ET pathways during induction of ISR against both hemibiotrophic and necrotrophic pathogens (Salas-Marina et al., 2011).

It is unlikely that SA is the long-distance signal in our study, as we did not observe induction of SA in TvWT-treated plant xylem sap that correlated with ISR, with levels of SA staying relatively unchanged between the different mutants and treatments (Fig. 10F). Our study cannot exclude that SA is not required for ISR, as SA deficient plants were not available for this study. However, it is possible that, similar to its role in SAR (Vernooij et al., 1994; Klessig et al., 2018), SA may be required locally for activation of ISR, but is not the mobile signal. Interestingly, our transcriptome data clearly demonstrated simultaneous upregulation of 12-OPDA and SA biosynthesis and response genes during TvWT root colonization. This raises a question of whether the two pathways are synergistic rather than antagonistic like the well-documented interaction between SA and JA. In support of this idea, studies have shown that genes uniquely regulated by 12-OPDA require activation by bZIP motif-binding transcription factors TGA2, TGA5, and TGA6 (Stotz et al., 2013), all of which interact with NPR1 in SA-mediated defense responses (Zhang et al., 2003). A recent finding showed that both 12-OPDA and SA levels correlated with resistance against *C. graminicola*, with susceptible mutants

accumulating significantly decreased levels of both metabolites (Huang, 2017). Several studies also showed that treatment with either OPDA or SA resulted in increased glutathione (GSH) levels and enhanced cellular reduction potential (Koornneef et al., 2008; Park et al., 2013). Specifically, 12-OPDA binding to cyclophilin 20-3 (CYP20-3) resulted in increased biosynthesis of cysteine and accumulation of GSH, which in turn increased cellular reduction potential, driving expression of several OPDA-responsive genes (Park et al., 2013). Other studies showed that GSH also functioned as a signal for SA-mediated defenses acting through NPR1 (Ghanta et al., 2011), and was required for activation of SA signaling through the accumulation of H_2O_2 (Han et al., 2013). In support of the synergy between OPDA and SA, treatment of *Arabidopsis* rosettes with SA increased AOS activity and OPDA accumulation, while JA levels remained the same (Laudert and Weiler, 1998). The relevance of potential OPDA-SA synergism for ISR induction remains to be studied.

ISR requires functional LOX10 and *T. virens* peptide signal Sm1

As reported in this study, *LOX10* transcriptional activation as early as 2 to 6 hr during interaction between maize roots and *T. virens* required functional peptide signal Sm1 (Fig. 1A). Such early activation is consistent with a previous report showing Sm1 is constitutively expressed and secreted continuously by fungal hyphae even in the absence of a host (Djonovic et al., 2006). Previous studies showed that expression of *LOX10* was overexpressed in the roots of constitutively ISR-active *lox3* mutants (Gao et al., 2008; Constantino et al., 2013). Importantly, expression of *LOX3* in maize roots was suppressed by TvWT in a Sm1-dependent manner (Constantino et al., 2013). These results imply that Sm1-mediated induction of ISR involves

suppression of *LOX3*, the negative regulator of ISR response, resulting in the transcriptional activation and accumulation of LOX10, which in turn produces 12-OPDA as a xylem resident mobile signal for ISR induction. Remarkably, the inability of *Δsm1* to induce ISR was also due to the inability to induce OPDA accumulation, since complementation with OPDA of xylem sap *Δsm1*-treated B73 rescued TvWT-induced levels of ISR (Fig. 13). The exact mode of action on plant cells by Sm1 remains to be further explored. Here we provide additional evidence that Sm1 is a major peptide signal for ISR by demonstrating that the enhanced ISR activation of *Δsir1* mutant is likely due to a 3-fold greater expression of *SM1* (Fig. 1C). The antagonistic interactions between 2 different SSCPs, Sm1 and Sir1, indicate that the individual peptides secreted by *T. virens* may be responsible for different aspects of regulating maize-fungal symbiosis.

A surprising finding of this study is that while TvWT-treated *lox10* mutants displayed ISS phenotype, this phenotype was lost in *lox3lox10* double mutants (Fig. 4). This result implies that functional LOX3 is the major reason behind ISS phenotype in *lox10* mutant plants, again reinforcing the previously reported LOX3 negative role in ISR regulation. Unfortunately, our metabolite profiling of xylem sap from different plant and fungal genotype combinations did not yield any candidates responsible for ISS thus far. The concept of ISS is not a new, as a recent study reported that different accessions of *A. thaliana* treated with different strains of *P. fluorescens* led to either ISR or ISS against bacterial pathogens (Haney et al., 2015). Their findings and our results emphasize the importance of both plant and symbiont genotypes in shaping the outcomes of their interaction.

Is ethylene required for ISR?

Unexpectedly, our study found that treatment of ET-deficient mutant *acs2acs6* with TvWT still induced ISR (Fig. 14C and 14D), suggesting that ET may not be as important for ISR induction. In support of this notion, TvWT colonization of B73, *lox10*, and *lox3* resulted in significantly decreased levels of ET precursor, ACC, content in xylem sap (Fig. 15). The decrease in ACC may be attributed to fungal ACC deaminase (ACCD) activity, which breaks ACC down to ammonia and α-ketobutyrate (Glick et al., 1994), as putative ACCD genes were identified in *Trichoderma* genomes (Kubicek et al., 2011). The reduction of ET results in increased gibberellin (GA) and IAA signaling and improved plant growth (Glick et al., 2007; Hermosa et al., 2012). Pea plants treated with *Variovorax paradoxus*, a rhizobacterium that encodes ACCD, also resulted in enhanced plant growth and yield compared to pea plants treated with mutants disrupted in ACCD activity (Belimov et al., 2009). ACCD silenced mutants of *T. asperellum* lost the ability to enhance root elongation in canola (Viterbo et al., 2010) and could no longer improve salt tolerance (Brotman et al., 2013).

Our results appear to contradict previous studies on ET role in ISR. For example, *Arabidopsis* ET-insensitive mutants, which include *etr1* and *ein2* through *ein7*, treated with *P. fluorescens* WCS417r displayed loss of ISR against *Pseudomonas syringae* pv. *tomato* (Pst), but retained the ability to trigger SAR (Knoester et al., 1999). Similar to our results, induction of ISR with WCS417r was not associated with increased ET levels or upregulation of ET biosynthesis genes ACC synthase (*ACS*) and ACC oxidase (*ACO*). Interestingly, while the mutant *eir1* was only ET insensitive in the roots, WCS417r could still induce ISR when introduced to plant leaves, suggesting that the ET response pathway must remain intact for induction of ISR. Taken

together, our findings indicate that the loss of ET biosynthesis may have no bearing on whether ISR can still occur as long as ET response components stay functional.

Does the balance between TvWT-induced growth promotion and ISR involve differential regulation of 12-OPDA and JA?

In the field of symbiont-host interactions, one of the mysteries that remains to be explored is the mechanism by which PGPR/PGPF induce ISR defense and promote plant growth simultaneously. Plant growth and defense tradeoff can occur depending on environmental cues, prompting the plant to devote more resources towards defense responses or towards growth in the absence of stresses (Huot et al., 2014). In maize, improper balancing between plant growth and defense could be best observed with *lox3* mutants, which overproduces defense hormones SA, JA, and ET in the roots and displays constitutive ISR, but has reduced germination rate, reduced height by ~25-30%, and premature senescence (Gao et al., 2008). Our results showed that *T. virens* enhanced growth of treated *lox10* plants, suggesting that growth promotion and ISR are distinct pathways (Fig. 3). Interestingly, while the *T. virens* mutant *Δsm1* provided moderately better growth promotion effect than TvWT on B73, inferring that without the Sm1-dependent induction of ISR, more plant resources are diverted to growth instead.

There is overwhelming evidence that increased JA and ET content results in impaired plant growth and development (Wasternack and Hause, 2013; Huang et al., 2017; Dubois et al., 2018). Exogenous JA treatment resulted in reduced root growth, leaf expansion, and hypocotyl growth in seedling plants (Wasternack and Hause, 2013). Most recently, overexpression of plastid lipase (*PLIP*) genes was shown to result in significantly higher accumulation of JA,

reducing vegetative growth even when *Arabidopsis* was grown in nutrient rich media (Wang et al., 2018). *Arabidopsis* mutants with constitutive ET response displayed dwarfism, sterility, and premature senescence (Qu et al., 2007), while tobacco mutants with decreased ET sensitivity displayed enhanced growth (Tao et al., 2015).

If JA and ET are major signals for ISR induction by beneficial microorganisms, but both inhibit growth, then it remains unclear how the symbionts could also promote plant growth. The identification of 12-OPDA, rather than JA or ET, as an ISR signal provides an intriguing venue to explore how this widely reported growth-defense balance by *T. virens* is achieved. Currently, studies on the effect of 12-OPDA on plant growth suggest an inhibitory role like JA, though the concentrations used in those studies may not have been biologically relevant. Addition of 25 and 50 μM 12-OPDA to growth media inhibited *M. polymorpha* growth; however, the concentrations used were much higher than those used in our study (Yamamoto et al., 2015). While 12-OPDA was shown to promote *Arabidopsis* (Col-0 and Ws backgrounds) seed dormancy, their study also used much higher concentrations (10 and 50 μM) in the growth media (Dave et al., 2011). In our study, it is possible that by upregulation of 12-OPDA biosynthesis and downregulation of JA biosynthesis and response may be one strategy by which *T. virens* and perhaps other beneficial microorganisms can achieve this balance. This idea warrants further investigation, but has not been part of this study.

Hypothetical model of oxylipin regulation of ISR response

A summary of the maize ISR process induced by *T. virens* is presented (Fig. 19). *T. virens* root colonization results in the suppression of *LOX3* (negative regulator of ISR) in a Sm1-

dependent manner, which allows the upregulation of *LOX10*. Upregulation of *LOX10* and the 12-OPDA biosynthesis genes (*AOS1a, b, c*, and *AOC1*) drives the biosynthesis of 12-OPDA. The downregulation of JA biosynthesis and signaling genes results in the accumulation of 12-OPDA, which can be transported along the xylem to confer systemic resistance throughout the rest of the plant.

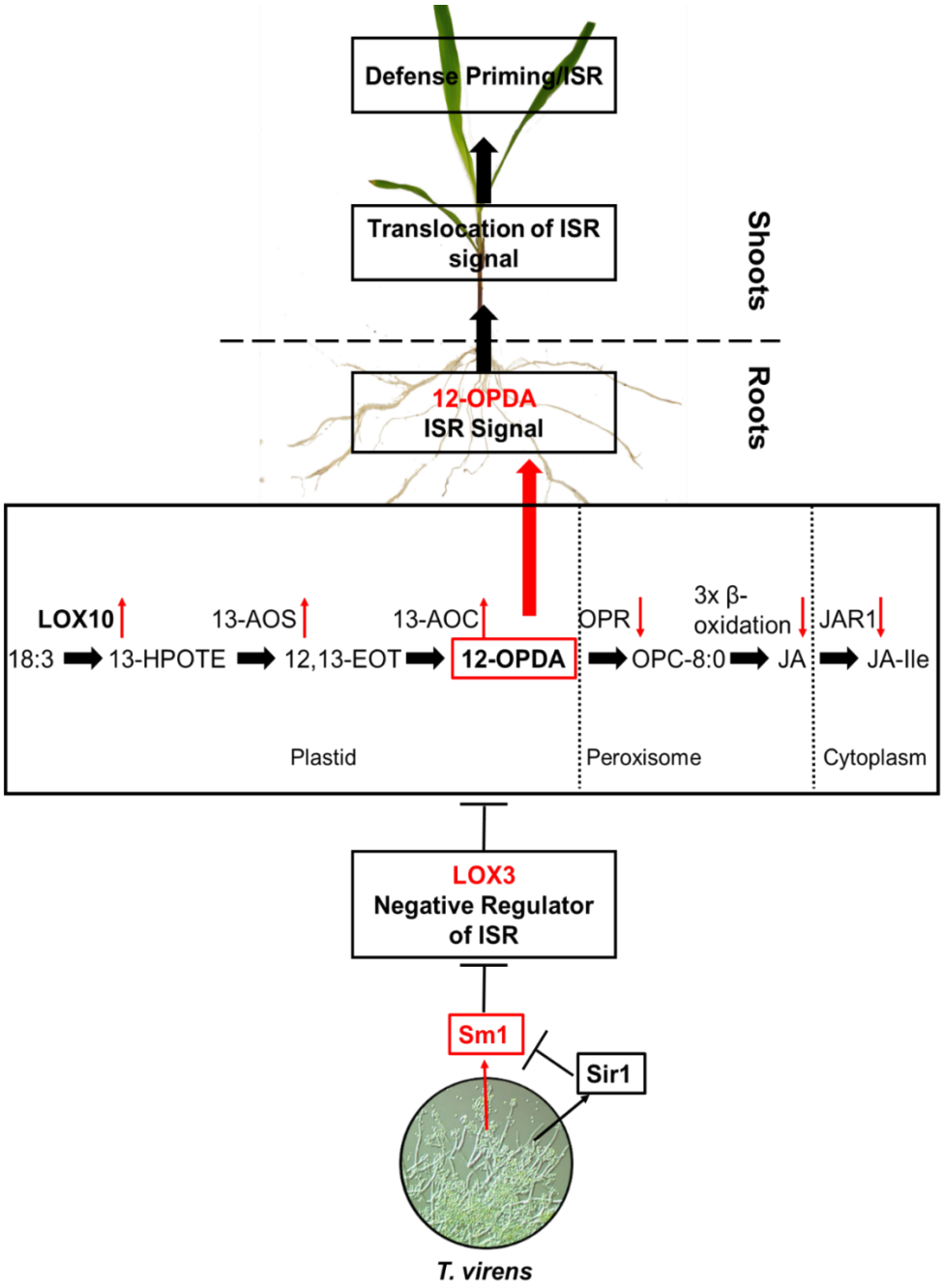

FIGURE 19. Hypothetical model of *T. virens*-triggered ISR in maize.

The below-ground interactions between maize roots and *T. virens* result in the transcriptional and metabolic reprogramming of the roots that leads to synthesis of long-distance ISR signal(s) that travel systemically along the xylem to confer resistance throughout the plant against a broad range of pathogen infection. The fungus suppresses *LOX3* and induces *LOX10* expression, either sequentially or concurrently, in a Sm1-dependent manner. One ISR signal, 12-OPDA, is able to significantly improve systemic resistance and rescue susceptibility.

CHAPTER IV

9-LIPOXYGENASE LOX12 IS A POSITIVE REGULATOR OF *TRICHODERMA VIRENS* TRIGGERED INDUCED SYSTEMIC RESISTANCE (ISR) AND GROWTH

INTRODUCTION

The plant rhizosphere contains many diverse microorganisms ranging from harmful pathogens to plant growth promoting rhizobacteria/fungus (PGPR/PGPF), which provide various benefits to host plants. Among the PGPF, *Trichoderma* spp. are soil-borne fungi found ubiquitously and studied extensively for their ability to impart agriculturally relevant traits, such as enhancing plant growth, mycoparasitism and antibiosis against harmful soilborne pathogens, and triggering induced systemic resistance (ISR) in host plants (Yedidia et al., 1999; Howell et al., 2000; Lorito et al., 2010; Druzhinina et al., 2011; Hermosa et al., 2012). ISR induction by *Trichoderma* spp. is modulated by small secreted peptide elicitors. The small secreted peptide Sm1 from *T. virens* is required to induce ISR in cotton and maize, as the knockout mutant *Δsm1* could no longer induce ISR in treated plants (Djonovic et al., 2006; Djonovic et al., 2007; Constantino et al., 2013). Another peptide elicitor is Suppressor of Induced Resistance, Sir1, formerly known as protein ID 77560 (Joint Genome Institute, *T. virens* version 2), which acts as a negative regulator of ISR (Lamdan et al., 2015). Treatment of maize with the knockout mutant *Δsir1* of *T. virens* resulted in enhanced resistance against the necrotrophic pathogen *Cochliobolus heterostrophus* as compared to treatment with wild-type (WT) *T. virens*. ISR occurs upon root colonization by the beneficial microbes, which are capable of priming of plant defenses to allow rapid and robust responses against systemic pathogen infection (Pieterse et al., 2014a). While no

long-distance signal required for ISR has been identified, in general, Jasmonic acid (JA) and ethylene (ET) have been implicated as the primary plant hormones that mediate the ISR response, at least, in local tissues colonized by symbionts (Pieterse et al., 2014b). Interestingly, the *eir1* mutant of *Arabidopsis thaliana*, insensitive to ET only in the roots, still retained capacity for ISR when treated with *Pseudomonas fluorescens* WCS417r in the plant leaves, suggesting that the ET response pathway must remain intact for local induction of ISR (Knoester et al., 1999). Induction of ISR by WCS417r also had no effect on ET levels or expression of ET biosynthesis genes ACC synthase (*ACS*) and ACC oxidase (*ACO*) in *Arabidopsis*. Additionally, our work presented in Chapter 3 show that JA and ET are not essential for ISR induction, as JA-deficient *opr7opr8* double mutant and ET-deficient *acs2acs6* double mutant both retained the capacity for *T. virens*-induced ISR. Therefore, the actual long-distance signals for ISR have yet to be identified. In contrast to ISR, another distinct pathway for plant systemic resistance is systemic acquired resistance (SAR), which occurs in response to a prior pathogen infection, mediated by salicylic acid (SA) instead, and better characterized (Pieterse et al., 2014a). Several SAR long-distance signals have been identified, including azelaic acid (AzA), pipecolic acid (Pip), methyl salicylate (MeSA), glycerol-3-phosphate (G3P), and dehydroabietinal (DA) (Klessig et al., 2018; Shan and He, 2018).

Along with JA and JA-like derivatives, plants produce an estimated 650 different oxylipins (Borrego and Kolomiets, 2016). Recent studies have shown that induction of ISR involves oxylipins other than JA (Constantino et al., 2013). Oxylipins make up a group of oxidized lipid signals that regulate many aspects of plant physiology, which include root growth and development, reproductive organ development, acclimation to abiotic stresses, and defense responses against pathogens and herbivores (Howe and Jander, 2008; Wasternack and Hause,

2013). Oxylipin synthesis is initiated by lipoxygenase (LOX) enzymes, which catalyze the oxygenation of polyunsaturated fatty acids linoleic acid (C18:2) and linolenic acid (C18:3) at position C-9 or C-13 (Feussner and Wasternack, 2002; Andreou et al., 2009). The carbon position determines whether the LOX is identified as a 9-LOX or 13-LOX. The products of LOX enzymes are fed into seven different branches, which include the allene oxide synthase (AOS) branch, which produces JA and other jasmonates, and hydroperoxide lyase (HPL) branch, which produces six carbon (C6) compounds called green leaf volatiles (GLVs) (Matsui, 2006). The 13-LOX products, which include JA and GLVs, are better characterized, while 9-LOX products are largely unexplored.

While 9-LOX pathway has been linked to several plant functions, such as germination, growth and development, and defense against infection and herbivory (Vellosillo et al., 2007; Nalam et al., 2012), the specific functions of the majority of 9-oxylipins remain elusive. For example, LOX1 in pepper (*Capsicum annuum*) and *Arabidopsis* has been demonstrated to positively regulate plant defense against several pathogens, as the *lox1* mutants accumulated less reactive oxygen species (ROS) and SA and expressed defense response genes at lower levels (Hwang and Hwang, 2010). Another study showed that activity from both 9-LOX and α-dioxygenase (α-DOX), another fatty acid oxygenase, were required for both local defense and activation of SAR in *Arabidopsis* (Vicente et al., 2012). The mutants *lox1*, *dox1*, and *lox1 dox1* were all impaired in their response to *Pseudomonas syringae* pv tomato (*Pst*) infection. The *lox1 dox1* double mutant displayed reduced levels of 9-ketooctadecatrienoic acid (9-KOT), which was found to demonstrate strong antimicrobial activity in vitro against several pathogens, including *Botrytis cinerea*, *Phytophthora infestans*, and *Fusarium oxysporum* (Prost et al., 2005), regulate plant hormone homeostasis. Several 9-LOX derived 10-oxo-11-phytoenoic acid (10-OPEA) and

other cyclopentanones and cyclopentenones were detected at high levels in maize in response to infection by *C. heterostrophus* and insect herbivory (Christensen et al., 2015; Christensen et al., 2016). Pathogenic fungi *Aspergillus flavus* and *Fusarium verticillioides* grown in media containing 10-OPEA were inhibited in growth, while corn earworm (*Helicoverpa zea*) that fed on 10-OPEA-treated leaves were stunted in growth. Furthermore, these 9-LOX products were collectively called "Death Acids," as exogenous application induced expression of a unique set of defense response genes, increased cysteine protease activity, and resulted in potent programmed cell death.

Among the 13 different maize LOXs, LOX3, LOX4, LOX5, and LOX12 are 9-LOXs, while LOX1 and LOX2 have both 9-LOX and 13-LOX activity (Borrego and Kolomiets, 2016; Ogunola et al., 2017). The maize LOX3 plays an important role in regulating defense, as *lox3* mutants displayed robust constitutive systemic resistance against a variety of seed, foliar, root, and stalk pathogens, including the hemibiotrophic foliar and stalk pathogen *Colletotrichum graminicola*, necrotrophic foliar pathogen *C. heterostrophus*, and root pathogen *Exserohilum pedicellatum* (Gao et al., 2007; Isakeit et al., 2007; Constantino et al., 2013). Expression of *LOX3* was detected exclusively in maize roots, with no expression detected in leaves even when infected with *C. graminicola* (Constantino et al., 2013). Roots of *lox3* mutants accumulated significantly higher levels of defense phytohormones jasmonic acid (JA), salicylic acid (SA), and ethylene (ET), and overexpressed genes involved with biosynthesis of those phytohormones (Gao et al., 2008). LOX3 was also shown as a negative regulator of *T. virens*-triggered ISR, as expression of *LOX3* was suppressed in response to root colonization with *T. virens* (Constantino et al., 2013). Furthermore, transfusion of xylem sap collected from untreated *lox3* mutants conferred strong systemic resistance in receiver WT (B73) plants,

suggesting that sap contained root-derived molecule(s) with potent defense signaling activity. Taken together, these findings provided evidence that LOX3 is a root-exclusive negative regulator of *T. virens*-induced ISR.

Of the maize 9-LOXs, LOX4 and LOX5 share ~95% amino acid sequence identity and are differentially expressed spatially and in response to different stimuli (Park et al., 2010). Specifically, *LOX4* was expressed predominantly in below-ground tissue and in response to JA treatment, while *LOX5* expression was mainly in above-ground tissue and in response to JA, SA, wounding, and herbivory. These data suggest that LOX5 has important functions in plant defense, especially against insect herbivory, and is evidenced by *lox5* mutants being significantly more susceptible to insect herbivory (Park, 2012). The roles of LOX4 as a defense gene and LOX5 as a susceptibility gene in maize interactions with *C. graminicola* has been well established (Park, 2012; Constantino, 2017; Damarwinasis, 2018). LOX4 and LOX5 have opposing functions, as *lox4* mutants display enhanced susceptibility to *Colletotrichum graminicola*, causal agent of anthracnose stalk rot and leaf blight, while *lox5* mutants exhibited increased resistance against *C. graminicola* (Park, 2012; Damarwinasis, 2018). A recent study found that GLVs released by *C. graminicola*-infected plants influenced neighbor plants into greater susceptibility to infection by hemibiotrophic and necrotrophic pathogens and greater expression of *LOX5* and *LOX12* (Constantino, 2017). Interestingly, *LOX5* expression was recently found to be overexpressed in *lox4* mutants under drought conditions (Huang, 2017). These studies suggest that LOX5 and LOX12 may act as susceptibility factors, with increased *LOX5* expression being the reason behind increased susceptibility of *lox4* mutants. Expression of the other 9-LOX, *LOX12*, is found in below-ground tissue with highest expression measured in the mesocotyl tissue (Christensen et al., 2014). Furthermore, *LOX12* expression was also greatly

induced in response to infection by *Fusarium verticillioides*, with the *lox12* mutants displaying increased susceptibility to *F. verticillioides* infection due to decreased accumulation of 12-OPDA (JA precursor) and JA, and attenuated expression of JA biosynthesis genes (Christensen et al., 2014).

In Chapter 3, metabolite and phytohormone analysis identified a 9-LOX derived α-ketol, 9-hydroxy-10-oxo-12(Z), 15(Z)-octadecadienoic acid (KODA) that accumulated at higher levels in xylem sap of plants displaying robust ISR response, such as WT *T. virens* (TvWT)-treated B73 and untreated and TvWT-treated *lox3*. Transfusion of KODA at concentrations of 100 nM and above at 10 µL volumes significantly enhanced receiver plant resistance against *C. graminicola* infection in a dose-dependent manner. Transcriptome analysis also revealed overexpression of 9-LOX genes *LOX4*, *LOX5*, and *LOX12* in *lox3* mutant roots, suggesting that the 9-LOX derived oxylipins from these three 9-LOXs play a major role in regulating *T. virens*-induced ISR in maize. To test this hypothesis, we screened several 9-LOX maize mutants and showed that function of LOX12, but not LOX4 or LOX5, is required to establish *T. virens*-induced ISR. Instead of ISR, *T. virens*-colonized *lox12* mutants became more susceptible to pathogen infection, thus displaying an induced systemic susceptibility (ISS) phenotype. The ISS phenotype was also independent of two of *T. virens* peptide elicitors, as treatment with either *T. virens* ISR-deficient mutant *Δsm1* or ISR-enhancing mutant *Δsir1* resulted in ISS.

RESULTS

Overexpression of 9-LOX genes in *lox3* mutant roots identify positive ISR regulator candidates

Previous studies have established maize LOX3 as a key negative regulator of plant defense, with *lox3* mutants over-accumulating defense phytohormones and displaying constitutive ISR (Gao et al., 2007; Gao et al., 2008; Constantino et al., 2013). Expression levels of the different 9-LOX, 13-LOX, and JA biosynthesis genes in *lox3* roots were determined compared to wild-type (WT) B73 inbred through qPCR analysis to identify genes that may be responsible for increased synthesis of OPDA and KODA and resulting constitutive ISR phenotype of *lox3* mutant. (Table 2). Of the 13-LOXs tested, expression of *LOX10* was significantly overexpressed in *lox3* roots compared to B73 roots by ~11-fold. LOX10 provides hydroperoxy fatty acid substrate for both the13-AOS pathway for wound-induced biosynthesis of 12-OPDA and JA, and for the HPL pathway for GLV biosynthesis (Christensen et al., 2013). Expression of the other 13-LOXs, which include *LOX7* and *LOX8,* were not statistically different between *lox3* and B73 roots. Among the genes that comprise the AOS branch for JA biosynthesis, *AOS1c, AOC,* and *OPR7* were significantly upregulated in *lox3* mutant roots, with expression increased up to ~3-, 48-, and 11-fold higher than in B73 roots, respectively. Of the 9-LOX genes screened, *LOX4, LOX5*, and *LOX12* were expressed to higher levels in *lox3* mutant roots, with ~20-, 6-, and 8-fold increases compared to B73, respectively. These data suggest that the upregulated 9-LOX genes may act as positive regulators of ISR in maize.

Function	Gene	Fold	Probability	Result
9- Lipoxygenase	LOX4	20.436	0.005	UP
	LOX5	6.165	0.007	UP
	LOX12	8.51	0.056	UP
13-Lipoxygenase	LOX7	1.822	0.332	
	LOX8	0.932	0.679	
	LOX10	10.819	0.078	UP

TABLE 2: Fold induction of expression of selected LOX genes in *lox3* mutant roots as compared to WT roots by using qPCR.

The 9-LOXs, LOX4 or LOX5, are not required for *T. virens*-mediated ISR

After establishing that 9-LOXs, *LOX4*, *5* and *12*, were overexpressed in *lox3* mutant roots and were good candidates for production of KODA as an ISR long-distance signal, I screened the respective mutants for any alteration in *T. virens*-induced ISR. To test if LOX4 and LOX5 played a role in regulating *T. virens*-induced ISR, untreated and WT *T. virens* (TvWT)-treated B73 inbred (the recurrent WT parent line for the mutants tested in this study) and knock-out mutants, *lox4-7*, *lox5-3*, and *lox4-7 lox5-3* double mutant (*lox4lox5*) were infected with *Colletotrichum graminicola*, the causal agent of anthracnose leaf blight. Lesion areas were compared across the different maize lines and *T. virens* treatments to assess disease progression. Untreated B73 were susceptible, while TvWT-treated B73 displayed the expected ISR phenotype, with significantly smaller lesions developing on the infected leaves (Fig. 20). Consistent with previous reports (Park, 2012; Damarwinasis, 2018), untreated *lox4-7* plants were significantly more susceptible than B73, with larger lesions developing on *lox4-7* leaves compared to untreated B73 leaves, while untreated *lox5-3* mutant leaves developed significantly smaller lesions than on untreated B73 leaves. In the absence of *T. virens*, lesions on *lox4lox5* double mutant were similar to those observed with *lox5-3* mutant, suggesting that the lack of the susceptibility gene, LOX5, overrides the effect of disruption of the defense gene, LOX4. When treated with TvWT, however, *lox4-7* mutants developed significantly smaller lesions in response to *C. graminicola* infection than untreated *lox4-7*, which were comparable to TvWT-treated B73 lesions. The smaller lesions of TvWT-treated *lox4-7* suggest that the capacity for ISR remained intact and that LOX4 function is not important in establishing ISR. TvWT-treated *lox5-3* remained unchanged from untreated *lox5-3*, with significantly smaller lesions comparable to

TvWT-treated B73 and untreated *lox5-3*. This, along with TvWT-treated *lox4lox5* behaving the exact same way as *lox5-3*, strongly confirmed that LOX5, not LOX4, is the main reason behind the observed resistance of the double mutant. Furthermore, TvWT treatment had no additional effects on *lox5-3* and *lox4lox5* resistance, suggesting that while *lox3* mutant overexpressed *LOX4* and *LOX5*, these 9-LOXs were not the positive regulators of ISR, at least in response to *T. virens*-induced ISR in maize.

To confirm that both LOX4 and LOX5 are not involved in ISR, we further screened how *T. virens* secreted peptide elicitors of ISR, Sm1 and Sir1, affected *lox4* and *lox5* mutants and their responses to *C. graminicola* infection. The *lox4-7*, *lox5-3*, and *lox4lox5* mutants and B73 were treated with *Δsm1*, an ISR-negative mutant (Djonovic et al., 2007), and *Δsir1*, an ISR-enhancing mutant previously known as *Δ77560* (Lamdan et al., 2015), and subsequently infected with *C. graminicola*. Consistent with previous reports, *Δsm1*-treated B73 no longer displayed ISR (Djonovic et al., 2007), while *Δsir1*-treated B73 exhibited enhanced ISR compared to TvWT-treated B73 (Fig. 21). Interestingly, treatment of *lox4-7* with either *Δsm1* or *Δsir1* resulted in significantly enhanced resistance similar to TvWT-treated *lox4-7*. This surprising finding suggests that the ISR phenotype observed with *lox4-7* was not Sm1-dependent as it was for B73. Rather, LOX4 may play a role in only allowing ISR to occur in the presence of *T. virens* Sm1. Similar to what was previously observed, both *lox5-3* and *lox4lox5* remained resistant against *C. graminicola* infection when treated with either *Δsm1* or *Δsir1*. These data suggest that the resistance observed with *lox5-3* and *lox4lox5* mutants occur regardless of presence or absence of *T. virens* and that LOX5 may in fact be a susceptibility gene to *C. graminicola* infection, that may function only at local site of infection. Altogether, while LOX4 is clearly not required for

ISR induction, the function of LOX5 as the susceptibility gene in locally infected tissue is clear, however, its relevance to ISR will have to be elucidated further.

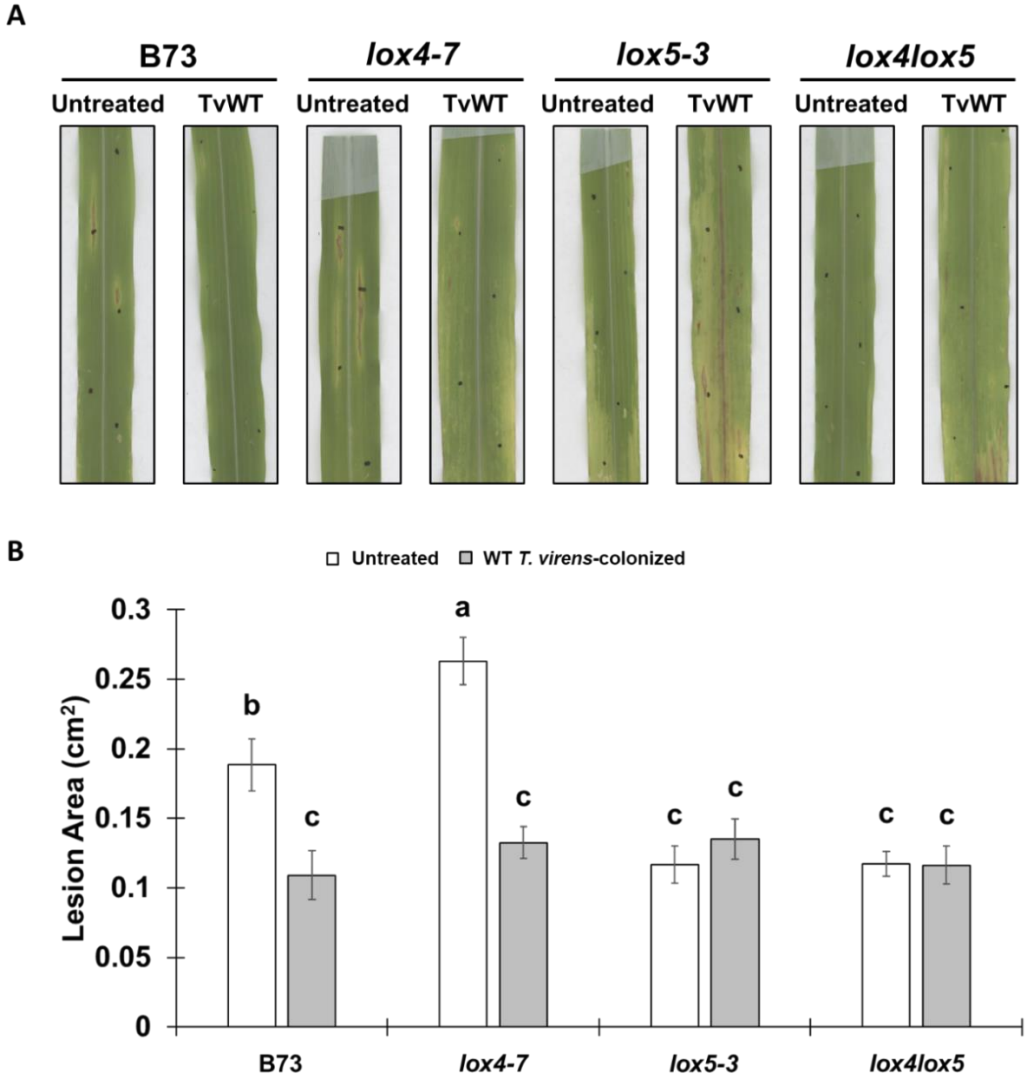

FIGURE 20. LOX4 does not play any major roles in regulation of *T. virens*-triggered ISR against hemibiotrophic pathogen *C. graminicola*.

(A) Lesions developed on 3rd leaves of untreated or TvWT-treated B73 inbred line, *lox4-7*, *lox5-3*, and *lox4lox5* double mutant plants infected with *C. graminicola*.

(B) Measurements of lesion area caused by *C. graminicola* infection on leaves of untreated or TvWT-treated B73 inbred line, *lox4-7*, *lox5-3*, and *lox4lox5* double mutant plants. Values represent means ± standard deviation SD (n=5), with letters indicating significant differences between treatments (Tukey's HSD test, $p < 0.05$).

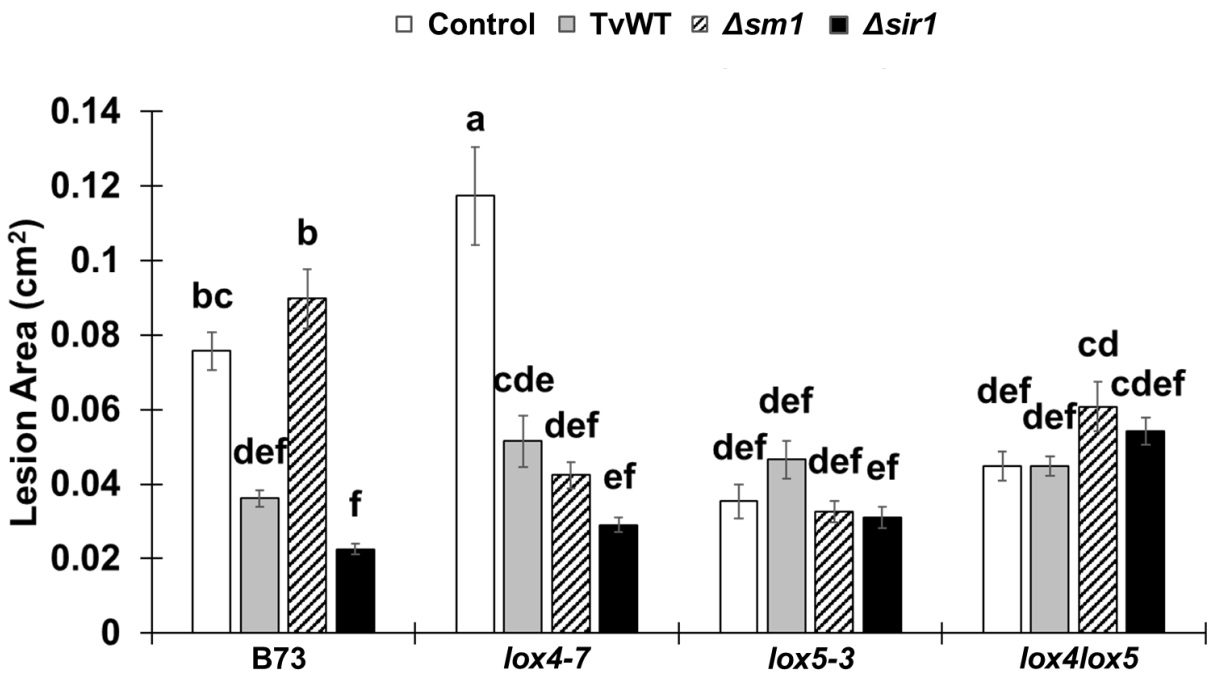

FIGURE 21. LOX4 and LOX5 are not impacted by *T. virens* fungal elicitors Sm1 or Sir1. Measurements of lesion area caused by *C. graminicola* infection on leaves of untreated or TvWT-, *Δsm1*-, and *Δsir1*-treated B73 inbred line, *lox4-7*, *lox5-3*, and *lox4lox5* double mutant plants. Values represent means ± standard deviation SD (n=5), with letters indicating significant differences between treatments (Tukey's HSD test, $p < 0.05$).

LOX12 is a positive regulator of *T. virens*-mediated ISR

In order to test the role of the only other predominant 9-LOX in the maize genome, LOX12, in regulating *T. virens*-induced ISR, I utilized the same approach used to test *lox4* and *lox5* mutants as described above B73 and *lox12-1* mutant in the B73 background and at BC7 stage were either untreated or treated with TvWT and subsequently challenged with *C. graminicola* foliar infection. Surprisingly, untreated *lox12-1* leaves developed smaller lesions in response to *C. graminicola* infection compared to untreated B73 (Fig. 22A). This resistance, however, was lost when *lox12-1* mutants were treated with TvWT. Rather, leaves of TvWT-treated *lox12-1* developed significantly larger lesions compared to untreated *lox12-1*, displaying ISS phenotype. In the absence of *T. virens* colonization, another independent mutant allele of *LOX12*, *lox12-2,* in the B73 background and at BC5 stage, also displayed heightened resistance compared to untreated near-isogenic WT against *C. graminicola* infection (Fig. 22B). Similar to *lox12-1* allele, TvWT-treated *lox12-2* displayed ISS, with significantly larger lesions developing on infected leaves compared to untreated *lox12-2* mutants. Altogether, these results suggest that LOX12 function is required for establishing *T. virens*-induced ISR. Interestingly, in addition to the lack of ISR phenotype of TvWT-treated *lox12* mutants, *lox12-1* also lost shoot growth promotion due to TvWT root colonization, suggesting that LOX12 acts as a positive regulator of above-ground growth (Fig. 23). This is in sharp contrast to *lox10* mutants reported in Chapter 3, which retained *T. virens* growth promotion effect but displayed ISS instead of ISR when treated with TvWT.

LOX12 expression was upregulated by *T. virens* treatment, as qPCR analysis revealed that TvWT treatment induced expression of *LOX12* in B73 roots under hydroponic conditions

across all time points tested, with the highest induction occurring at 12 and 48 hr after treatment (Fig. 24A). Furthermore, transgenic *Arabidopsis* mutants expressing β-glucuronidase (*GUS*) under the control of maize LOX12 promoter (*pLOX12::GUS*) displayed strong GUS activity upon treatment with TvWT (Fig. 24B). Interestingly, GUS staining was strongest not in the roots, but in the vasculature tissue of coleoptiles and in the above-ground organs. Vasculature-centered expression pattern is indicative to the potential signaling properties of the LOX12 oxylipin product(s). Overall, these findings show that expression of *LOX12* is induced in response to TvWT treatment and reinforces the conclusion that LOX12 functions as a positive regulator of ISR.

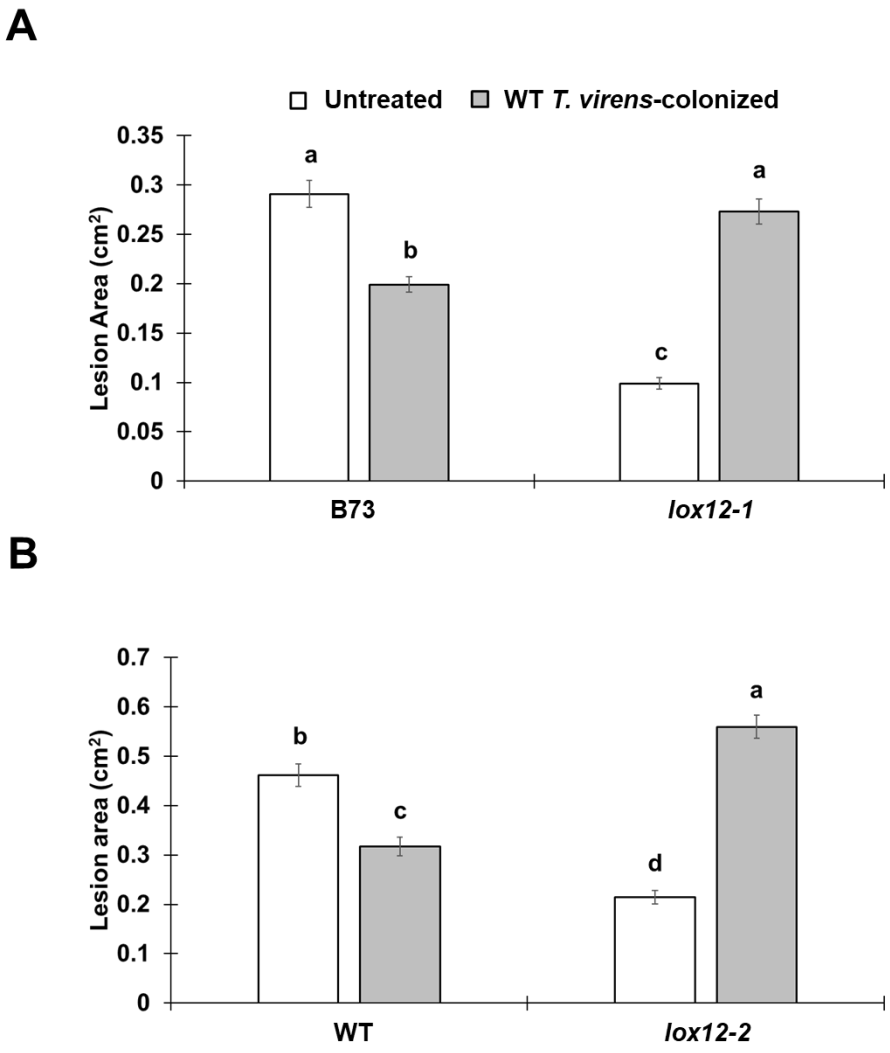

FIGURE 22. LOX12 acts as a positive regulator of *T. virens*-triggered ISR against hemibiotrophic pathogen *C. graminicola*.

(A) Measurements of lesion area caused by *C. graminicola* infection on leaves of untreated or TvWT-treated B73 inbred line and *lox12-1* mutant plants. Values represent means ± standard deviation SD (n=5), with letters indicating significant differences between treatments (Tukey's HSD test, $p < 0.05$).

(B) Measurements of lesion area caused by *C. graminicola* infection on leaves of untreated or TvWT-treated B73 inbred line and *lox12-2* mutant plants. Values represent means ± standard deviation SD (n=5), with letters indicating significant differences between treatments (Tukey's HSD test, $p < 0.05$).

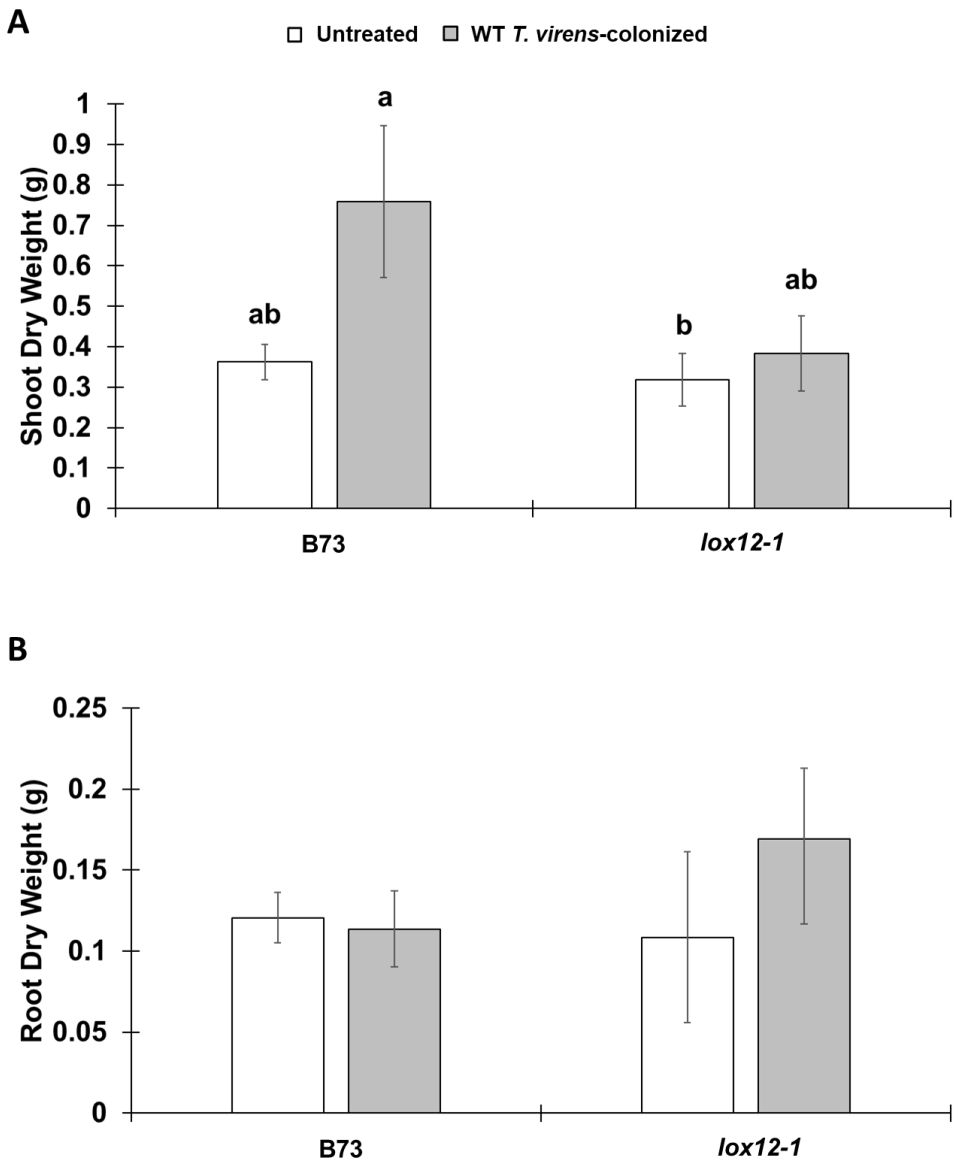

FIGURE 23. LOX12 is required for *T. virens* shoot growth promotion.

Measurements of average shoot and root tissue dry weight of untreated and TvWT-treated B73 and *lox12-1* plants. Values represent means ± standard deviation SD (n=5), with letters indicating significant differences between treatments (Tukey's HSD test, $p < 0.05$).

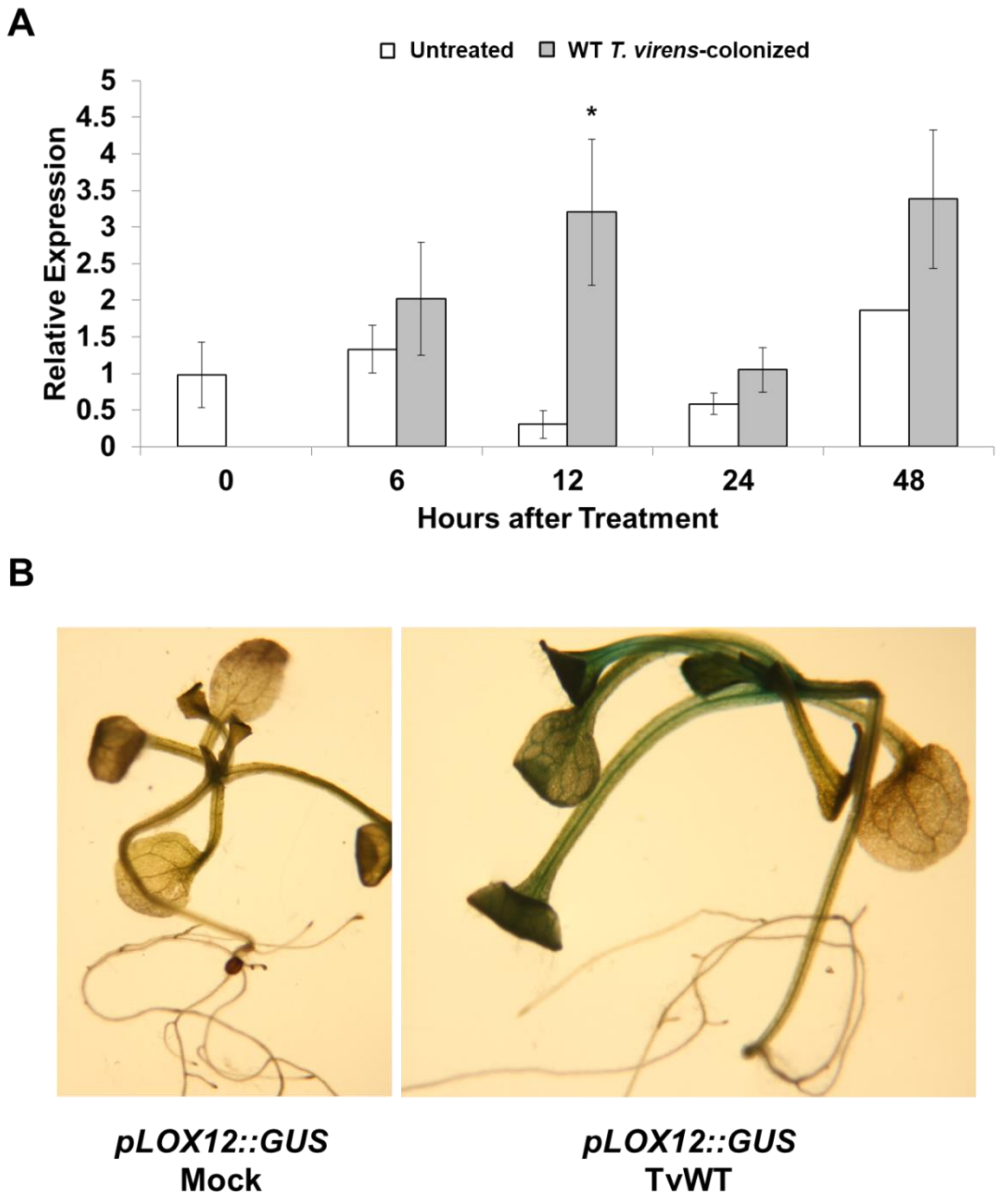

FIGURE 24. *LOX12* expression is induced by *T. virens*.

(A) Expression of *LOX12* via qPCR was determined in B73 seedling roots after treatment with TvWT at 6, 12, 24, and 48 hours after treatment compared to untreated control plants. Relative expression was calculated from cycle threshold values using the $2^{-\Delta\Delta Ct}$ method. Values represent means ± standard deviation SD (n=3) relative to control plants and were normalized to transcript levels of *α-Tubulin* (*α-TUB*). Statistical significance (* represents $p < 0.05$) was determined with Tukey's HSD test compared to control.

(B) Transgenic *Arabidopsis* expressing β-glucuronidase (*GUS*) under control of maize LOX12 promoter (*pLOX12::GUS*) were treated with TvWT and stained for GUS activity.

lox12 ISS phenotype may be due to the loss of *LOX10* induction

The maize LOX3 has been established as a negative regulator of ISR (Constantino et al., 2013), so one possible reason behind the ISS phenotype observed with *lox12* mutants is aberrant expression of *LOX3*. To test this hypothesis, I measured expression of *LOX3* in B73 and *lox12-1* seedlings grown in hydroponic conditions at 6 and 30 hr after treatment with TvWT. The time points 6 hr and 30 hr represented recognition between maize and *T. virens* and initial *T. virens* colonization of maize roots, respectively. The untreated *lox12-1* mutants expressed *LOX3* at levels ~2-fold greater than untreated B73 at both 6 and 30 hr (Fig. 25). Surprisingly, *LOX3* transcript accumulation in TvWT-treated *lox12-1* was induced 30-fold higher than TvWT-treated B73 at 6 hr and 2-fold higher at 30 hr after treatment. This abnormal upregulation of *LOX3* transcripts suggests that LOX3 overexpression may be the primary reason behind the ISS phenotype of TvWT-treated *lox12* mutants. To test this idea, I generated *lox3-4 lox12-1* double mutant (*lox3lox12*) to observe interactions with *T. virens* and test for capacity for ISR. Untreated and TvWT-, *Δsm1*-, and *Δsir1*-treated B73, the single mutants *lox3-4* and *lox12-1*, and *lox3lox12* were challenged with *C. graminicola*, and lesion area was measured and compared across maize mutants and treatments. As was previously reported (Constantino et al., 2013), untreated and TvWT-treated *lox3-4* displayed constitutive ISR, with TvWT treatment having no additive effects on *lox3-4* resistance (Fig. 26). Surprisingly, *lox12-1* retained the ISS phenotype when treated with either *Δsm1* or *Δsir1*, suggesting that these *T. virens* peptide elicitors had no bearing on *lox12* ISS phenotype. Untreated by *T. virens lox3lox12*double mutant displayed increased resistance similar to that observed with *lox12-1* single mutant. Interestingly, as with *lox12-1*, *lox3lox12* also displayed ISS phenotype when treated with TvWT, *Δsm1*, or *Δsir1*. These results

suggest that loss of LOX3 was insufficient to prevent the ISS phenotype in *lox12* mutants and that overexpression of LOX3 in *lox12* mutant is not the reason for ISS. Conversely, the constitutive ISR phenotype of *lox3* mutants could be attributed to a overexpression of *LOX12*.

If abnormal upregulation of *LOX3* in *lox12* mutants was not the reason behind the ISS, then perhaps the loss of induction of a positive regulator of ISR may be the reason instead. In Chapter 3, we established that the LOX10 acts as a positive regulator of ISR through direct production of 12-OPDA and promotion of 9-LOX-derived KODA biosynthesis. To determine whether disruption of *lox12* results in altered expression of *LOX10*, we extracted RNA from roots of *lox12-1* and *lox3lox12* grown in hydroponic conditions and treated with TvWT at 6 and 30 hr and performed qPCR. The analyses revealed that, as reported in Chapter 3, expression of *LOX10* was induced in B73 roots 6 hr after TvWT treatment (Fig. 27A). Interestingly, *LOX10* was not induced in either *lox12-1* or *lox3lox12* roots at 6 hr after TvWT treatment. These results suggest that LOX10 may contribute to the ISS phenotype of both *lox12-1* and *lox3lox12* mutants. On the other hand, *LOX12* expression remained relatively unchanged in both *lox10-3* and *lox3lox10* mutants (Fig. 27B). These findings suggest that LOX10 and LOX12 do not reciprocally regulate each other, with LOX12 acting upstream of *T. virens*-induced *LOX10* expression. Altogether, these findings place LOX12 as acting downstream of LOX3 and upstream of LOX10 in regulating ISR.

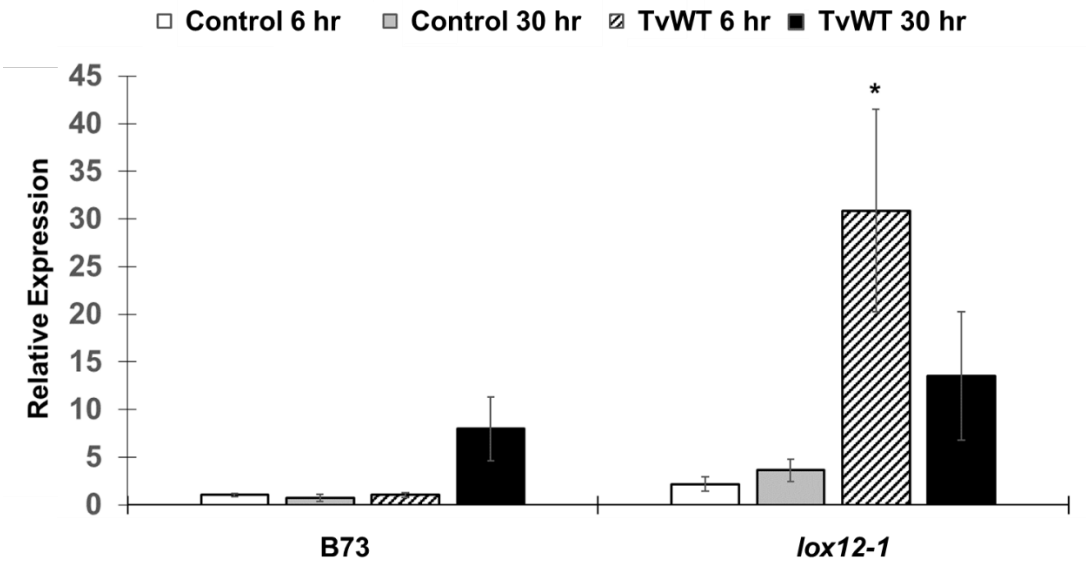

FIGURE 25. *LOX3* expression in *lox12-1* mutant is strongly induced by *T. virens*. Expression of *LOX3* via qPCR was determined in B73 and *lox12-1* seedling roots after treatment with TvWT at 6 and 30 hours after treatment compared to untreated control plants. Relative expression was calculated from cycle threshold values using the $2^{-\Delta\Delta Ct}$ method. Values represent means ± standard deviation SD (n=3) relative to control plants and were normalized to transcript levels of *α-Tubulin* (*α-TUB*). Statistical significance (* represents $p < 0.05$) was determined with Tukey's HSD test.

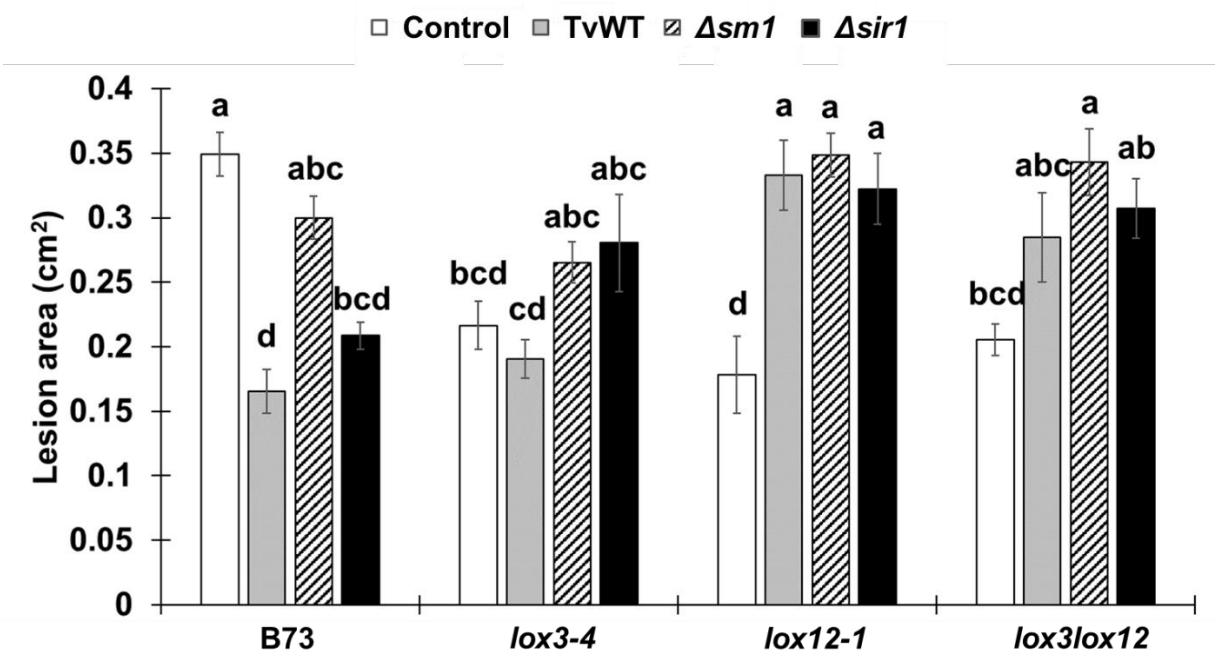

FIGURE 26. Loss of LOX12 function in *lox3* mutant is the cause for ISS phenotype. Measurements of lesion area caused by *C. graminicola* infection on leaves of untreated or TvWT-, *Δsm1*-, and *Δsir1*-treated B73 inbred line, *lox3-4*, *lox12-1*, and *lox3lox12* double mutant plants. Values represent means ± standard deviation SD (n=5), with letters indicating significant differences between treatments (Tukey's HSD test, $p < 0.05$).

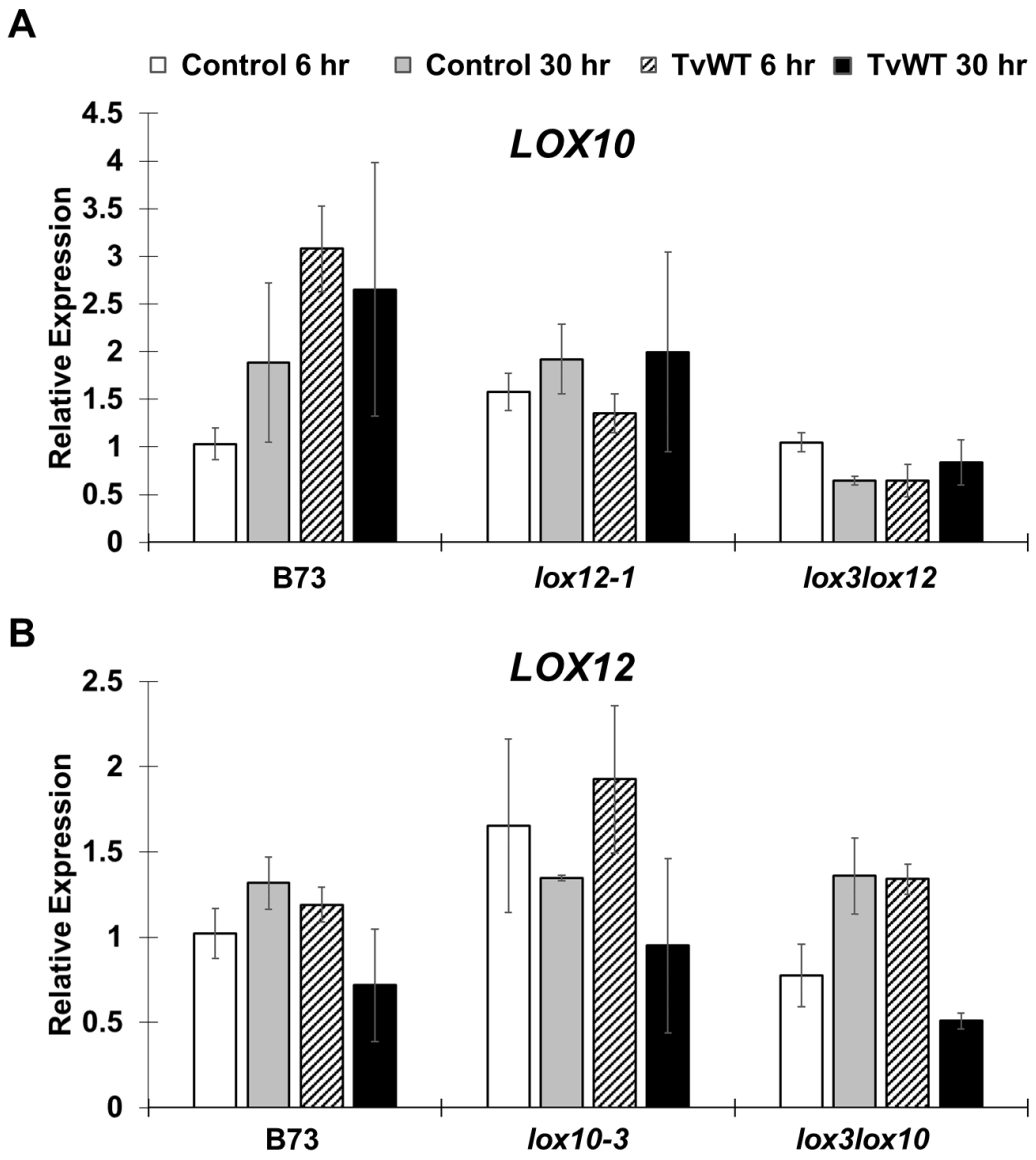

FIGURE 27. *LOX10* induction by *T. virens* requires functional LOX12.

(A) Expression of *LOX10* via qPCR was determined in B73, *lox12-1*, and *lox3lox12* seedling roots after treatment with TvWT at 6 and 30 hours after treatment compared to untreated control plants. Relative expression was calculated from cycle threshold values using the $2^{-\Delta\Delta Ct}$ method. Values represent means ± standard deviation SD (n=3) relative to control plants and were normalized to transcript levels of *α-Tubulin* (*α-TUB*).

(B) Expression of *LOX12* via qPCR was determined in B73, *lox10-3*, and *lox3lox10* seedling roots after treatment with TvWT at 6 and 30 hours after treatment compared to untreated control plants. Relative expression was calculated from cycle threshold values using the $2^{-\Delta\Delta Ct}$ method. Values represent means ± standard deviation SD (n=3) relative to control plants and were normalized to transcript levels of *α-Tubulin* (*α-TUB*).

DISCUSSION

The maize 9-LOX, LOX12, plays a major role as a positive regulator of ISR

In this study, we sought to determine if 9-LOX derived oxylipins have a role in the positive regulation of ISR in *T. virens*-colonized maize plants. The signaling pathways of JA and ET have long been proposed as the key components in regulating ISR signaling in plants (Pieterse et al., 2014a). Chapter 3 describes our results that shows that JA precursor, 12-OPDA, and not JA itself is a likely long-distance signal for ISR. Recent evidence suggests that 9-LOX-derived oxylipins also play major roles in regulating both local and systemic resistance against pathogen infection. Maize 9-LOX, LOX3, acts as a negative regulator of ISR, as *lox3* mutants display strong, constitutive systemic resistance against a variety of pathogens (Gao et al., 2007; Isakeit et al., 2007; Constantino et al., 2013). In Chapter 3, I screened oxylipin content in xylem sap of ISR-positive and negative plants and identified the α-ketol, KODA, as an ISR signal that could enhance resistance against pathogen infection in a dose-dependent effect at extremely low nM concentrations. Maize mutants disrupted in LOX10, a 13-LOX, displayed ISS phenotype and had lower levels of KODA. KODA itself, however, is produced through 9-LOX and 9-AOS activity, implying that there must be a 9-LOX responsible for KODA biosynthesis. Therefore, I screened available 9-LOX mutants to test whether any 9-LOX gene is involved induction of ISR by *T. virens*. I reasoned that such a 9-LOX may be overexpressed in the roots of *lox3* mutant that displays strong ISR response even in the absence of *T. virens* colonization. Table 2 shows that those 9-LOX genes are *LOX4*, *LOX5*, and *LOX12*. Interestingly, a recent study revealed that *lox3* mutant kernels, which are resistant against *Fusarium verticillioides*, overexpress these

three genes as well in response to *Fusarium* infection and that these mutants displayed increased susceptibility to *Fusarium* infection (Battilani et al., 2018). That study validated these 9-LOX genes as vital to maize resistance and potential regulators of ISR. ISR tests of the 9-LOX knockout mutants revealed that LOX4 is not required for ISR induction by *T. virens*. *lox4* mutants responded to *T. virens* by displaying strong ISR against *C. graminicola*, implying that this gene is not required for ISR (Fig. 20). The function of LOX5 in ISR could not be established conclusively as *LOX5* is a susceptibility gene to *C. graminicola* in locally infected leaf tissue (Constantino, 2017; Damarwinasis, 2018). *lox5* mutants were resistant to infection regardless of *T. virens* treatment. To test for the role of this gene in *Trichoderma*-colonized roots would require use of grafting approaches, which is impossible in monocot species.

A key finding in this Chapter was that among the 9-LOXs tested, LOX12 was identified as a positive regulator of *T. virens*-induced ISR, as *lox12* mutants lost ISR response and exhibited increased susceptibility to *C. graminicola* infection in response to root colonization by *T. virens* (Fig. 22). Additionally, expression of *LOX12* was strongly induced in B73 roots treated with *T. virens* (Fig. 24A), and transgenic *Arabidopsis* expressing *pLOX12::GUS* accumulated high levels of GUS in the vasculature tissues of coleoptile and above-ground organs in response to *T. virens* treatment (Fig. 24B). The ISS phenotype of *lox12* and the induction of *LOX12* expression in response to *T. virens* suggests that LOX12 function is required for *T. virens*-induced ISR. These results support the hypothesis that 9-oxylipins play a major role in ISR signaling. A role for 9-LOXs in ISR was also proposed in recent studies that showed silencing the 9-LOX, *PvLOX2,* by RNA interference (RNAi) in beans resulted in loss of mycorrhizae-induced resistance (MIR) against the foliar pathogen *Sclerotinia sclerotiorum* (Mora-Romero et al., 2015a; Mora-Romero et al., 2015b). AM fungal colonization of tomato roots resulted in

strong induction of *LOXA* and *AOS3*, which are directly associated with biosynthesis of 9-LOX derived oxylipin (Garrido et al., 2010; López-Ráez et al., 2010). Aside from regulating ISR, 9-oxylipins also appear to regulate SAR, as *Arabidopsis* 9-LOX mutant, *lox1*, α-DOX mutant *dox1*, and *lox1 dox1* double mutant were all impaired in local defense and SAR activation against *Pst* infection (Vicente et al., 2012). Altogether, these studies demonstrated the defensive activity of 9-LOX derived oxylipins (Vellosillo et al., 2007; Mosblech et al., 2009). While the specific 9-LOX derived oxylipins responsible for ISR or SAR were not identified in any of these studies, we have provided additional evidence of the importance of the 9-LOX products in regulating plant-symbiont interactions.

lox12 ISS phenotype is not associated with overexpression of LOX3 but may be due to loss of *LOX10* induction by *T. virens*

Interestingly, treatment of *lox12* mutants with both ISR-deficient mutant *Δsm1* (Djonovic et al., 2007) and ISR-enhancing mutant *Δsir1* (Lamdan et al., 2015) resulted in increased susceptibility, a phenomenon called (ISS) (Fig. 26). I showed that *lox12* ISS is unaffected by either of the *T. virens* secreted peptide elicitors. As LOX3 is an established negative regulator of ISR and a target by *T. virens* for suppression in maize roots (Constantino et al., 2013), the likely explanation for *lox12* ISS phenotype was an upregulation of *LOX3* in roots. Supporting this hypothesis, qPCR analysis showed that *lox12* mutants overexpressed *LOX3* ~30-fold higher than B73 when treated with WT *T. virens* (Fig. 25). Contradicting this hypothesis, though, is that the double mutant *lox3lox12* also displayed ISS phenotype when treated with *T. virens* (Fig. 26). This finding confirms that the *lox3* mutant constitutive ISR phenotype required LOX12 function

and that LOX3 is not the driver of ISS. In Chapter 3, we established that LOX10, a 13-LOX, is a positive regulator for ISR, with expression in roots upregulated transiently in response to *T. virens* treatment. qPCR analysis revealed that neither *lox12* nor *lox3lox12* mutant responded to *T. virens* by induction of *LOX10* (Fig. 27A), confirming the hypothesis that LOX10 is the reason behind *lox12* ISS. These results also support the notion that 9-LOX pathway and 9-oxylipin signals (such as KODA) must precede the 13-LOX pathway and 13-oxylipin signals (such as 12-OPDA) for induction of ISR.

Maize 9-LOXs, LOX3 and LOX12, appear to play opposing roles, with LOX3 acting as a negative regulator and LOX12 as a positive regulator of *T. virens*-induced ISR. While *lox3* mutant roots accumulate higher levels of 12-OPDA and JA, *lox12* mutants accumulate less, leading to increased susceptibility to *Fusarium* infection (Christensen et al., 2014). Several studies on arbuscular mycorrhizae (AM) fungi and plant 9-LOXs also demonstrate contrasting roles of 9-LOXs with regards to MIR. Silencing of the 9-LOX, *LOX2,* in beans resulted in loss of MIR and decreased expression of *LOX6*, the 13-LOX responsible for JA biosynthesis (Mora-Romero et al., 2015b). The bean LOX2 activity is reminiscent of maize LOX12, as loss of either resulted in decreased JA biosynthesis and loss of ISR/MIR. Another study showed that potato 9-LOX, *AOS3*, was upregulated in response to AM fungal colonization, resulting in higher accumulation of KODA and other 9-oxylipins in the roots (Morcillo et al., 2016). This corroborates data in Chapter 3, where increased KODA levels in xylem sap strongly correlated with ISR, while decreased levels of KODA, especially in *lox10* mutants correlated with lack of resistance and ISS phenotype. RNA-mediated silencing of *AOS3* resulted in increased 13-LOX and JA biosynthesis genes, JA, and root colonization by AM fungus. While not a 9-LOX, potato AOS3 appears to function in a similar manner to maize LOX3 as negative regulators of JA

biosynthesis. Unfortunately, outside of root colonization and JA biosynthesis, no data were provided on whether over-colonization resulted in hindering plant growth or improved MIR, making a comparison difficult.

There is also evidence that both 9- and 13-LOX pathways are required for establishing ISR. Upregulation of tomato 9-LOX, *LOXA*, and 9-AOS, *AOS3*, genes were limited to the AM fungus-colonized parts of the roots and required the activation of JA pathway (León-Morcillo et al., 2012). Another study showed that JA perception was required to regulate AM colonization in tomato roots, as jasmonic acid deficient mutant 1 (*jai1*) was over-colonized, while exogenous foliar treatment with methyl-JA (MeJA) resulted in decreased root colonization by AM fungus (Herrera-Medina et al., 2008). Taken together, these studies infer that 9- and 13-LOX pathway crosstalk is required to both control colonization and MIR. This clearly supports my results in Chapter 3 and this chapter, as both the 13-LOX, LOX10, and 9-LOX, LOX12, are required for *T. virens*-induced ISR.

Conclusion

This study built upon the findings from Chapter 3 and identified LOX12, a 9-LOX, as a positive regulator of ISR that acts in concert with LOX10. Like *lox10* mutants, *lox12* mutants also displayed increased susceptibility in response to *T. virens* root colonization. The exact 9-oxylipin produced by LOX12 has yet to be identified, but the likely candidate is KODA, a 9-LOX derived α-ketol, since it has been demonstrated to positively affect ISR. Based on expression patterns of *lox10* and *lox12* mutants, we also conclude that LOX12 acts upstream of LOX10, with LOX12 activity required for *T. virens* induction of *LOX10* expression in maize

roots. The exact hierarchy of LOX10 and LOX12 in positive regulation of ISR will require construction of l*ox10lox12* double and *lox3lox10lox12* triple mutants currently underway in our laboratory.

CHAPTER V

SUMMARY

Major agricultural advances must occur to contend with the increasing global population and the increasing demand for food and resources without increasing pollution or environmental damage through the overuse of fertilizer and chemical pesticides. The study of plant-microbe interactions is one potential avenue to meet these demands, as many of these microbes can provide benefits for plant hosts, such as enhanced growth, better nutrient uptake, abiotic stress tolerance, and improved resistance against pathogen infection and herbivory. One form of enhanced plant resistance is induced systemic resistance (ISR), which primes plant defenses for rapid and robust responses against infections locally and systemically. One beneficial microbe, *Trichoderma virens*, is well documented for its ability to enhance plant growth and trigger ISR in host plants. The main objectives of this project were to identify important genes and signal molecules that regulate *T. virens*-induced ISR in maize

Maize LOX10, a 13-LOX involved in wound-induced jasmonic acid (JA) biosynthesis, was both induced in B73 inbred wild-type maize roots in response to the beneficial fungus *T. virens* and overexpressed in constitutive ISR *lox3* mutant roots. Treating *lox10* mutants with *T. virens* resulted in increased susceptibility against infection by the foliar hemibiotrophic pathogen *Colletotrichum graminicola*. We have called this phenotype induced systemic susceptibility (ISS). Metabolite profiling of xylem sap collected from untreated or *T. virens*-treated B73, *lox3*, and *lox10* identified 12-OPDA, 13-LOX and 13-AOS derived precursor of JA biosynthesis, and 9-hydroxy-10-oxo-12(Z),15(Z)-octadecadienoic acid (KODA), 9-LOX and 9-AOS derived α-

ketol, as two oxylipins whose accumulation corresponded to ISR-positive plants. Demonstrating signaling roles, low volume transfusion of OPDA or KODA in biologically relevant (nM) concentrations enhanced receiver plant resistance in a dose-dependent manner, while JA-Ile transfusion resulted in increased susceptibility. Surprisingly, both JA-deficient mutant *opr7opr8* and ethylene (ET)-deficient mutant *acs2acs6* retained the capacity for *T. virens*-induced ISR, suggesting that neither phytohormone is required. Transcriptome analysis of *T. virens*-treated B73 revealed that genes for 12-OPDA biosynthesis (*LOX10, AOS1a, b, c,* and *AOC1*) were upregulated in response to *T. virens*, but subsequent genes for JA biosynthesis and signaling were downregulated. Altogether, these results portray 12-OPDA and KODA, rather than JA or ET, as the key regulators of *T. virens* ISR.

In addition to *LOX10*, *lox3* roots overexpressed three 9-LOX genes, *LOX4*, *LOX5*, and *LOX12*, suggesting that 9-oxylipins also play a role in regulating ISR. Screening *T. virens*-treated *lox4*, *lox5*, and *lox12* for ISR phenotype revealed that LOX12 acts as a positive regulator of ISR, as *lox12* mutants displayed ISS phenotype in response to *T. virens* colonization. Furthermore, *lox3lox12* double mutant displayed ISS phenotype as well in response to *T. virens*, demonstrating that the constitutive ISR of *lox3* is contingent on LOX12 function. Interestingly, both *lox12* and *lox3lox12* mutant roots lack the induction of *LOX10* expression in response to *T. virens*, suggesting that LOX12 activity is required for the initiation of ISR. Altogether, these results place LOX12 upstream of LOX10 and downstream of LOX3 and portrays ISR as a complex pathway that requires both 9- and 13-oxylipins to operate.

REFERENCES

Alonso-Ramirez, A., Poveda, J., Martin, I., Hermosa, R., Monte, E., and Nicolas, C. (2014). Salicylic acid prevents *Trichoderma harzianum* from entering the vascular system of roots. Molecular Plant Pathology **15,** 823-831.

Andreou, A., Brodhun, F., and Feussner, I. (2009). Biosynthesis of oxylipins in non-mammals. Progress in Lipid Research **48,** 148-170.

Baek, J.M., and Kenerley, C.M. (1998). The *arg2* gene of *Trichoderma virens*: cloning and development of a homologous transformation system. Fungal Genetics and Biology **23,** 34-44.

Battilani, P., Lanubile, A., Scala, V., Reverberi, M., Gregori, R., Falavigna, C., Dall'Asta, C., Park, Y.S., Bennett, J., and Borrego, E.J. (2018). Oxylipins from both pathogen and host antagonize jasmonic acid-mediated defence via the 9-lipoxygenase pathway in *Fusarium verticillioides* infection of maize. Molecular Plant Pathology **19,** 2162-2176.

Belimov, A.A., Dodd, I.C., Hontzeas, N., Theobald, J.C., Safronova, V.I., and Davies, W.J. (2009). Rhizosphere bacteria containing 1-aminocyclopropane-1-carboxylate deaminase increase yield of plants grown in drying soil via both local and systemic hormone signalling. New Phytologist **181,** 413-423.

Blechert, S., Bockelmann, C., Fusslein, M., Von Schrader, T., Stelmach, B., Niesel, U., and Weiler, E.W. (1999). Structure-activity analyses reveal the existence of two separate groups of active octadecanoids in elicitation of the tendril-coiling response of *Bryonia dioica* Jacq. Planta **207,** 470-479.

Borrego, E.J., and Kolomiets, M.V. (2016). Synthesis and functions of jasmonates in maize. Plants **5,** 41.

Brotman, Y., Landau, U., Cuadros-Inostroza, A., Tohge, T., Fernie, A.R., Chet, I., Viterbo, A., and Willmitzer, L. (2013). *Trichoderma*-plant root colonization: escaping early plant defense responses and activation of the antioxidant machinery for saline stress tolerance. PLoS Pathog **9,** e1003221.

Christensen, S.A. (2011). The function of the lipoxygenase *ZmLOX10* in maize interactions with insects and pathogens (Texas A & M University).

Christensen, S.A., and Kolomiets, M.V. (2011). The lipid language of plant–fungal interactions. Fungal Genetics and Biology **48,** 4-14.

Christensen, S.A., Huffaker, A., Hunter, C.T., Alborn, H.T., and Schmelz, E.A. (2016). A maize death acid, 10-oxo-11-phytoenoic acid, is the predominant cyclopentenone signal present during multiple stress and developmental conditions. Plant Signaling & Behavior **11,** e1120395.

Christensen, S.A., Huffaker, A., Kaplan, F., Sims, J., Ziemann, S., Doehlemann, G., Ji, L., Schmitz, R.J., Kolomiets, M.V., and Alborn, H.T. (2015). Maize death acids, 9-lipoxygenase–derived cyclopente (a) nones, display activity as cytotoxic phytoalexins and transcriptional mediators. Proceedings of the National Academy of Sciences **112,** 11407-11412.

Christensen, S.A., Nemchenko, A., Park, Y.S., Borrego, E., Huang, P.C., Schmelz, E.A., Kunze, S., Feussner, I., Yalpani, N., Meeley, R., and Kolomiets, M.V. (2014). The Novel Monocot-Specific 9-Lipoxygenase *ZmLOX12* Is Required to Mount an Effective Jasmonate-Mediated Defense Against *Fusarium verticillioides* in Maize. Molecular Plant-Microbe Interactions **27,** 1263-1276.

Christensen, S.A., Nemchenko, A., Borrego, E., Murray, I., Sobhy, I.S., Bosak, L., DeBlasio, S., Erb, M., Robert, C.A., Vaughn, K.A., Herrfurth, C., Tumlinson, J., Feussner, I., Jackson, D., Turlings, T.C., Engelberth, J., Nansen, C., Meeley, R., and Kolomiets, M.V. (2013). The maize lipoxygenase, *ZmLOX10*, mediates green leaf volatile, jasmonate and herbivore-induced plant volatile production for defense against insect attack. The Plant Journal **74,** 59-73.

Conrath, U., Beckers, G.J., Flors, V., Garcia-Agustin, P., Jakab, G., Mauch, F., Newman, M.A., Pieterse, C.M., Poinssot, B., Pozo, M.J., Pugin, A., Schaffrath, U., Ton, J., Wendehenne, D., Zimmerli, L., and Mauch-Mani, B. (2006). Priming: getting ready for battle. Molecular Plant-Microbe Interactions **19,** 1062-1071.

Constantino, N.N. (2017). Pathogen Triggered Plant Volatiles Induce Systemic Susceptibility in Neighboring Plants (Texas A & M University).

Constantino, N.N., Mastouri, F., Damarwinasis, R., Borrego, E.J., Moran-Diez, M.E., Kenerley, C.M., Gao, X., and Kolomiets, M.V. (2013). Root-expressed maize lipoxygenase 3 negatively regulates induced systemic resistance to *Colletotrichum graminicola* in shoots. Frontiers in Plant Science **4,** 510.

Contreras-Cornejo, H.A., Macías-Rodríguez, L., Beltrán-Peña, E., Herrera-Estrella, A., and López-Bucio, J. (2011). *Trichoderma*-induced plant immunity likely involves both hormonal-and camalexin-dependent mechanisms in *Arabidopsis thaliana* and confers resistance against necrotrophic fungi *Botrytis cinerea*. Plant Signaling & Behavior **6,** 1554-1563.

Czechowski, T., Stitt, M., Altmann, T., Udvardi, M.K., and Scheible, W.-R. (2005). Genome-wide identification and testing of superior reference genes for transcript normalization in Arabidopsis. Plant physiology **139,** 5-17.

Damarwinasis, R. (2018). *ZmLOX4* and *ZmLOX5* genes play contrasting roles in defense against *Colletotrichum graminicola* (Texas A & M University).

Dave, A., Hernandez, M.L., He, Z., Andriotis, V.M., Vaistij, F.E., Larson, T.R., and Graham, I.A. (2011). 12-oxo-phytodienoic acid accumulation during seed development represses seed germination in *Arabidopsis*. The Plant Cell **23,** 583-599.

Djonovic, S., Pozo, M.J., Dangott, L.J., Howell, C.R., and Kenerley, C.M. (2006). Sm1, a proteinaceous elicitor secreted by the biocontrol fungus *Trichoderma virens* induces plant defense responses and systemic resistance. Molecular Plant-Microbe Interactions **19,** 838-853.

Djonovic, S., Vargas, W.A., Kolomiets, M.V., Horndeski, M., Wiest, A., and Kenerley, C.M. (2007). A proteinaceous elicitor Sm1 from the beneficial fungus *Trichoderma virens* is required for induced systemic resistance in maize. Plant Physiology **145,** 875-889.

Druzhinina, I.S., Seidl-Seiboth, V., Herrera-Estrella, A., Horwitz, B.A., Kenerley, C.M., Monte, E., Mukherjee, P.K., Zeilinger, S., Grigoriev, I.V., and Kubicek, C.P. (2011). *Trichoderma*: the genomics of opportunistic success. Nature Reviews Microbiology **9,** 749-759.

Dubois, M., Van den Broeck, L., and Inze, D. (2018). The Pivotal Role of Ethylene in Plant Growth. Trends in Plant Science **23,** 311-323.

Engelberth, J., Alborn, H.T., Schmelz, E.A., and Tumlinson, J.H. (2004). Airborne signals prime plants against insect herbivore attack. Proceedings of the National Academy of Sciences **101,** 1781-1785.

Farag, M.A., and Pare, P.W. (2002). C6-Green leaf volatiles trigger local and systemic VOC emissions in tomato. Phytochemistry **61,** 545-554.

Feussner, I., and Wasternack, C. (2002). The lipoxygenase pathway. Annual Review of Plant Biology **53,** 275-297.

Floková, K., Feussner, K., Herrfurth, C., Miersch, O., Mik, V., Tarkowská, D., Strnad, M., Feussner, I., Wasternack, C., and Novák, O. (2016). A previously undescribed jasmonate compound in flowering *Arabidopsis thaliana*–The identification of cis-(+)-OPDA-Ile. Phytochemistry **122,** 230-237.

Funk, C.D. (2001). Prostaglandins and leukotrienes: advances in eicosanoid biology. Science **294,** 1871-1875.

Gao, X., Starr, J., Gobel, C., Engelberth, J., Feussner, I., Tumlinson, J., and Kolomiets, M. (2008). Maize 9-lipoxygenase *ZmLOX3* controls development, root-specific expression of defense genes, and resistance to root-knot nematodes. Molecular Plant-Microbe Interactions **21,** 98-109.

Gao, X., Shim, W.B., Gobel, C., Kunze, S., Feussner, I., Meeley, R., Balint-Kurti, P., and Kolomiets, M. (2007). Disruption of a maize 9-lipoxygenase results in increased resistance to fungal pathogens and reduced levels of contamination with mycotoxin fumonisin. Molecular Plant-Microbe Interactions **20,** 922-933.

Garrido, J.M.G., Morcillo, R.J.L., Rodríguez, J.Á.M., and Bote, J.A.O. (2010). Variations in the mycorrhization characteristics in roots of wild-type and ABA-deficient tomato are

accompanied by specific transcriptomic alterations. Molecular Plant-Microbe Interactions **23,** 651-664.

Ghanta, S., Bhattacharyya, D., and Chattopadhyay, S. (2011). Glutathione signaling acts through NPR1-dependent SA-mediated pathway to mitigate biotic stress. Plant Signaling & Behavior **6,** 607-609.

Gleason, C., Leelarasamee, N., Meldau, D., and Feussner, I. (2016). OPDA Has Key Role in Regulating Plant Susceptibility to the Root-Knot Nematode *Meloidogyne hapla* in *Arabidopsis*. Frontiers in Plant Science **7,** 1565.

Glick, B.R., Jacobson, C.B., Schwarze, M.M., and Pasternak, J. (1994). 1-Aminocyclopropane-1-carboxylic acid deaminase mutants of the plant growth promoting rhizobacterium *Pseudomonas putida* GR12-2 do not stimulate canola root elongation. Canadian Journal of Microbiology **40,** 911-915.

Glick, B.R., Todorovic, B., Czarny, J., Cheng, Z.Y., Duan, J., and McConkey, B. (2007). Promotion of plant growth by bacterial ACC deaminase. Critical Reviews in Plant Sciences **26,** 227-242.

Gorman, Z., Christensen, S., He, Y., Yan, Y., Borrego, E., and Kolomiets, M. (2017). Volatiles from LOX10 promote maize susceptibility to *Colletotrichum graminicola* by hijacking jasmonic and salicylic acids antagonism. In PHYTOPATHOLOGY (AMER PHYTOPATHOLOGICAL SOC 3340 PILOT KNOB ROAD, ST PAUL, MN 55121 USA), pp. 1-2.

Guo, H.M., Li, H.C., Zhou, S.R., Xue, H.W., and Miao, X.X. (2014). Cis-12-oxo-phytodienoic acid stimulates rice defense response to a piercing-sucking insect. Molecular Plant **7,** 1683-1692.

Han, Y., Chaouch, S., Mhamdi, A., Queval, G., Zechmann, B., and Noctor, G. (2013). Functional Analysis of Arabidopsis Mutants Points to Novel Roles for Glutathione in Coupling H_2O_2 to Activation of Salicylic Acid Accumulation and Signaling. Antioxidants & Redox Signaling **18,** 2106-2121.

Haney, C.H., Samuel, B.S., Bush, J., and Ausubel, F.M. (2015). Associations with rhizosphere bacteria can confer an adaptive advantage to plants. Nature Plants **1,** 1-9.

Haque, E., Osmani, A.A., Ahmadi, S.H., Ogawa, S., Takagi, K., Yokoyama, M., and Ban, T. (2016). KODA, an α-ketol derivative of linolenic acid provides wide recovery ability of wheat against various abiotic stresses. Biocatalysis and Agricultural Biotechnology **7,** 67-75.

Harman, G.E. (2011). Multifunctional fungal plant symbionts: new tools to enhance plant growth and productivity. New Phytol **189,** 647-649.

Havko, N.E., Major, I.T., Jewell, J.B., Attaran, E., and Howe, G.A. (2016). Control of carbon assimilation and partitioning by jasmonate: an accounting of growth–defense tradeoffs. Plants **5,** 7.

Heil, M., and Bostock, R.M. (2002). Induced systemic resistance (ISR) against pathogens in the context of induced plant defences. Annals of Botany **89,** 503-512.

Hermosa, R., Viterbo, A., Chet, I., and Monte, E. (2012). Plant-beneficial effects of *Trichoderma* and of its genes. Microbiology **158,** 17-25.

Herrera-Medina, M.J., Tamayo, M.I., Vierheilig, H., Ocampo, J.A., and García-Garrido, J.M. (2008). The jasmonic acid signalling pathway restricts the development of the arbuscular mycorrhizal association in tomato. Journal of Plant Growth Regulation **27,** 221.

Howe, G.A., and Jander, G. (2008). Plant immunity to insect herbivores. Annual Review of Plant Biology **59,** 41-66.

Howe, G.A., Lightner, J., Browse, J., and Ryan, C.A. (1996). An octadecanoid pathway mutant (JL5) of tomato is compromised in signaling for defense against insect attack. The Plant Cell **8,** 2067-2077.

Howell, C.R., Hanson, L.E., Stipanovic, R.D., and Puckhaber, L.S. (2000). Induction of Terpenoid Synthesis in Cotton Roots and Control of Rhizoctonia solani by Seed Treatment with Trichoderma virens. Phytopathology **90,** 248-252.

Huang, H., Liu, B., Liu, L., and Song, S. (2017). Jasmonate action in plant growth and development. Journal of Experimental Botany **68,** 1349-1359.

Huang, P.-C. (2017). Oxylipin Signals Govern Drought and Salt Tolerance and Resistance to Pathogens (Texas A&M University).

Huot, B., Yao, J., Montgomery, B.L., and He, S.Y. (2014). Growth–defense tradeoffs in plants: a balancing act to optimize fitness. Molecular Plant **7,** 1267-1287.

Hwang, I.S., and Hwang, B.K. (2010). The pepper 9-lipoxygenase gene CaLOX1 functions in defense and cell death responses to microbial pathogens. Plant Physiol **152,** 948-967.

Isakeit, T., Gao, X., and Kolomiets, M. (2007). Increased resistance of a maize mutant lacking the 9-Lipoxygenase gene, *ZmLOX3*, to root rot caused by *Exserohilum pedicellatum*. Journal of Phytopathology **155,** 758-760.

Jogaiah, S., Abdelrahman, M., Tran, L.P., and Ito, S.I. (2018). Different mechanisms of *Trichoderma virens*-mediated resistance in tomato against Fusarium wilt involve the jasmonic and salicylic acid pathways. Molecular Plant Pathology **19,** 870-882.

Kachroo, A., and Kachroo, P. (2009). Fatty Acid-derived signals in plant defense. Annu Rev Phytopathol **47,** 153-176.

Katagiri, F., and Tsuda, K. (2010). Understanding the plant immune system. Molecular Plant-Microbe Interactions **23,** 1531-1536.

Kittikorn, M., Shiraishi, N., Okawa, K., Ohara, H., Yokoyama, M., Ifuku, O., Yoshida, S., and Kondo, S. (2010). Effect of fruit load on 9,10-ketol-octadecadienoic acid (KODA), GA and jasmonic acid concentrations in apple buds. Scientia Horticulturae **124,** 225-230.

Klessig, D.F., Choi, H.W., and Dempsey, D.A. (2018). Systemic Acquired Resistance and Salicylic Acid: Past, Present, and Future. Molecular Plant-Microbe Interactions **31,** 871-888.

Knoester, M., Pieterse, C.M.J., Bol, J.F., and Van Loon, L.C. (1999). Systemic resistance in *Arabidopsis* induced by rhizobacteria requires ethylene-dependent signaling at the site of application. Molecular Plant-Microbe Interactions **12,** 720-727.

Koornneef, A., Leon-Reyes, A., Ritsema, T., Verhage, A., Den Otter, F.C., Van Loon, L.C., and Pieterse, C.M. (2008). Kinetics of salicylate-mediated suppression of jasmonate signaling reveal a role for redox modulation. Plant Physiology **147,** 1358-1368.

Korolev, N., David, D.R., and Elad, Y. (2008). The role of phytohormones in basal resistance and *Trichoderma*-induced systemic resistance to *Botrytis cinerea* in *Arabidopsis thaliana*. Biocontrol **53,** 667-683.

Kubicek, C.P., Herrera-Estrella, A., Seidl-Seiboth, V., Martinez, D.A., Druzhinina, I.S., Thon, M., Zeilinger, S., Casas-Flores, S., Horwitz, B.A., Mukherjee, P.K., Mukherjee, M., Kredics, L., Alcaraz, L.D., Aerts, A., Antal, Z., Atanasova, L., Cervantes-Badillo, M.G., Challacombe, J., Chertkov, O., McCluskey, K., Coulpier,

F., Deshpande, N., von Dohren, H., Ebbole, D.J., Esquivel-Naranjo, E.U., Fekete, E., Flipphi, M., Glaser, F., Gomez-Rodriguez, E.Y., Gruber, S., Han, C., Henrissat, B., Hermosa, R., Hernandez-Onate, M., Karaffa, L., Kosti, I., Le Crom, S., Lindquist, E., Lucas, S., Lubeck, M., Lubeck, P.S., Margeot, A., Metz, B., Misra, M., Nevalainen, H., Omann, M., Packer, N., Perrone, G., Uresti-Rivera, E.E., Salamov, A., Schmoll, M., Seiboth, B., Shapiro, H., Sukno, S., Tamayo-Ramos, J.A., Tisch, D., Wiest, A., Wilkinson, H.H., Zhang, M., Coutinho, P.M., Kenerley, C.M., Monte, E., Baker, S.E., and Grigoriev, I.V. (2011). Comparative genome sequence analysis underscores mycoparasitism as the ancestral life style of *Trichoderma*. Genome Biology **12,** R40.

Lamdan, N.L., Shalaby, S., Ziv, T., Kenerley, C.M., and Horwitz, B.A. (2015). Secretome of *Trichoderma* interacting with maize roots: role in induced systemic resistance. Molecular & Cellular Proteomics **14,** 1054-1063.

Laudert, D., and Weiler, E.W. (1998). Allene oxide synthase: a major control point in *Arabidopsis thaliana* octadecanoid signalling. The Plant Journal **15,** 675-684.

León-Morcillo, R.J., Ángel, J., Vierheilig, H., Ocampo, J.A., and García-Garrido, J.M. (2012). Late activation of the 9-oxylipin pathway during arbuscular mycorrhiza formation in tomato and its regulation by jasmonate signalling. Journal of Experimental Botany **63,** 3545-3558.

Li, C., Liu, G., Xu, C., Lee, G.I., Bauer, P., Ling, H.Q., Ganal, M.W., and Howe, G.A. (2003). The tomato suppressor of prosystemin-mediated responses2 gene encodes a fatty acid desaturase required for the biosynthesis of jasmonic acid and the production of a systemic wound signal for defense gene expression. The Plant Cell **15,** 1646-1661.

López-Ráez, J.A., Verhage, A., Fernandez, I., Garcia, J.M., Azcon-Aguilar, C., Flors, V., and Pozo, M.J. (2010). Hormonal and transcriptional profiles highlight common and differential host responses to arbuscular mycorrhizal fungi and the regulation of the oxylipin pathway. Journal of Experimental Botany **61,** 2589-2601.

Lorito, M., Woo, S.L., Harman, G.E., and Monte, E. (2010). Translational Research on Trichoderma: From 'Omics to the Field.

Martinez-Medina, A., Appels, F.V.W., and van Wees, S.C.M. (2017). Impact of salicylic acid- and jasmonic acid-regulated defences on root colonization by *Trichoderma harzianum* T-78. Plant Signaling & Behavior **12,** e1345404.

Matsui, K. (2006). Green leaf volatiles: hydroperoxide lyase pathway of oxylipin metabolism. Current Opinion in Plant Biology **9,** 274-280.

Maynard, D., Groger, H., Dierks, T., and Dietz, K.J. (2018). The function of the oxylipin 12-oxophytodienoic acid (OPDA) in cell signaling, stress acclimation and development. Journal of Experimental Botany.

Mendes, R., Garbeva, P., and Raaijmakers, J.M. (2013). The rhizosphere microbiome: significance of plant beneficial, plant pathogenic, and human pathogenic microorganisms. FEMS Microbiology Reviews **37,** 634-663.

Miersch, O., Kramell, R., Parthier, B., and Wasternack, C. (1999). Structure–activity relations of substituted, deleted or stereospecifically altered jasmonic acid in gene expression of barley leaves. Phytochemistry **50,** 353-361.

Monte, I., Ishida, S., Zamarreno, A.M., Hamberg, M., Franco-Zorrilla, J.M., Garcia-Casado, G., Gouhier-Darimont, C., Reymond, P., Takahashi, K., Garcia-Mina, J.M.,

Nishihama, R., Kohchi, T., and Solano, R. (2018). Ligand-receptor co-evolution shaped the jasmonate pathway in land plants. Nature Chemical Biology **14,** 480-488.

Mora-Romero, G.A., Cervantes-Gamez, R.G., Galindo-Flores, H., Gonzalez-Ortiz, M.A., Felix-Gastelum, R., Maldonado-Mendoza, I.E., Perez, R.S., Leon-Felix, J., Martinez-Valenzuela, M.C., and Lopez-Meyer, M. (2015a). Mycorrhiza-induced protection against pathogens is both genotype-specific and graft-transmissible. Symbiosis **66,** 55-64.

Mora-Romero, G.A., Gonzalez-Ortiz, M.A., Quiroz-Figueroa, F., Calderon-Vazquez, C.L., Medina-Godoy, S., Maldonado-Mendoza, I., Arroyo-Becerra, A., Perez-Torres, A., Alatorre-Cobos, F., Sanchez, F., and Lopez-Meyer, M. (2015b). PvLOX2 silencing in common bean roots impairs arbuscular mycorrhiza-induced resistance without affecting symbiosis establishment. Functional Plant Biology **42,** 18-30.

Moran-Diez, M.E., Trushina, N., Lamdan, N.L., Rosenfelder, L., Mukherjee, P.K., Kenerley, C.M., and Horwitz, B.A. (2015). Host-specific transcriptomic pattern of Trichoderma virens during interaction with maize or tomato roots. BMC Genomics **16,** 8.

Morcillo, R.J.L., Navarrete, M.I.T., Bote, J.A.O., Monguio, S.P., and García-Garrido, J.M. (2016). Suppression of allene oxide synthase 3 in potato increases degree of arbuscular mycorrhizal fungal colonization. Journal of Plant Physiology **190,** 15-25.

Mosblech, A., Feussner, I., and Heilmann, I. (2009). Oxylipins: structurally diverse metabolites from fatty acid oxidation. Plant Physiology and Biochemistry **47,** 511-517.

Mueller, S., Hilbert, B., Dueckershoff, K., Roitsch, T., Krischke, M., Mueller, M.J., and Berger, S. (2008). General detoxification and stress responses are mediated by oxidized lipids through TGA transcription factors in *Arabidopsis*. The Plant Cell **20,** 768-785.

Mueller, U.G., and Sachs, J.L. (2015). Engineering microbiomes to improve plant and animal health. Trends in Microbiology **23,** 606-617.

Mukherjee, P.K., and Kenerley, C.M. (2010). Regulation of morphogenesis and biocontrol properties in *Trichoderma virens* by a VELVET protein, Vel1. Applied and Environmental Microbiology **76,** 2345-2352.

Mukherjee, P.K., Horwitz, B.A., Herrera-Estrella, A., Schmoll, M., and Kenerley, C.M. (2013). *Trichoderma* research in the genome era. Annual Review of Phytopathology **51,** 105-129.

Nalam, V.J., Keeretaweep, J., Sarowar, S., and Shah, J. (2012). Root-derived oxylipins promote green peach aphid performance on Arabidopsis foliage. Plant Cell **24,** 1643-1653.

Ogunola, O.F., Hawkins, L.K., Mylroie, E., Kolomiets, M.V., Borrego, E., Tang, J.D., Williams, W.P., and Warburton, M.L. (2017). Characterization of the maize lipoxygenase gene family in relation to aflatoxin accumulation resistance. PloS One **12,** e0181265.

Park, S.W., Li, W., Viehhauser, A., He, B., Kim, S., Nilsson, A.K., Andersson, M.X., Kittle, J.D., Ambavaram, M.M., Luan, S., Esker, A.R., Tholl, D., Cimini, D., Ellerstrom, M., Coaker, G., Mitchell, T.K., Pereira, A., Dietz, K.J., and Lawrence, C.B. (2013). Cyclophilin 20-3 relays a 12-oxo-phytodienoic acid signal during stress responsive regulation of cellular redox homeostasis. Proceedings of the National Academy of Sciences **110,** 9559-9564.

Park, Y.S. (2012). Diverse functions of the two segmentally duplicated 9-lipoxygenases ZmLOX4 and ZmLOX5 of maize (Texas A & M University).

Park, Y.S., Kunze, S., Ni, X., Feussner, I., and Kolomiets, M.V. (2010). Comparative molecular and biochemical characterization of segmentally duplicated 9-lipoxygenase genes ZmLOX4 and ZmLOX5 of maize. Planta **231,** 1425-1437.

Pena-Cortés, H., Albrecht, T., Prat, S., Weiler, E.W., and Willmitzer, L. (1993). Aspirin prevents wound-induced gene expression in tomato leaves by blocking jasmonic acid biosynthesis. Planta **191,** 123-128.

Penrose, D.M., Moffatt, B.A., and Glick, B.R. (2001). Determination of 1-aminocycopropane-1-carboxylic acid (ACC) to assess the effects of ACC deaminase-containing bacteria on roots of canola seedlings. Canadian Journal of Microbiology **47,** 77-80.

Pieterse, C.M., Van der Does, D., Zamioudis, C., Leon-Reyes, A., and Van Wees, S.C. (2012). Hormonal modulation of plant immunity. Annual Review of Cell and Developmental Biology **28,** 489-521.

Pieterse, C.M., Zamioudis, C., Berendsen, R.L., Weller, D.M., Van Wees, S.C., and Bakker, P.A. (2014a). Induced systemic resistance by beneficial microbes. Annual Review of Phytopathology **52,** 347-375.

Pieterse, C.M., van Wees, S.C., van Pelt, J.A., Knoester, M., Laan, R., Gerrits, H., Weisbeek, P.J., and van Loon, L.C. (1998). A novel signaling pathway controlling induced systemic resistance in *Arabidopsis*. The Plant Cell **10,** 1571-1580.

Pieterse, C.M.J., Zamioudis, C., Van der Does, D., and Van Wees, S.C.M. (2014b). Signalling Networks Involved in Induced Resistance.

Ponce De Leon, I., Schmelz, E.A., Gaggero, C., Castro, A., Alvarez, A., and Montesano, M. (2012). *Physcomitrella patens* activates reinforcement of the cell wall, programmed cell death and accumulation of evolutionary conserved defence signals, such as salicylic acid

and 12-oxo-phytodienoic acid, but not jasmonic acid, upon *Botrytis cinerea* infection. Molecular Plant Pathology **13,** 960-974.

Pozo, M.J., Van Der Ent, S., Van Loon, L., and Pieterse, C.M. (2008). Transcription factor MYC2 is involved in priming for enhanced defense during rhizobacteria-induced systemic resistance in *Arabidopsis thaliana*. New Phytologist **180,** 511-523.

Prost, I., Dhondt, S., Rothe, G., Vicente, J., Rodriguez, M.J., Kift, N., Carbonne, F., Griffiths, G., Esquerre-Tugaye, M.T., Rosahl, S., Castresana, C., Hamberg, M., and Fournier, J. (2005). Evaluation of the antimicrobial activities of plant oxylipins supports their involvement in defense against pathogens. Plant Physiology **139,** 1902-1913.

Qu, X., Hall, B.P., Gao, Z., and Schaller, G.E. (2007). A strong constitutive ethylene-response phenotype conferred on *Arabidopsis* plants containing null mutations in the ethylene receptors ETR1 and ERS1. BMC Plant Biology **7,** 3.

Sakamoto, D., Nakamura, Y., Sugiura, H., Sugiura, T., Asakura, T., Yokoyama, M., and Moriguchi, T. (2010). Effect of 9-Hydroxy-10-oxo-12(Z), 15(Z)-octadecadienoic Acid (KODA) on Endodormancy Breaking in Flower Buds of Japanese Pear. Hortscience **45,** 1470-1474.

Salas-Marina, M.A., Silva-Flores, M.A., Uresti-Rivera, E.E., Castro-Longoria, E., Herrera-Estrella, A., and Casas-Flores, S. (2011). Colonization of *Arabidopsis* roots by *Trichoderma atroviride* promotes growth and enhances systemic disease resistance through jasmonic acid/ethylene and salicylic acid pathways. European Journal of Plant Pathology **131,** 15-26.

Salas-Marina, M.A., Isordia-Jasso, M.I., Islas-Osuna, M.A., Delgado-Sanchez, P., Jimenez-Bremont, J.F., Rodriguez-Kessler, M., Rosales-Saavedra, M.T., Herrera-Estrella,

A., and Casas-Flores, S. (2015). The Epl1 and Sm1 proteins from *Trichoderma atroviride* and *Trichoderma virens* differentially modulate systemic disease resistance against different life style pathogens in *Solanum lycopersicum*. Frontiers in Plant Science **6,** 77.

Scalschi, L., Sanmartin, M., Camanes, G., Troncho, P., Sanchez-Serrano, J.J., Garcia-Agustin, P., and Vicedo, B. (2015). Silencing of OPR3 in tomato reveals the role of OPDA in callose deposition during the activation of defense responses against *Botrytis cinerea*. The Plant Journal **81,** 304-315.

Shan, L.B., and He, P. (2018). Pipped at the Post: Pipecolic Acid Derivative Identified as SAR Regulator. Cell **173,** 286-287.

Shoresh, M., Yedidia, I., and Chet, I. (2005). Involvement of Jasmonic Acid/Ethylene Signaling Pathway in the Systemic Resistance Induced in Cucumber by *Trichoderma asperellum* T203. Phytopathology **95,** 76-84.

Shoresh, M., Harman, G.E., and Mastouri, F. (2010). Induced systemic resistance and plant responses to fungal biocontrol agents. Annu Rev Phytopathol **48,** 21-43.

Song, S., Qi, T., Fan, M., Zhang, X., Gao, H., Huang, H., Wu, D., Guo, H., and Xie, D. (2013). The bHLH subgroup IIId factors negatively regulate jasmonate-mediated plant defense and development. PLoS Genetics **9,** e1003653.

Song, Y., Chen, D., Lu, K., Sun, Z., and Zeng, R. (2015). Enhanced tomato disease resistance primed by arbuscular mycorrhizal fungus. Frontiers in Plant Science **6,** 786.

Stelmach, B.A., Muller, A., Hennig, P., Laudert, D., Andert, L., and Weiler, E.W. (1998). Quantitation of the octadecanoid 12-oxo-phytodienoic acid, a signalling compound in plant mechanotransduction. Phytochemistry **47,** 539-546.

Stotz, H.U., Mueller, S., Zoeller, M., Mueller, M.J., and Berger, S. (2013). TGA transcription factors and jasmonate-independent COI1 signalling regulate specific plant responses to reactive oxylipins. Journal of Experimental Botany **64,** 963-975.

Stumpe, M., Gobel, C., Faltin, B., Beike, A.K., Hause, B., Himmelsbach, K., Bode, J., Kramell, R., Wasternack, C., Frank, W., Reski, R., and Feussner, I. (2010). The moss *Physcomitrella patens* contains cyclopentenones but no jasmonates: mutations in allene oxide cyclase lead to reduced fertility and altered sporophyte morphology. New Phytologist **188,** 740-749.

Taki, N., Sasaki-Sekimoto, Y., Obayashi, T., Kikuta, A., Kobayashi, K., Ainai, T., Yagi, K., Sakurai, N., Suzuki, H., Masuda, T., Takamiya, K., Shibata, D., Kobayashi, Y., and Ohta, H. (2005). 12-oxo-phytodienoic acid triggers expression of a distinct set of genes and plays a role in wound-induced gene expression in *Arabidopsis*. Plant Physiology **139,** 1268-1283.

Tao, J.J., Cao, Y.R., Chen, H.W., Wei, W., Li, Q.T., Ma, B., Zhang, W.K., Chen, S.Y., and Zhang, J.S. (2015). Tobacco Translationally Controlled Tumor Protein Interacts with Ethylene Receptor Tobacco Histidine Kinase1 and Enhances Plant Growth through Promotion of Cell Proliferation. Plant Physiology **169,** 96-+.

Thaler, J.S., Humphrey, P.T., and Whiteman, N.K. (2012). Evolution of jasmonate and salicylate signal crosstalk. Trends in Plant Science **17,** 260-270.

Tsuchisaka, A., Yu, G.X., Jin, H.L., Alonso, J.M., Ecker, J.R., Zhang, X.M., Gao, S., and Theologis, A. (2009). A Combinatorial Interplay Among the 1-Aminocyclopropane-1-Carboxylate Isoforms Regulates Ethylene Biosynthesis in *Arabidopsis thaliana*. Genetics **183,** 979-1003.

Tzeng, T.H., Lyngholm, L.K., Ford, C.F., and Bronson, C.R. (1992). A restriction fragment length polymorphism map and electrophoretic karyotype of the fungal maize pathogen *Cochliobolus heterostrophus*. Genetics **130,** 81-96.

Vellosillo, T., Martinez, M., Lopez, M.A., Vicente, J., Cascon, T., Dolan, L., Hamberg, M., and Castresana, C. (2007). Oxylipins produced by the 9-lipoxygenase pathway in *Arabidopsis* regulate lateral root development and defense responses through a specific signaling cascade. The Plant Cell **19,** 831-846.

Vernooij, B., Friedrich, L., Morse, A., Reist, R., Kolditz-Jawhar, R., Ward, E., Uknes, S., Kessmann, H., and Ryals, J. (1994). Salicylic acid is not the translocated signal responsible for inducing systemic acquired resistance but is required in signal transduction. The Plant Cell **6,** 959-965.

Vicente, J., Cascón, T., Vicedo, B., García-Agustín, P., Hamberg, M., and Castresana, C. (2012). Role of 9-lipoxygenase and α-dioxygenase oxylipin pathways as modulators of local and systemic defense. Molecular Plant **5,** 914-928.

Vick, B.A., and Zimmerman, D.C. (1984). Biosynthesis of Jasmonic Acid by Several Plant-Species. Plant Physiology **75,** 458-461.

Viterbo, A., Landau, U., Kim, S., Chernin, L., and Chet, I. (2010). Characterization of ACC deaminase from the biocontrol and plant growth-promoting agent *Trichoderma asperellum* T203. FEMS Microbiology Letters **305,** 42-48.

Vlot, A.C., Dempsey, D.A., and Klessig, D.F. (2009). Salicylic Acid, a multifaceted hormone to combat disease. Annual Review of Phytopathology **47,** 177-206.

Wang, K., Guo, Q., Froehlich, J.E., Hersh, H.L., Zienkiewicz, A., Howe, G.A., and Benning, C. (2018). Two Abscisic Acid-Responsive Plastid Lipase Genes Involved in Jasmonic Acid Biosynthesis in *Arabidopsis thaliana*. The Plant Cell **30,** 1006-1022.

Wang, S., Saito, T., Ohkawa, K., Ohara, H., Shishido, M., Ikeura, H., Takagi, K., Ogawa, S., Yokoyama, M., and Kondo, S. (2016). alpha-Ketol linolenic acid (KODA) application affects endogenous abscisic acid, jasmonic acid and aromatic volatiles in grapes infected by a pathogen (*Glomerella cingulata*). Journal of Plant Physiology **192,** 90-97.

Wang, Y., Ohara, Y., Nakayashiki, H., Tosa, Y., and Mayama, S. (2005). Microarray analysis of the gene expression profile induced by the endophytic plant growth-promoting rhizobacteria, *Pseudomonas fluorescens* FPT9601-T5 in *Arabidopsis*. Molecular Plant-Microbe Interactions **18,** 385-396.

Wasternack, C. (2007). Jasmonates: an update on biosynthesis, signal transduction and action in plant stress response, growth and development. Annals of Botany **100,** 681-697.

Wasternack, C., and Hause, B. (2013). Jasmonates: biosynthesis, perception, signal transduction and action in plant stress response, growth and development. An update to the 2007 review in Annals of Botany. Annals of Botany **111,** 1021-1058.

Whitman, D.W., and Eller, F.J. (1990). Parasitic wasps orient to green leaf volatiles. Chemoecology **1,** 69-76.

Xia, A., Feng-ying, D., Song, G., Fan-jun, C., Li-xing, Y., and Ri-liang, G. (2014). Transcriptional regulation of expression of the maize aldehyde dehydrogenase 7 gene (ZmALDH7B6) in response to abiotic stresses. Journal of Integrative Agriculture **13,** 1900-1908.

Yamamoto, Y., Ohshika, J., Takahashi, T., Ishizaki, K., Kohchi, T., Matusuura, H., and Takahashi, K. (2015). Functional analysis of allene oxide cyclase, MpAOC, in the liverwort *Marchantia polymorpha*. Phytochemistry **116,** 48-56.

Yan, Y., Christensen, S., Isakeit, T., Engelberth, J., Meeley, R., Hayward, A., Emery, R.J., and Kolomiets, M.V. (2012). Disruption of OPR7 and OPR8 reveals the versatile functions of jasmonic acid in maize development and defense. The Plant Cell **24,** 1420-1436.

Yedidia, I., Benhamou, N., and Chet, I. (1999). Induction of defense responses in cucumber plants (*Cucumis sativus* L.) by the biocontrol agent *Trichoderma harzianum*. Applied and Environmental Microbiology **65,** 1061-1070.

Yokoyama, M., Yamaguchi, S., Inomata, S., Komatsu, K., Yoshida, S., Iida, T., Yokokawa, Y., Yamaguchi, M., Kaihara, S., and Takimoto, A. (2000). Stress-induced factor involved in flower formation of *Lemna* is an α-ketol derivative of linolenic acid. Plant and Cell Physiology **41,** 110-113.

Zhang, Y.L., Tessaro, M.J., Lassner, M., and Li, X. (2003). Knockout analysis of *Arabidopsis* transcription factors TGA2, TGA5, and TGA6 reveals their redundant and essential roles in systemic acquired resistance. The Plant Cell **15,** 2647-2653.